Institut für Nutzpflanzenwissenschaften und Ressourcenschutz (INRES)

der

Rheinische Friedrich-Wilhelms-Universität Bonn

Non-destructive evaluation of complex interactions between *Heterodera schachtii* and *Rhizoctonia solani* on sugar beet as affected by cultivar resistance

Inaugural - Dissertation

zur

Erlangung des Grades

Doktor der Agrarwissenschaften

(Dr.agr.)

der

Hohen Landwirtschaftlichen Fakultät

der

Rheinischen Friedrich-Wilhelms-Universität

zu Bonn

vorgelegt am 15.11.2010

von

Christian Hillnhütter

aus

Siegen, Deutschland

Non-destructive evaluation of complex interactions between *Heterodera schachtii* and *Rhizoctonia solani* on sugar beet as affected by cultivar resistance

The beet cyst nematode *Heterodera schachtii* and *Rhizoctonia* crown and root rot caused by the fungus *Rhizoctonia solani* anastomosis group 2-2IIIB were investigated for the presence of synergistic interactions on sugar beet.

Three levels of cultivar resistance were tested for their response to the fungus and nematode alone and in combination. A cultivar susceptible to both pathogens, one tolerant to *R. solani* and one resistant to *H. schachtii* were used. Synergistic damage was caused by the disease complex on the tolerant and the susceptible cultivars. Conversely, the resistant cultivar showed less damage by the disease complex than *R. solani* inoculated alone. Staggered time of inoculation of the two pathogens was used to investigate the effect of plant age on the development of the disease complex. It was demonstrated that younger plants were more susceptible to the disease complex. Besides destructive analysis of plant-pathogen interactions, hyperspectral leaf reflectance was used to test it's suitability for detection of symptoms caused by each organism alone or in combination. Calculation of the Normalized Differenced Vegetation Index allowed discrimination of plants impacted by the disease complex as well as *R. solani* treated alone from plants of the absolute control and the *H. schachtii* treated plants.

Nuclear magnetic resonance imaging was tested for detection of belowground symptoms caused by *R. solani* and/or *H. schachtii*. The treatment with *H. schachtii* alone showed excessive lateral root development. Morphology of the roots was different to control plants. The roots were thicker near the locus of nematode inoculation. *Rhizoctonia solani* rotting on the beet was also detected by Nuclear Magnetic Resonance imaging. Signal intensity (water content) was lower where rotting occurred. The disease complex treated plants showed more severe rotting on the Nuclear Magnetic Resonance image near the site of nematode penetration.

Hyperspectral leaf reflectance images were processed to obtain more exact data for symptom discrimination. By calculation of several spectral vegetation indices it was possible to discriminate symptoms caused by *H. schachtii*, *R. solani* or the disease complex as opposed to healthy plants by means of leaf reflectance. Spectral vegetation indices were highly correlated with pathogen induced symptoms when obtained from hyperspectral images including soil reflectance. A supervised classification technique based on spectral reflectance was tested to differentiate between four levels of leaf symptoms caused by *Rhizoctonia* crown and root rot and resulted in an overall accuracy of 79 %.

Aerial and near-range hyperspectral sensors were tested on detection, discrimination and quantification of symptoms caused by *Rhizoctonia* crown and root rot and the beet cyst nematode in a field experiment. Georeferenced maps were constructed with ground truth data which was then correlated to different aerial and near-range hyperspectral datasets. Symptoms could be discriminated by variable temporal onset in the cropping season. By supervised classification of aerial data it was possible to quantify damage of either *R. solani* or *H. schachtii* with an overall accuracy of 78 %. More severe damage by concomitant pathogen occurrence, but no synergistic damage was observed by the disease complex under natural field conditions.

Berührungslose Untersuchung von Wechselbeziehungen zwischen *Heterodera schachtii* und *Rhizoctonia solani* an Zuckerrüben unter Berücksichtigung des Einflusses von Sortenresistenzen auf die Interaktionen

Der Einfluss des gemeinsamen Auftretens von Rübenzystennematoden (*Heterodera schachtii*) und der durch *Rhizoctonia solani* hervorgerufenen späten Rübenfäule wurde auf die Bildung synergistischer Interaktionen an Zuckerrüben untersucht.

Drei unterschiedlich resistente Zuckerrübensorten wurden auf mögliche Interaktionen zwischen Pilz und Nematode getestet. Eine Sorte war gegen beide Schadorganismen anfällig, eine tolerant gegenüber *R. solani* und eine resistent gegenüber *H. schachtii*. Die anfällige und die tolerante Sorte zeigten einen synergistischen Schaden, verursacht durch den Krankheits-Komplex. Hingegen gab es bei der *H. schachtii* resistenten Sorte keine synergistischen Schadeffekte. Um den Einfluss des Entwicklungsstadiums der Pflanzen auf die Interaktion zu untersuchen, wurde eine zeitlich verzögerte Inokulation des Krankheits-Komplexes realisiert. Wie erwartet waren jüngere, weniger entwickelte Pflanzen dem gleichzeitigen Auftreten von *H. schachtii* und *R. solani* gegenüber anfälliger. Neben den konventionell destruktiven Methoden der Versuchsauswertung wurde die Blattreflektion mittels eines hyperspektralen Sensors aufgenommen. Diese berührungslose Methode wurde auf ihre Sensibilität gegenüber der Entdeckung von Symptomen von jeweils einem oder beiden Organismen zusammen untersucht. Durch die Berechnung des Normalized Differenced Vegetation Index aus den hyperspektralen Daten war es möglich Symptome von Pflanzen mit dem Krankheits-Komplex von Pflanzen ohne diesen zu unterscheiden.

Die nukleare Magnetresonanztomographie wurde als berührungslose Technik eingesetzt, um unterirdische Schäden, hervorgerufen durch *H. schachtii* und/oder *R. solani*, nachzuweisen. Die mit *H. schachtii* inokulierten Pflanzen bildeten verstärkt Seitenwurzeln. Auch die durch *R. solani* hervorgerufene Fäule konnte durch Magnetresonanztomographie diagnostiziert werden. Pflanzen mit dem Krankheits-Komplex zeigten auf den Resonanzbildern eine deutlich stärkere Fäule am Rübenkörper nahe der Penetrationsstellen der Nematoden.

Um die aussagekräftigsten Daten für eine Symptomdiskriminierung zu erhalten, wurden hyperspektrale Bilder auf unterschiedliche Weise prozessiert. Anhand mehrerer spektraler Vegetations Indizes war es möglich die verschieden inokulierten Pflanzen voneinander zu unterscheiden. Die Indizes korrelierten am stärksten mit den Symptomen, wenn die Reflektion des Bodens in die Auswertung der Bilder einbezogen wurde. Mittels einer überwachten Klassifizierung konnten durch *R. solani* hervorgerufene Blattsymptome mit einer Genauigkeit von 79 % bestimmt werden.

In einem Feldversuch wurden flugzeug- und handgetragene hyperspektrale Sensoren auf Detektion, Diskriminierung und Quantifizierung von Symptomen der Rübenfäule und des Rübenzystennematoden untersucht. Georeferenzierte Karten wurden aus Bonitur Daten erstellt und anschließend mit hyperspektralen Daten korreliert. Symptome durch die beiden Versuchsorganismen konnten durch das zeitlich versetzte Auftreten unterschieden werden. Durch eine überwachte Klassifizierung der Luftbilddaten war es möglich Schäden sowohl durch *R. solani* als auch durch *H. schachtii* mit einer Genauigkeit von 78 % zu bestimmen. Ein synergistischer Schaden konnte durch das gleichzeitige Auftreten der beiden Versuchsorganismen im Feld nicht nachgewiesen werden.

TABLE OF CONTENTS

CHAPTER 1: GENERAL INTRODUCTION

1. THE SUGAR BEET CROP

Sugar beet (*Beta vulgaris* L. ssp. vulgaris var. altissima Döll) belongs to the family *Chenopodiaceae* (Franke, 1997). The storage organ of the sugar beet plant is usually called tuber, although about 90 % of the tuber is root origin, the upper 10 % (the crown) being derived from the hypocotyl.

The tuber contains high concentrations of sucrose and is mainly used for sugar extraction, as well as for bio-ethanol and bio-gas production. In 1747 the chemist Marggraf detected the similarity of sugar obtained from sugar beet to that coming from sugar cane. Since the Napoleon wars the sugar beet crop has had an upsurge in production in Europe and in the USA (Nürnberg, 1965). Breeding increased the total content of sugar from 1.6 - 20 % (Elliot & Weston, 1993).

Today the EU, the USA and the Russian Federation are the biggest sugar beet producers with an overall harvested area of 1.5 Mill ha (FAO, 2010). The production and the price of sugar beet have recently decreased in the EU due to political decisions related to agricultural subsidies and due to strong competition with sugar from sugar cane. Conversely, the use of sugar beet for production of ethanol could give sugar beet production upsurge (von Blottnitz & Curran, 2007).

Due to the long history of sugar beet cultivation in Germany and the high proportion of sugar beet in crop rotations, many leaf and soil-borne pathogens severely limit yield. The most important soil-borne pathogens are *Heterodera schachtii* and *Rhizoctonia solani*.

2. THE BEET CYST NEMATODE *HETERODERA SCHACHTII*

The beet cyst nematode (BCN) *Heterodera schachtii* (Schmidt) is a sedentary endoparasite. Besides sugar beet *H. schachtii* has a wide host range including mustard, canola and

cabbage. Eighty percent of the plants in the families *Chenopodiaceae* and *Cruciferae* are hosts for the nematode (Börner, 1990). The nematode originated in Europe and followed the sugar beet around the world in infested planting material.

Damage: *Heterodera schachtii* was the first pathogen of sugar beet to be recognized (Schacht, 1859). It causes severe damage to sugar beet with yield losses of up to 25 % and is still considered the most important pest in sugar beet production worldwide (Cooke, 1987; Schlang, 1991). Depending on soil-type, the economic threshold of *H. schachtii* ranges from 500 - 1000 second stage juveniles (J2) and eggs 100 ml^{-1} soil (Müller, 1990; Cooke, 1993).

Symptoms: Occurrence and symptom development of *H. schachtii* infested sugar beet plants in the field is manifested as patches that expand slowly in the direction of mechanical cultivation (Petherbridge & Jones, 1944). The nematodes have limited mobility in the soil which limits natural spread (Jones, 1980; Avendano et al., 2004). Infested plants show stunted growth, decreased chlorophyll content in leaves and symptoms of wilt late in the growing season especially when the plants are exposed to heat and/or water stress conditions (Cooke, 1987; Schmitz et al., 2006). Belowground symptoms include the development of compensatory secondary roots that result in the typical "bearded" root symptom and an overall beet deformity (Decker, 1969; Cooke, 1987). When removed from the soil, white or brown citrus shaped females or cysts can be observed attached to the roots.

Life cycle: The BCN has a high rate of multiplication with between 200 - 500 eggs produced per female (Raski, 1950). After the first mould, J2 hatch from the eggs in the cysts and invade the plant roots (Börner, 1990). Juveniles penetrate the elongation zone behind the root tip (Moriarty, 1964) and also the beet (Decker, 1969). The J2 initiate the formation of giant cells (syncytium) in the roots (Bleve-Zachero & Zachero, 1987) which serve as nurse cells. The formation of the syncytium reduces intercellular and vascular transport of water and nutrients (Wyss, 1997). Females become sedentary in the third juvenile stage due to swelling and ultimately break through the outer root epidermis. Male adults leave the roots, fertilize the females and die. The mature females die after egg lying is completed and their body wall becomes the cyst which contains the eggs of the next generation. These cysts can remain

intact for five years in the soil. A generation is completed when the females develop eggs which contain J2 ready to hatch.

Influence of abiotic factors: According to the temperature sum-model of Čuri & Smoray (1966), *H. schachtii* required a total degree days of 437 °C for completion of one generation. Due to the lack of diapause, BCN can produce two or three generations per year in central Europe when favourable soil conditions and host plants are present (Duggan, 1959; Müller, 1990).

In addition to temperature, soil physics plays a role in the life cycle. Soil texture and moisture content as well as aeration influence nematode behaviour and population development (Nejad & Dern, 1979; Cooke, 1984). Heavy soils with small pore size and poor aeration reduce nematode activity (Wallace, 1955). Extremely low soil moisture levels can induce dormancy and complete drying is lethal to *H. schachtii* (Goffart, 1951).

Sampling: For long term successful sugar beet production and nematode management the spatial distribution and the density of BCN populations has to be determined before planting. The most commonly and currently used labour intensive sampling methods are based on a narrow sampling grid of the entire field and this gives reliable data on distribution in the field and pre-plant density of BCN. However, Evans et al. (2002) reported missing whole population clusters of potato cyst nematode when using a 20 m raster grid. Targeted sampling of nematode clusters after sugar beet harvest gives information on the density, but not the exact distribution of infection loci of BCN in a field. Sampling of the soil at the edge of fields, where the beets are temporarily stored is the cheapest method for quantification of BCN population densities, but gives no information on spatial distribution in that field. The decision to invest integrated pest management (IPM) to prevent yield losses in sugar beet requires knowledge of the initial nematode population prior to planting, because the main damage caused by BCN occurs early in the season when the tap root is damaged (Gierth, 2004).

Plant protection: Modern BCN management utilizes a combination of nematicides, tolerant and/or resistant cultivars, rotation with non-host crops and the incorporation of resistant green manure crops such as mustard and oil radish in the cropping program (Schlang, 1996).

3. *RHIZOCTONIA* CROWN AND ROOT ROT

The soil-borne multinucleate basidiomycete *Rhizoctonia solani* Kühn (teleomorph *Thanatephorus cucumeris* [Frank] Donk) is the most important *Rhizoctonia* species in the world. Species of *Rhizoctonia* infect over 500 plants, mainly in the families *Compositae*, *Gramineae*, *Leguminosae*, *Solanaceae* and *Cruziferae* (Ogoshi, 1996). Because of large variation in the behaviour of the fungus, it has often been considered a complex-species (Cubeta & Vigalys, 1997) and according to the hyphal fusion behaviour, fourteen anastomosis groups and 21 subgroups have been determined to date (Carling et al., 2002; Harikrishnan & Yang, 2004). Several anastomosis groups have been reported in sugar beet, such as AG 1, AG 2-1, AG 2-2, AG 3, AG 4 and AG 5 (Naito et al., 1976; Herr, 1996; Lees et al., 2002).

Damage: *Rhizoctonia* crown and root rot (RCRR) caused by *R. solani* AG 2-2IIIB (Zens et al., 2002) is one of the most important sugar beet diseases in the world and causes yield losses of up to 50 percent (Herr, 1996; Büttner et al., 2004). In the USA up to 24 % of the sugar beet cropping area is endangered by RCRR and in the EU 5 % of the sugar beet areas are infested (Harveson, 2008).

Symptoms: Occurrence of RCRR also manifest as patches in the field and are often not visible until late in the cropping season, around August and September. First symptoms include wilting, chlorosis and black constrictions on the petioles near the crown of the beet (Zens et al., 2002). Wilted leaves collapse, developing a rosette of necrotic leaves around the beet crown. Rotting typically progresses from the petioles to the crown and then down into the beet and lateral roots. Late in the season roots are often completely rotten and the surface of the beet is black, whereas the internal beet tissue is light to dark brown.

Life cycle: *Rhizoctonia solani* can survive for long period of time exceeding five years when growing saprophytically on crop residues (Herzog & Wartenberg, 1958) and as sclerotia or melanized mycelium in soil (Roberts & Herr, 1979; Hyakumachi & Ui, 1982). Ruppel (1991) reported a reduction in survival when AG 2-2 was buried deep in field soil. The most predominant occurrence however is in the upper five centimetres of soil (Ruppel, 1991). Richards (1921) reported that *R. solani* invaded the beet body near the petioles. Also Baker (1970) and Herr (1996) concurred that RCRR initiated invasion of the plant at the base of the leaf petioles above the ground surface. Penetration of *R. solani* into plant tissue is an active process that involves the production of enzymes such as cutinase, cellulose and pektinase. Infection can also be passive through wounds, stomata or lenticels (Baker & Bateman, 1978; Weinhold & Sinclair, 1996).

Influence of abiotic factors: Hyphal growth of *R. solani* starts at 15 °C and development reaches an optimum between 25-33 °C (Whitney & Duffus, 1986; Engelkes & Windels, 1994). High soil-humidity, soil compaction and soils with high organic matter content result in higher inoculum potential of *R. solani*, whereas dry or sandy soils are suboptimal for the development of the pathogen (Glenn & Sivasithamparam, 1990).

Sampling: Determination of spatial distribution and quantification of *R. solani* in a naturally infested field is time consuming, labour intense and therefore expensive. Sampling methods often used, are the soil pellet sampling method of Henis et al. (1978) or the soil fraction plating after Boosalis & Scharen (1959). Due to the patchy occurrence of *R. solani*, similar problems like for the BCN exist regarding determination of distribution and quantification. In addition, the detection and quantification of specific anastomosis groups of *R. solani*, in the present case AG 2-2, is even more difficult. The hyphal anastomosis test is the oldest method to determine the anastomosis group of a specific isolate. More recent techniques for detection are ELISA based (Thornton & Gilligan, 1999) and also real time PCR is often used for quantification (Ophel-Keller et al., 2008).

Plant protection: The control of RCRR is problematical due to the fact that fungicides for seed or soil treatment are not highly effective and/or not registered for use, e.g. in Europe

(Buhre et al., 2009). Management of *R. solani*, therefore, is primarily achieved with tolerant sugar beet cultivars.

4. INTERACTIONS BETWEEN NEMATODES AND FUNGAL PATHOGENS

While nematodes are quite capable of causing severe plant injury and reduction in crop production, they are often involved with other disease causing organisms occupying the same ecological niche. Such associations leading to more than additive damage are referred as "complex diseases", the name having been derived from the presence of two or more disease-causing organisms (Jenkins & Taylor, 1967). Concomitant occurrence is common in nature and the limitation of research to single pathogens is unrealistic since the soil contains an extensive flora and fauna of microorganisms which may cause plant diseases (Back et al., 2002).

Types of damage: Combinations of plant parasitic nematodes and soil-borne fungal pathogens frequently result in a loss that is more than additive such as the breaking of resistance or the production of symptoms differing from those usually produced by either organism alone. Damage is differentiated between synergistic, neutral and additive. The definition of synergistic damage is that "the magnitude of host response to concurrent pathogens exceeds the sum of the separate responses to each pathogen" (Shurtleff & Averre, 1997). Where nematodes and fungi are known to interact and cause plant damage that equates to the sum of individual damage, the association may be described as neutral. More difficult to identify are neutral associations that can result in similar plant damage to that seen in additive associations, where the nematode and the pathogen are not known to interact with each other (Barker & McGawley, 1998; Back et al., 2002).

Besides the different levels of damage, there needs to be a differentiation between direct and indirect interaction of the organisms within the disease complex. Indirect interactions are initiated by the changes that each organism causes to the plant on which both depend (Pitcher, 1978). Direct interactions imply that the nematode is a vector of the pathogen; the pathogen enters the plant through wounding caused by the nematode (Bergeson, 1972;

Barker & McGawley, 1998). Stress on the plant can also decrease plant resistance and cause increased damage.

Evaluation of disease complexes: Ever since Atkinson (1892) first observed that the severity of *Fusarium* wilt of cotton was enhanced in the presence of root-knot nematodes, vast numbers of studies have focused on the study of potential interrelationships between nematodes and associated organisms. Nevertheless, Sikora & Carter (1987) concluded that the literature on interactions between nematodes and other pathogens is often unclear. They questioned a number of published concepts and hypotheses as well as experimental designs and statistical analyses that indicated the existence of interactions. Therefore, Khan & Dasgupta (1993) suggested that a disease complex should be considered multi-causal only if its causal factors are both biologically and statistically established. Wallace (1983) recommended that a range of biotic parameters should be included in these types of studies and that multivariate statistical analyses should be used. Experimental designs for investigation of disease complexes often include; bridging, layering, or grafting of roots or stem tissues, and double-root or split-root techniques (Khan, 1993).

Rhizoctonia solani in disease complexes: Soil-borne disease complexes involving species of *Rhizoctonia* and nematodes have led to synergistic increases in damage. Reynolds & Hanson (1957) reported an increase of *Rhizoctonia* damping-off in cotton in the presence of *Meloidogyne incognita*. The cereal cyst nematode *Heterodera avenae* in complex with *R. solani* AG 8 led to additive damage to wheat plants in greenhouse trials (Meagher & Chambers, 1970), but no clear indications for interactions were found in field trials (Meagher et al., 1978). Stelter & Meinl (1967) and Back et al. (2006) demonstrated an increase in damage due to the interaction between potato cyst nematodes and *R. solani* on potato.

Field observations have indicated that higher levels of RCRR damage occur on sugar beets when BCN and RCRR are present simultaneously (Schlang, Daub & Sikora, personal communication). Whereas numerous reports have been published on interactions between soil-borne fungal pathogens and plant parasitic nematodes (Powell, 1971; Bergeson, 1972; Pitcher, 1978; Sikora & Carter, 1987; Taylor, 1990; Back et al., 2002), little to nothing is known about such complex interactions on sugar beet.

<u>Plant protection</u>: Management options for the control of a disease complex involving BCN and RCRR have not been investigated. Should the presence of RCRR in the plant influence resistance to BCN, yield would be drastically affected and standard management practices would need redesigning.

5. METHODS USED FOR DISEASE COMPLEX ANALYSIS

In the present investigations the existence of a BCN-RCRR disease complex on sugar beet was examined. One of the main objectives of the experiments was to develop a non-destructive technique of detection and analysis. Nuclear magnetic resonance imaging (NMRi) was used to visualize the effects of BCN and RCRR alone and in combination on belowground parts of the plant.

In addition to the soil and root imaging technique, leaf reflectance was monitored to detect effects of a disease complex on the sugar beet canopy. Furthermore, analysis of hyperspectral leaf reflectance was evaluated for discrimination and quantification of BCN and RCRR as opposed to labour intense rating and sampling.

5.1. Nuclear magnetic resonance imaging

Nuclear magnetic resonance imaging is primarily a non-invasive imaging technique used to visualize detailed internal structures. The main driving force for development of non-invasive methods has been the medical profession, but recently a number of such techniques have become applicable to plant science (Jahnke et al., 2009). Nuclear magnetic resonance (NMR) is a relatively new technology with the first image published by Lauterbur in 1973. By comparison the first human X-ray image was taken more than 100 years ago by Röntgen (1895).

NMRi provides much greater contrast between different tissues than X-ray based computer tomography does. This technique uses the phenomenon of nuclear magnetic resonance to image protons of water. Plants are largely composed of water molecules and each water molecule has two hydrogen protons. If plants enter the magnetic field of the scanner the

magnetic moments of the ^{1}H protons change, aligning with the direction of the field. The hydrogen nuclei start producing different rotating magnetic fields detectable by the scanner. When the magnetic fields are switched off, the protons return to their equilibrium. These physical principles allow construction of an image, because the protons in different tissues return to their equilibrium state at different rates. This is reflected in proton relaxation times (the rate at which ^{1}H nuclei return to equilibrium after excitation from an externally applied pulse). Image contrast in NMRi depends not only on water distribution within the tissue, but also on physiological functions explained by degrees of water binding. Like classical histopathology with light microscopy, varied strategies for image acquisition with NMRi can provide both detailed anatomical and functional information (MacFall et al., 1994). The information gained by NMRi can include *in vivo* distribution of metabolites, water flow in the vascular tissue and physical properties such as water diffusion and relaxation mechanisms in different cellular compartments (Köckenberger, 2001). Software programs allow formation of a three dimensional image with a spatial resolution of up to 30 μm^3 voxel^{-1} (pixel element of a 3D image) by stacking individual slices of tissue one on the top of the other. It is this advantage which is likely to be exploited more in future. Nuclear magnetic resonance imaging should be used in developmental plant science, particularly in breeding programmes to improve the resistance of commercially valuable crops to disease stress.

Reviewing the literature, over the last decade this method has received substantial attention with respect to plant studies (MacFall et al., 1994; Pearce et al., 1994) and has been used to measure 3D structures in plant and soil (Köckenberger et al., 2004). The opaqueness of soil makes the observation of root systems impossible by optical means. Model NMRi studies involving packed clay soil columns have indicated that two- and three-dimensional images of static and dynamic water phenomena can be obtained for soils, but only where the soil has a modest iron content and there is an adequate water content (Amin et al., 1994). However, publications of Bottomley et al. (1993) showed the suitability of NMRi to create three dimensional images of root geometry or water changes occurring in roots.

It may be possible to use NMRi to study issues of biotic interactions with roots, e.g. where nematodes such as *H. schachtii* change root structure, or rotting fungus like *R. solani* damage beet tissue (Jahnke et al., 2009). Pests and diseases of plants have been investigated using

NMRi technique. Fungal infection of plants or young trees was investigated at the stem level but not the root (MacFall et al., 1994; Pearce et al., 1994). Xylem blockage by the bacterium *Xylella fastidiosa* on grapes has also been investigated (Shackel et al., 2002). Only one study concerning nematodes was conducted to date in which the effect of *Bursaphelenchus xylophilus* infestation on Japanese black pine was investigated (Utsuzawa et al., 2005). Also the disease development of *Rhizoctonia solani* on sugar beet was investigated by NMRi, but no results were presented (Halloin et al., 1992).

5.2. Hyperspectral leaf reflectance

The use of hyperspectral leaf reflectance (HLR) for the detection of damage caused by plant parasitic nematodes and/or soil-borne pathogens for optimization of plant protection management is a "best-fit technology". There are a number of biological and technical factors that favour the use of reflectance recording sensors for these two pest groups: i) damage caused by root infections is visible in the foliage at different times in the growing season; ii) nematode and disease infestations are clustered in the field; iii) movement out of a cluster is slow due to low nematode and pathogen mobility; iv) introduction of new infection loci into a field are rare; v) precision detection used in one season can be applicable for future crops; and vi) chemical and biological control technologies are available that allow site-specific treatment. The use of this knowledge to develop site-specific plant health management can significantly reduce yield losses due to these two pest groups and can lead to a high cost/ benefit return for the grower.

Steddom et al. (2005) stated that remote sensing (RS) is the practice of gathering information on an object without touching it and that most such technologies measure different parts of electromagnetic radiation such as heat or light. Plants depend on radiant energy for conversion of solar energy into organic substances. The leaf can absorb light in the visible part (VIS) of the electromagnetic spectrum (400 - 700 nm), where the spectrum of reflectance is quiet low, with a peak at about 550 nm in the green region. In the near infrared (NIR) short-wave region (700 - 1400 nm) reflectance increases up to 50 percent, whereas in the long-wave (1400 - 2500 nm) reflectance decreases due to water absorbance. Leaves not only absorb and reflect light but light also is transmitted through the leaf.

Applications involving RS and HLR analysis are currently being refined and used for determination of plant stress causal agents and also spatial distributions of both plant pathogens (Laudien et al., 2004) and plant parasitic nematodes (Heath et al., 2000; Nutter et al., 2002) in crops. As noted by Back et al. (2002), a further development of this type of technology is likely to be invaluable for the prediction of disease complexes, and will be targeted in this work.

Disturbance or destruction of normal root functioning induced by soil-borne nematodes or pathogens decreases the content of water, chlorophyll, carotinoids and anthocyanin levels in the leaves, which simultaneously leads to shifts in reflectance of the electromagnetic spectrum. The use of reflectance in the visible NIR and NIR spectrum, therefore, can be effectively used to detect disease symptoms even before they are visible.

The first aerial images of damage caused by a soil-borne plant disease were made in the year 1927 when Taubenhaus et al. (1929) took pictures from an US Army airplane at an altitude of 75 to 150 m to detect symptom development of cotton root rot caused by *Phymatotrichum omnivorum*. The first use of infrared (IR) imagery for detection of plant parasitic nematodes was conducted in the early 1960´s by Norman & Fritz (1965) to detect the burrowing nematode *Radopholus similis* in citrus trees before visible symptom development. This work resulted in a reduction in sampling and the introduction of site-specific nematicide treatment. Gausman et al. (1975) used a spectroradiometer and detected differences in cotton leaf reflection levels in nematode infested compared to control plants. Plants with high populations of the reniform nematode *Rotylenchulus reniformis* showed lower leaf reflectance compared to the control plants at wavelengths of 500 to 2500 nm. Leaves of nematode parasitized plants were thinner and more compact in the inner cellular layers and, therefore, caused lower light reflection.

Using multispectral video imagery Cook et al. (1999) were able to discriminate between damage by the root-knot nematode *Meloidogyne incognita* and root rot due to *P. omnivorum* alone as well as in combination. This was the first attempt to detect symptoms of a disease complex by HLR.

Heath et al. (2000) conducted experiments to predict the number of *Globodera pallida* and *G. rostochiensis* parasitizing potato plants using non-destructive hyperspectral measurements. High correlations were found between the numbers of juveniles per gram of potato roots and the Normalized Difference Vegetation Index (NDVI) developed by Rouse et al. (1974).

Hyperspectral sensors offer contiguous band placement over a wide spectral range and are superior to multispectral sensors with fewer spectral bands (Schowengerdt, 1997). The development of narrowband hyperspectral sensors was an important development in RS due to the greater amount of data obtained. With the combination of GIS and RS technologies Nutter et al. (2002) were able to map the spatial distribution of soybean cyst nematode, *Heterodera glycines*, in soybean fields. Appropriate calibrations were made for different atmospheric conditions by collecting data at different times in the growing season simultaneously by satellite, aircraft and near-range sensors.

Lawrence et al. (2004) used aerial and handheld near-range hyperspectral sensors to detect *R. reniformis* in cotton for data analysis with the MATHLAB program in combination with self-organizing maps developed by Kohonen (1998), obtained a prediction accuracy that ranged between 83 and 97 percent. They suggested the need for research on the effects of different soil types and in scaling leaf level measurements into a commercially viable orbital or suborbital system to validate the robustness of this approach (Lawrence et al., 2007).

Hyperspectral data is highly adaptable to the identification of soil-borne pests and diseases because of the higher amount of data available as a result of the narrower bands. The identification of the most sensitive bands of hyperspectral data for a specific pest group seems promising. Rupe et al. (2005) for example, isolated four bands out of 300 which were most responsive to distributions of *H. glycines* in soybean fields. These bands were found in near-range reflectance by the Maximum R^2 procedure.

Band extraction was often used for development of spectral vegetation indices (SVIs). Correlations of SVIs with yield, nutrient supply or damage by pathogens were reported for greenhouse and field experiments (Yang & Everitt, 2002; Bajwa et al., 2010; Mahlein et al.,

2010). SVIs are some of the standard tools for analysis of leaf reflectance data in crop management, because they are correlated to plant health, vitality and biomass. As pigment content provides information on the physiological state of leaves, pigment-specific SVIs may be useful in detecting stresses specific caused by *H. schachtii* and/or *R. solani*.

Besides the self-organizing maps, R^2 procedures and SVIs, the Spectral Angle Mapper (SAM) is another analytical tool (Yang et al., 2008) that has been reported as useful for supervised classification method for a variety of hyperspectral remote and near-range sensing applications (Clark et al., 2005; Mundt et al., 2005; Qin et al., 2009). With the SAM method developed by Kruse et al. (1993) it should be possible to classify symptoms caused by soil-borne organisms.

5.3. Leaf reflectance for detection of symptoms caused by soil-borne organisms in sugar beet

The sugar beet crop is highly suited for HLR analysis because it is a complanate growing plant with a planophile leaf structure (Franke, 1997). Furthermore, there is a direct relationship between root development and plant vitality (Nowatzki et al., 2009).

Very few studies have been conducted on the use of RS for the detection of soil-borne pests in sugar beet. Symptoms caused by *Heterodera schachtii*, studied by Sanwald (1979) using IR aerial images, resulted in a lack of significant changes in spectrometric reflectance. Using high spatial resolution digital multispectral video, Hope et al. (1999) detected RCRR in sugar beet caused by *R. solani*. Their goal was to use reflectance data to determine the most valuable vegetation index for classification of sugar beet root rot. The NDVI was considered the best predictor of RCRR infestation and is the most commonly used vegetation index. Spatial and temporal distribution as well as the economic impact of *R. solani* on sugar beet using multi- and hyperspectral, airborne and near-range data were successfully used to differentiate infected areas within a field (Laudien et al., 2004). The integration of a multi-temporal knowledge based approach might increase detection of disease symptoms.

6. OBJECTIVE OF THE STUDY

The overall goal of the research presented here was to analyse the existence of a disease complex involving *H. schachtii* and *R. solani* on sugar beet under greenhouse and natural conditions. Specifically designed experiments were developed to detect and discriminate changes in the plant by non-destructive methods.

The main objectives were to:

i. test the influence of different levels of cultivar resistance and staggered inoculation time on the existence of a disease complex

ii. use nuclear magnetic resonance for non-destructive imaging of roots and damage

iii. discriminate symptoms of disease complex by analysis of hyperspectral leaf reflectance

iv. transfer non-destructive technology to field scale and analyse disease complex under natural conditions

CHAPTER 2: GENERAL MATERIALS AND METHODS

In this chapter general materials and methods are described, whereas specific techniques and procedures employed in individual experiments are described within the respective chapters.

1. *HETERODERA SCHACHTII*

1.1. Origin, culturing and inoculation

Heterodera schachtii was obtained from the institutes' stock cultures. Nematodes were multiplied on *Brassica napus* cultivar Akela (Feldsaaten Freudenberger, Krefeld, Germany) in greenhouse pots filled with sterilized sand. Cysts were extracted using a standard wet-screen decantation method and then transferred to Oostenbrink dishes filled with 5mM $ZnCl_2$-solution for seven days to stimulate J2 emergence (Oostenbrink, 1960). The J2 were collected in 25 µm size sieves (Retsch, Haan, Germany), counted under the microscope and used directly for inoculation. Nematodes were inoculated into cavities (4 cm deep) in the soil with a pipette tip near the base of the plant.

1.2. Determination after experiment

After termination of experiments, cysts were extracted by the wet-screen decantation technique with a sieve combination of 500 µm and 250 µm aperture (Ayoub, 1980). The cysts were separated from organic matter as described by Müller (1980a). Cysts and organic matter residues from the 250 µm sieve were transferred to a 500 ml centrifuge tube, which was then filled with 400 ml of saturated (ρ = 1.23 g ml^{-1}) $MgSO_4$ (Merck, Darmstadt, Germany) solution and 10-13 g kaolin (AKW Eduard Kick GmbH, Amberg, Germany). The tubes were then centrifuged at 3,000 rpm (1,864 g) for five minutes and the supernatant containing the cysts transferred to 15 ml homogenization tubes (B. Braun, Melsungen, Germany) in which they were crushed with a handheld glass tissue homogenizer. The number of eggs and J2 per plant was counted under a stereoscope with fortyfold

magnification in a 2 ml RAS-Counting slide. The counting slide had sloping sides consisting of a 2 mm high plastic ring clued on a plastic plate of 75 × 37 mm (Hooper et al., 2005).

For the experiments in chapter five and six, the number of eggs and juveniles of *H. schachtii* was determined after the following protocol; 100 ml soil-samples were taken with a soil core sampling tool (Oakfield Apparatus Inc., Oakfield, WI, USA) based on specific sample grids. Cysts of nematodes were extracted (modified after Müller, 1980a) from each sample in a pail, whose bottom was cut off and replaced by a 100 µm sieve (Retsch, Haan, Germany). Samples were sieved until cysts and soil particles larger than 100 µm remained. Separation of the cysts from other remnants followed the method of Müller (1980a) described above.

2. *RHIZOCTONIA SOLANI*

2.1. Origin, culturing and inoculation

Rhizoctonia solani (AG2-2 IIIB) which causes RCRR, obtained from the Plant Protection Service North Rhine-Westphalia was used in all experiments.

A sand-flour protocol developed by Zens et al. (2002) was used for inoculum production in chapters three and five. The substrate consisted of 50 g sand, 1.5 g wheat flour and 7 ml tap water that was mixed inside a 200 ml Erlenmeyer flask and then sealed with a cotton plug. This growth substrate was autoclaved at 121 °C for 50 min. After cooling, the flasks were inoculated with three 5 mm mycelia pieces taken from 14 day old cultures growing on Potato Dextrose Agar (PDA) plates (PDB, Becton, Dickinson and Company, Le Pont de Claix, France + Agar, AppliChem, Darmstadt, Germany). The flasks were then incubated at 24 °C in the dark for 14 days and were shaken every second day to optimize fungal growth.

The soil was inoculated with *R. solani* using the protocol of Zens et al. (2002). Plastic pots (Ø 13 cm) were half-filled with planting soil containing 300 g of sand and field soil (1:1 v/v). The root system of four week old sugar beet plants were partially embedded into the bottom soil layer and then the roots covered by adding an additional 300 g of planting soil that was previously inoculated with 1.5 g of the sand-flour *R. solani* inoculum.

Rhizoctonia solani inoculation of the Magnetic Resonance Imaging experiment in chapter four followed the protocol described by Berdugo (2009). Anastomosis group 2-2IIIB was taken from pure isolates, and after two weeks growth on petri dishes, four pieces of 7 mm diameter were transferred under sterile conditions to Erlenmeyer flasks, containing 250 ml of PDB medium (Potato Dextrose Broth, Becton Dickinson, Franklin Lakes, NY, USA). The medium was previously autoclaved at 121 °C for 20 minutes. Flasks were shaken moderately at 100 rpm on a shaker placed at 25 °C in the dark. After 15 days, mycelium was taken from the medium by sieving the content of the Erlenmeyer flask through a sterile 5 µm pore size filter-paper. The mycelium was dripped off and subsequently homogenized in a blender (Waring products, Torrington, CT, USA) in order to make a stock solution (2 mg of *R. solani* mycelium per 1 ml of tap water). Each plant was then inoculated with 3 ml of stock solution in a cavity beside the beet crown.

2.2. Determination during and after experiment

Severity of *R. solani* beet rot was estimated for each beet based on Zens et al. (2002) scale of: 0 = healthy, no symptoms to 6 = beet completely rotten, plant dead. Aboveground leaf symptoms of RCRR were rated according to the scheme of Zens et al. (2002) which classifies leaf symptoms as wilting, yellowing or necrosis on a scale from 0 = plant healthy, no symptoms on the petioles to 6 = plant dead, leaf brown and necrotic (Fig. 2.1).

0=healthy   1=first constrictions   2=plant   3=plant wilting   4=crown dark brown,   5=crown black,   6=plant dead
on petioles   wilting   leaf yellowing   leaf yellow   necrosis on leaf

Figure 2.1   Shoot symptoms of sugar beet caused by *Rhizoctonia* crown and root rot (Berdugo et al., 2010).

3. PLANT CULTIVARS, GROWTH CONDITIONS AND EVALUATION CRITERIA

In chapter three, sugar beet cultivars Alyssa (susceptible, KWS GmbH, Einbeck, Germany), Calida (moderately tolerant to RCRR, KWS GmbH, Einbeck, Germany) and Sanetta (BCN resistant, Syngenta Seeds, Kleve, Germany) were used. For experiments in chapter four and five, sugar beet cultivar Alyssa was used and for the field experiment in chapter six the cultivar Beretta (susceptible to BCN and RCRR, tolerant to rhizomania, KWS GmbH, Einbeck, Germany) was used. For experiments under controlled conditions seeds of all cultivars were sown in multipots of 4.8 × 50 × 28 cm size. The experiments were conducted at 25/20 °C (day/night), a relative humidity of 70 ± 10 % and a photoperiod of 12 h d^{-1} (> 300 µmol m^{-2}s^{-1}, Phillips SGR 140, Hamburg, Germany). Four weeks after sowing, the seedlings were transplanted into experimental specific containers and soils, described in the respective chapters. Plants were fertilized every two weeks with 50 ml of a 2 % NPK fertilizer (18 + 12 + 18, Flory® 3Mega, Euflor, Munich, Germany). At termination of experiments the variables leaf, beet and root fresh weight were determined.

4. SYNERGY FACTOR DETERMINATION

Based on a definition of synergism (Shurtleff & Averre, 1997) the Abbott formula (Abbott, 1925) was modified and calculated for plant fresh weights as the *Synergy Factor* $= \Delta 1(c - s)/\{\Delta 2(c - h) + \Delta 3(c - r)\}$, where $\Delta 1 =$ the difference between the control and the simultaneous treatment; $c =$ plant weight of the control treatment; $s =$ plant weight of the simultaneous treatment; $\Delta 2 =$ difference in weight between the control and the BCN treatment; $h =$ plant weight of the BCN treatment; $\Delta 3 =$ difference in weight between control and the RCRR treatment; $r =$ plant weight of the RCRR treatment. If the *Synergy Factor* was 1 then interactions were additive and when it was higher than 1 they were synergistic.

5. STATISTICAL ANALYSIS

The statistical program SPSS 17 was used for analysis of data in all experiments (SPSS Inc., Chicago, IL, USA). Plant fresh weights and root length were tested for homogeneity of

variance and one way analysis of variance (ANOVA) used to determine if differences exist among treatments. Subgroups were separated using the Tukey's test, at a probability level of $p < 0.05$ or $p < 0.01$. Plant weights were further analysed by multi-factorial multivariate analysis of variance (MANOVA) at a probability level of 0.01 with the factors *R. solani*, *H. schachtii* and *R. solani × H. schachtii*. MANOVA was used to test for statistical significance of the interaction between the organisms (Sikora & Carter, 1987).

Above- and belowground plant weights were tested for correlation at a probability level of 0.01 using the Pearson's correlation coefficient. Correlations between plant weights, RCRR aboveground disease severity rating, *R. solani* beet rot rating and vegetation indices were also calculated. The Pearson's correlation coefficient was used for metric data and the Spearman's rank correlation coefficient for ordinal scaled data.

The *R. solani* beet rot rating values and the number of eggs and J2 per plant were compared using the t-test ($p < 0.05$). The control and BCN treatments were excluded from the t-test for the *R. solani* beet rot rating, because no infection was present. The control and *R. solani* treatments were not included in the t-test on J2 and eggs, because no nematodes were present in these treatments.

CHAPTER 3: INFLUENCE OF DIFFERENT LEVELS OF CULTIVAR RESISTANCE AND STAGGERED INOCULATION TIME ON DISEASE COMPLEXITY

1. INTRODUCTION

Interactions between *H. schachtii* and *R. solani* on sugar beet were investigated by Polychronopoulos (1970). He demonstrated higher seedling mortality rates in infested soil with both organisms than in control treatments. This may be due to the fact that under favourable conditions many root rot fungi combined with even low level nematode infections cause drastically higher seedling loss (Jenkins & Taylor, 1967). However, at the time of the studies of Polychronopoulos (1970) tolerant or resistant sugar beet cultivars for BCN and RCRR management were not available. Also *R. solani* anastomosis groupings specific for RCRR or for damping-off were not yet identified. In micro plot experiments, Müller (1980b) observed synergistic damage to sugar beet plants by *H. schachtii* and fungi of the genus *Fusarium*, *Cylindrocarpon*, *Rhizoctonia*, *Pythium* and *Verticillium*. It was not possible to ascertain which soil-borne fungal pathogen caused the synergistic damage in combination with BCN. This was, however, the first study reporting the existence of an interaction on sugar beet plants older than eight weeks (Müller, 1980b).

An important factor in the epidemiology of *H. schachtii* and *R. solani* is plant age (Olthof, 1983; Berdugo, 2009). They demonstrated that younger plants were more susceptible to *H. schachtii* or *R. solani* than older plants due to a more vital root system and a thicker epidermis, respectively.

Direct interactions between RCRR of *R. solani* (AG 2-2) and *H. schachtii* are improbable, because of the use of different plant infection sites. Whereas the nematode penetrates through the lateral roots in the zone of elongation behind the root tip (Moriarty, 1964; Franklin, 1972; Cooke, 1993), RCRR initiates invasion at the leaf petioles aboveground (Baker, 1970; Herr, 1996).

Investigations on the existence of a complex disease interaction between these two organisms have been simplified because of the availability of BCN and RCRR resistant or tolerant sugar beet cultivars which allows targeted experimental designs to evaluate interrelationships. Should the presence of RCRR in the plant influence resistance to BCN, yield will be drastically affected and standard management practices would need redesigning.

Hyperspectral leaf reflectance was recorded to calculate the vegetation index NDVI. This index was then tested on suitability to discriminate symptoms caused by either organism alone or in combination by means of leaf reflectance.

The objectives of the experiments were to:

i. investigate additive or synergistic interactions between BCN and RCRR when present concomitantly and when inoculated sequentially
ii. test the reaction of susceptible, tolerant and resistant cultivars to the disease complex BCN and RCRR
iii. use hyperspectral leaf reflectance as a means of non-destructive detection of symptoms caused by either organism alone or in combination

2. MATERIALS AND METHODS

2.1. Pathogen inoculation and disease impact evaluation

Plants were sown in multipots as described in chapter two. Four weeks after sowing they were transplanted into plastic pots (13 cm Ø) containing a 1 : 1 mixture (v/v) of sand and field soil that was steam-sterilized at 121°C for 120 minutes one day before. Plants were fertilized every two weeks with 50 ml of a 2 % NPK fertiliser (18 + 12 + 18, Flory® 3Mega; Euflor, Munich, Germany).

Nematodes and *R. solani* sand-flour inoculum was given to the plants following the protocol described in chapter two.

2.1.1. Simultaneous inoculation

Two experiments were conducted to examine the effects of simultaneous inoculation of the two pathogens on disease development using: *H. schachtii* resistant, *R. solani* tolerant and a susceptible cultivar to both organisms. There were four treatments per cultivar: 1) non-treated control; 2) *H. schachtii*; 3) *R. solani*; 4) *H. schachtii* with *R. solani*. Each treatment consisted of 12 plants.

The experiments were terminated four weeks after inoculation. The beet and lateral roots were washed free from soil and cysts and the number of nematodes per plant was determined as described in chapter two.

Root, beet, and shoot fresh weights were determined for each plant. Lateral roots were removed from the beet with a scalpel and root length measured with a root scanner (AGFA Snapscan 1236s™, Mortsel, Belgium) and the software WinRhizo Pro (Version 2004, Regent Instruments Inc., Quebec, Canada).

Severity of *R. solani* beet rot was estimated for each beet based on Zens et al. (2002) as aboveground symptoms of RCRR were rated according to the scheme of Zens et al. (2002) based on Figure 2.1.

2.1.2. Sequential inoculation

Two experiments were designed to test the effect of sequential inoculation with *R. solani* followed by a delayed introduction of *H. schachtii* on disease development. The studies were conducted with the susceptible cultivar Alyssa and had similar treatments (1 - 4) used for simultaneous inoculation and another treatment in which *H. schachtii* was inoculated two weeks after *R. solani*.

The experiments were harvested five weeks after inoculation and the same evaluation criteria as in the simultaneous inoculation experiment were undertaken, except root length was not determined.

2.2. Hyperspectral data acquisition and analysis

2.2.1.   Simultaneous inoculation

Hyperspectral reflectance of the foliage was measured at 0, 5, 8, 12, 16, 19, 22, 25 and 29 days past inoculation using a handheld spectrometer with a foreoptic contact probe and a leaf-clip holder (ASD FieldSpec Pro spectrometer, Analytical Spectral Devices Inc., Boulder, CO, USA). The contact probe foreoptic had a 10 mm spot size and an integrated halogen bulb light source. The ASD FieldSpec had a measuring range of 400 - 1050 nm and a spectral resolution of 1.421 nm. Sample reflectance was obtained by inserting a leaf into the leaf-clip and comparing leaf reflectance to the reflectance of a dark current as a minimum value and to the reflectance of the white standard (Spectralon Reflectance Standards, Labsphere, North Sutton, NH, USA). Spectra of 12 plants per treatment were recorded and each measurement was the average of ten scans. The measurements were always made on the same leaves of similar age.

2.2.2.   Sequential inoculation

RCRR aboveground disease severity rating and leaf reflectance were measured at 3, 7, 14, 21, 28 and 35 days after transplanting.

Hyperspectral data were exported as ASCII file using the software ASD ViewSpecPro (Analytical Spectral Devices Inc., Boulder, CO, USA) and then transferred to MS Office Excel where the Normalized Differentiated Vegetation Index (NDVI) was calculated. NDVI was developed by Rouse et al. (1974) to detect vegetation changes by comparing the reflectance of the strong light absorbing red region (RED) and the low light absorbing near infrared region (NIR) of plants, where RED was in the 620-640 nm band and NIR in the 740-760 nm band. $NDVI = \frac{(NIR-RED)}{(NIR+RED)}$ was calculated for all treatments from the spectral signatures recorded and is displayed in the results in a time series.

2.3. Statistical analysis

The ANOVA and MANOVA analysis were used as described in chapter two. The *R. solani* beet rot rating and the number of eggs and J2 per plant were compared using the t-test in the simultaneous inoculation experiment. In the sequential inoculation experiment the *R. solani* beet rot rating values and the number of eggs and J2 of *H. schachtii* per plant were compared using Tukey's test among the inoculated treatments respectively, with a probability level test of *p* < 0.05.

3. RESULTS

3.1. Simultaneous inoculation

Significant interactions between RCRR and BCN were detected in the three cultivars with different levels of resistance and tolerance to the two disease organisms.

Table 3.1 **The effects of disease complex of *Heterodera schachtii* and *Rhizoctonia solani* on fresh weight of leaf, root and beet and root length of three different sugar beet cultivars 29 days past inoculation.**

Cultivar	Treatment	Leaf [g]	Root [g]	Beet [g]	Root length [cm]
Alyssa Susceptible	Control	26.6±0.6a	6.6±0.4b	14.9±1.1a	2749±71 a
	Heterodera schachtii	27.7±1.1a	8.7±0.4a	12.0±1.2a	2510±84 a
	Rhizoctonia solani	11.4±3.3b	5.2±0.9b	6.7±1.8b	587±341b
	H. schachtii + R. solani	0.4±0.1c	0.4±0.1c	0.6±0.1c	15±3 b
Calida RCRR tolerant	Control	23.2±0.6a	8.2±0.3a	16.1±0.6a	3666±112a
	Heterodera schachtii	26.3±0.8a	9.4±0.5a	15.4±0.5a	3704±102a
	Rhizoctonia solani	7.2±2.5b	4.7±1.1b	3.5±0.9b	1117±419b
	H. schachtii + R. solani	4.6±2.6b	1.1±0.4c	2.7±2.0b	522±294b
Sanetta BCN resistant	Control	23.6±0.1bc	7.0±0.3a	13.4±0.8bc	3502±81 a
	Heterodera schachtii	24.5±0.9ab	7.7±0.5a	13.8±1.1ab	2749±132ab
	Rhizoctonia solani	8.8±3.3d	2.7±1.1b	5.8±2.4d	626±332c
	H. schachtii + R. solani	14.8±3.1cd	6.0±1.3ab	7.4±1.9cd	1908±526b

Displayed are the means±standard errors of each treatment. Different letters within each cultivar indicate significant difference after Tukey's test (*p* < 0.05; *n* = 12).

3.1.1. Susceptible cultivar: effect on root system and shoot weight

The strongest indications for the presence of an interaction between BCN and RCRR were detected on the susceptible cultivar Alyssa. Significant differences in plant fresh weight were observed among treatments (Tab. 3.1). There was a reduction in fresh leaf, beet and lateral root weight in the treatment with concomitant inoculation of *H. schachtii* and *R. solani* when compared to all other treatments (Tab. 3.1). The reduction in plant growth due to the interaction resulted a synergy factor higher than 1 (Tab. 3.2).

Table 3.2　**Influence of disease complex and plant resistance or tolerance on synergy factor of leaf, root and beet fresh weight and root length 29 days past inoculation.**

Cultivar	Plant variable	Synergistic effect	Synergy Factor
	Leaf weight	Yes	1.9
Alyssa	Root weight	Yes	1.8
Susceptible	Beet weight	Yes	1.3
	Root length	Yes	1.1
	Leaf weight	Yes	1.4
Calida	Root weight	Yes	1.5
RCRR tolerant	Beet weight	Additive	1.0
	Root length	Yes	1.3
	Leaf weight	No	0.6
Sanetta	Root weight	No	0.3
BCN resistant	Beet weight	No	0.8
	Root length	No	0.4

Furthermore, a statistical interaction was observed between the nematode and the fungus for the leaf and root weight (F = 11.71, df = 3, $p < 0.01$ and F = 37.78, df = 3, $p < 0.01$), respectively. A high correlation (r = 0.92, $p < 0.01$) was found between leaf weight and both, beet and lateral root weight which demonstrated a strong relationship between what is happening belowground with negative effects in the shoot of the sugar beet plants. Root rot severity was significantly higher in the concomitant treatments than when *R. solani* was present alone (Tab. 3.3).

Table 3.3   Influence of disease complex of *Heterodera schachtii* and *Rhizoctonia solani* on *R. solani* beet rot rating of different susceptible sugar beet cultivars 29 days past inoculation.

Cultivar	Treatment	*R. solani* beet rot rating
Alyssa	*Rhizoctonia solani*	5.5±0.4b
Susceptible	*H. schachtii + R. solani*	6.0±0.0a
Calida	*Rhizoctonia solani*	5.3±0.4a
RCRR tolerant	*H. schachtii + R. solani*	5.5±0.5a
Sanetta	*Rhizoctonia solani*	4.6±0.6a
BCN resistant	*H. schachtii + R. solani*	3.0±0.8a

Displayed are the means±standard errors of each *R. solani* inoculated treatment. Different letters within each cultivar indicate significant difference after Tukey's test ($p < 0.05$; $n = 12$).

The number of BCN eggs and J2 per plant was significant lower in the disease complex when compared to *H. schachtii* present alone (Tab. 3.4).

Table 3.4   Influence of disease complex of *Heterodera schachtii* and *Rhizoctonia solani* on the number of eggs and juveniles stage two per plant of three different susceptible cultivars 29 days past inoculation.

Cultivar	Treatment	J2/plant
Alyssa	*Heterodera* infested	6120±1041a
Susceptible	*H. schachtii + R. solani*	342±51 b
Calida	*Heterodera* infested	3560±571 a
RCRR tolerant	*H. schachtii + R. solani*	482±116 b
Sanetta	*Heterodera* infested	69±19 a
BCN resistant	*H. schachtii + R. solani*	48±9 b

Displayed are the means±standard errors of each treatment. Different letters within each cultivar indicate significant difference after Tukey's test ($p < 0.05$; $n = 12$).

3.1.2.   Susceptible cultivar: near-range sensing of crop status

The RCRR aboveground leaf symptom rating registered higher disease severity that developed at a faster rate in the concomitant verses *R. solani* treatment (Fig. 3.1A). The RCRR aboveground rating was correlated with leaf weight ($r = 0.91$, $p < 0.01$); and beet weights ($r = 0.85$, $p < 0.01$) and with *R. solani* beet rot rating ($r = 0.97$, $p < 0.01$). Plants inoculated concomitantly with *R. solani* and *H. schachtii* expressed damage through distinct leaf yellowing and black constrictions on the petioles near the beet 5 days past inoculation (dpi). Most leaves were necrotic 12 days later in the dual inoculations (Fig. 3.1A).

The NDVI values obtained were correlated ($r = -0.85$, $p < 0.01$) with the RCRR aboveground leaf symptom rating. The concomitant treatments induced lower NDVI beginning 5 dpi when

compared to all other treatments. The *R. solani* inoculated plants also had lower NDVI values beginning 5 dpi when compared to the control plants and those inoculated only with *H. schachtii*, the latter did not alter plant vitality over the duration of the experiment (Fig. 3.2A).

3.1.3. RCRR tolerant cultivar: effect on root system and shoot weight

Leaf and beet fresh weight and root length of the tolerant cultivar Calida were not affected by the *R. solani* verses the concomitant inoculations of *H. schachtii* with *R. solani*. Only fresh root weight of the concomitant treated plants was significantly lower than the other treatments (Tab. 3.1). However, the synergy factors for leaf and root weights and the root length were higher than 1, demonstrating a synergistic interaction between *H. schachtii* and *R. solani* (Tab. 3.2). An interaction (F = 14.29, df = 3, p < 0.01) was demonstrated between BCN and RCRR with regards to root weight. In addition, a significant correlation was detected of leaf with beet and root weight (r = 0.92, p < 0.01) in the tolerant cultivar. Inoculation of both pathogens resulted in similar levels of RCRR beet rot to that obtained with *R. solani* alone (Tab. 3.3). The number of eggs and J2 per plant was significantly lower in concomitant inoculation treatment compared to BCN alone (Tab. 3.4).

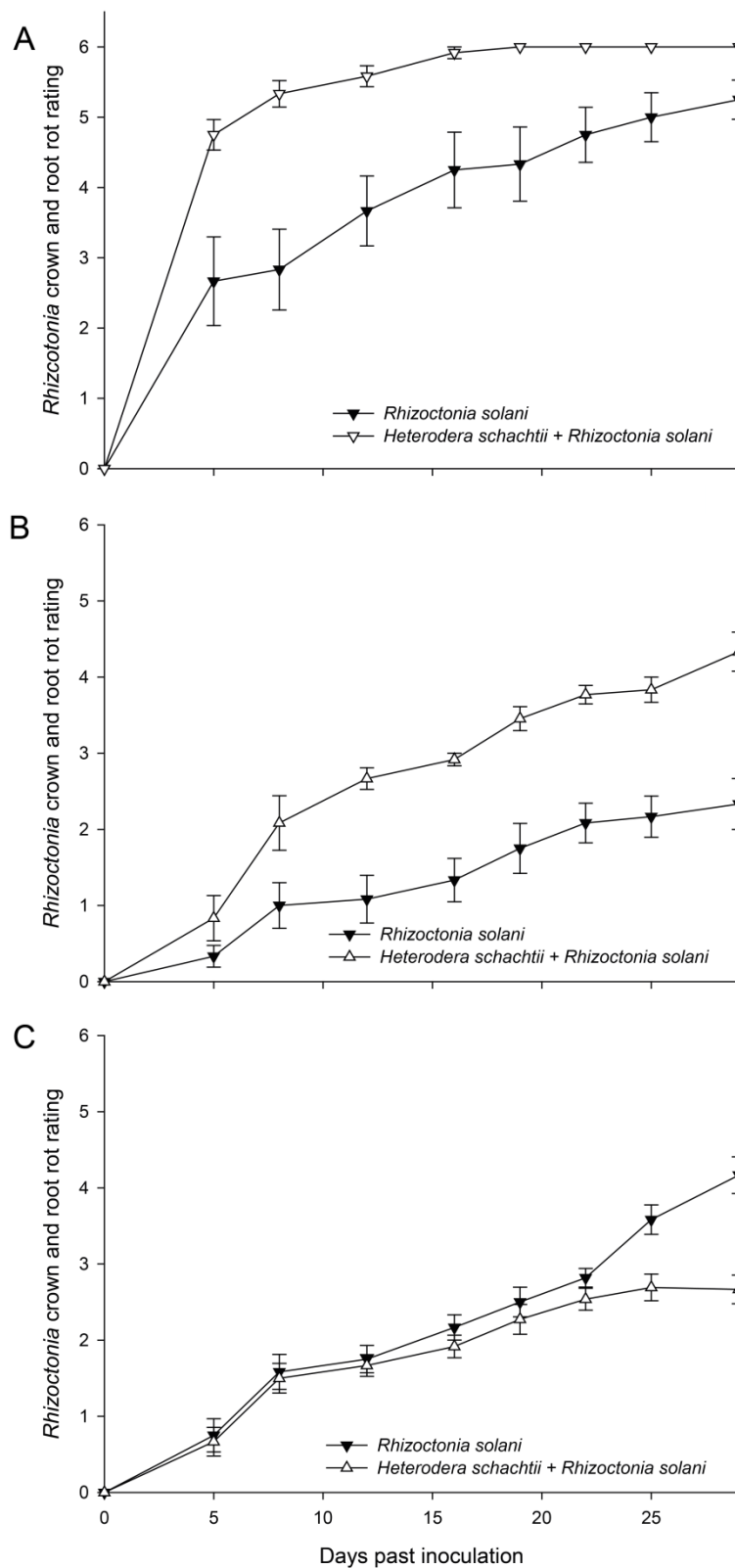**Figure 3.1** *Rhizoctonia* **crown rot and root rot rating of foliar leaf tissue of sugar beet cultivar susceptible Alyssa (A),** *Rhizoctonia* **crown and root rot tolerant Calida (B) and beet cyst nematode resistant Sanetta (C) in a time series of 29 days past inoculation. Plants were inoculated synced with** *Heterodera schachtii* **and** *Rhizoctonia solani.* **Bars indicate standard error of the mean (n = 12).**

3.1.4.   RCRR tolerant cultivar: near-range sensing of crop status

The aboveground RCRR leaf symptom ratings (Fig. 3.1B) were correlated with severity of *R. solani* beet rot (*r* = 0.94, *p* < 0.01). This correlation was supported by NDVI values calculated in a time series over 29 days past inoculation (*r* = -0.87, *p* < 0.01, Fig. 3.2B). The NDVI of *R. solani* alone compared to the simultaneous inoculations decreased beginning 5 dpi and was lower than that of BCN or the controls. The NDVI of the disease complex was significantly lower than the *R. solani* treated plants 22 and 25 dpi (Fig. 3.2B).

3.1.5.   *Heterodera schachtii* resistant cultivar: effect on root system and shoot weight

Plant fresh weight and root length were higher in all treatments conducted with the BCN resistant cultivar when compared to the *R. solani* treatment. Higher fresh weights were measured in the simultaneous treatments when compared to *R. solani* inoculated alone (Tab. 3.1). Synergism in the combined treatment was not detected as the synergy factor was below 1 (Tab. 3.2). The results, furthermore, demonstrated that there was no statistically based interaction between BCN and RCRR. However, leaf weights were highly correlated with the beet weights (*r* = 0.84, *p* < 0.01). In addition, *R. solani* beet rot was negatively correlated with the leaf weights (*r* = -0.75, *p* < 0.01). There were no significant differences in RCRR beet rot when the single and the combined inoculations were compared (Tab 3.3). The number of J2 and eggs produced by BCN decreased in the concomitant treatments when compared to BCN inoculated alone (Tab. 3.4).
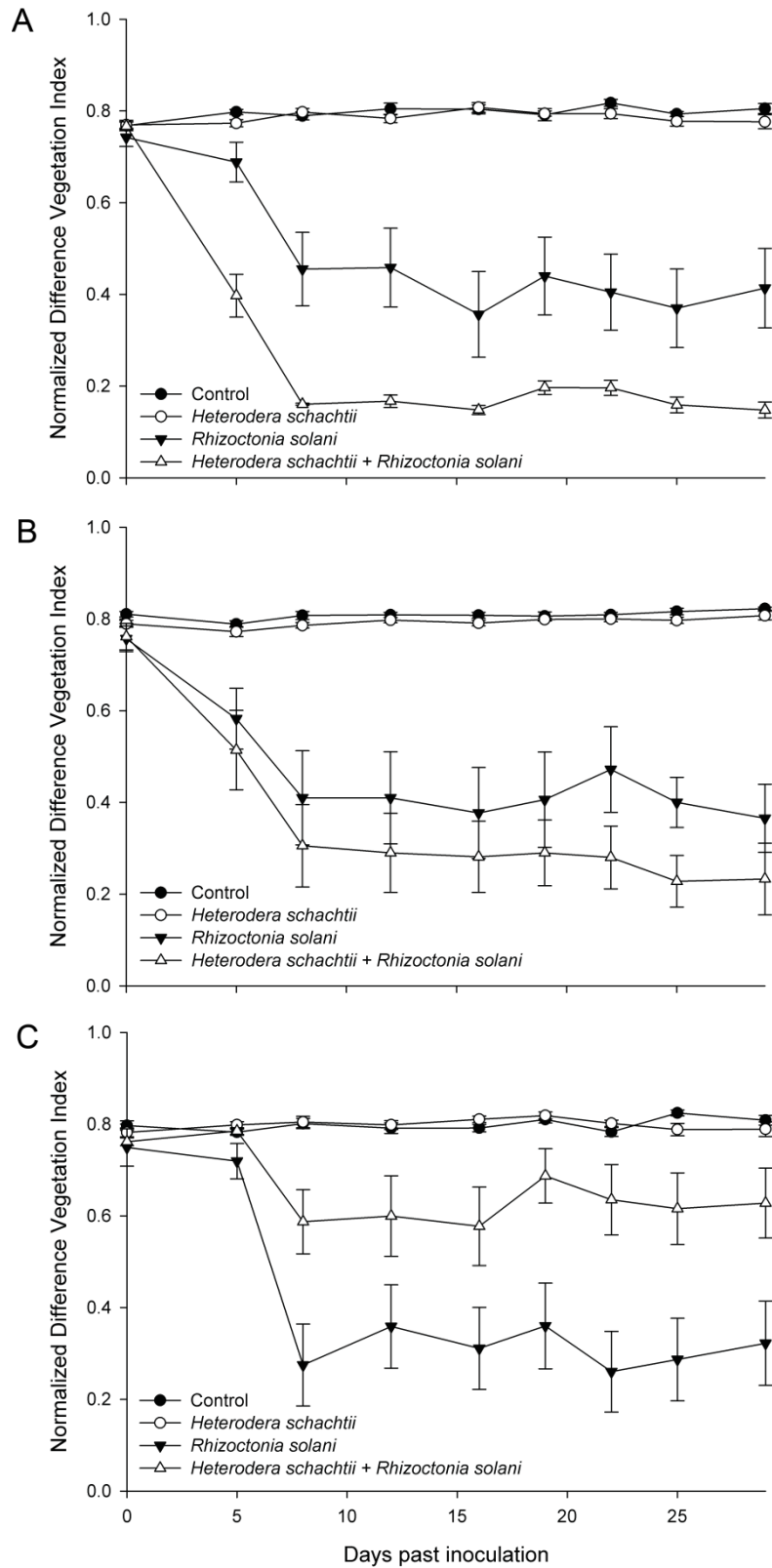
Figure 3.2   Effect of *Heterodera schachtii*, *Rhizoctonia solani* and their combination on NDVI values in a time series of 29 days past inoculation for cultivars Alyssa (A), Calida (B) and Sanetta (C). Bars represent standard error of the means (n = 12).

3.1.6.   *Heterodera schachtii* resistant cultivar: near-range sensing of crop status

Differences in the NDVI data between the treatments were obtained beginning 5 dpi (Fig. 3.2C). Plants inoculated with *R. solani* alone had significantly lower values from 5 to 29 dpi. Conversely, the concomitant treatments started to show a significantly lower NDVI values at 8 dpi. The RCRR leaf symptom rating (Fig. 3.1C) and the NDVI were correlated (r = -0.71, p < 0.01).

3.2. Sequential inoculation

A synergistic interaction was also detected in these experiments and demonstrated the importance of plant age on disease development.

3.2.1.   Plant and pathogen evaluation

Pre-inoculation with *R. solani* followed by the delayed introduction of BCN lead to significant reductions in beet fresh weight compared to the control. Root and leaf weights were not affected when compared to the control (Tab. 3.5). *Rhizoctonia solani* beet rot severity was also not significantly affected by sequential treatment over the individual treatments or the control. The presence of *R. solani* had a negative influence on the number of eggs and J2 per plant (Tab. 3.6). The results were similar to those obtained in the first experiment where the organisms were introduced simultaneously.

Table 3.5   **Effects of simultaneous and sequential inoculations of *Heterodera schachtii* and/or *Rhizoctonia solani* on plant fresh weights of susceptible cultivar Alyssa 35 days past inoculation.**

Treatment	Leaf [g]	Root [g]	Beet [g]
Control	16.7±1.5ab	7.2±0.6a	30.8±1.9a
Heterodera schachtii	17.2±1.0a	7.4±0.3a	19.6±1.6b
Rhizoctonia solani	8.0±1.7c	6.0±1.0ab	13.1±2.7bc
H. schachtii + *R. solani*	7.0±1.9c	3.0±0.8b	8.7±3.0 c
H. schachtii late + *R. solani*	10.0±2.1bc	5.1±1.1ab	15.0±3.6bc

Displayed are the means±standard errors of each treatment. Different letters within each column indicate significant difference after Tukey's test (p < 0.05; n = 12).

Table 3.6 **Effects of simultaneous and sequential inoculations of *Heterodera schachtii* and/or *Rhizoctonia solani* on number of eggs and juveniles stage two per plant of susceptible cultivar Alyssa 35 days past inoculation.**

Treatment	J2 plant^{-1}
Heterodera infested	2239±241a
H. schachtii + R. solani	817±272b
H. schachtii late *+ R. solani*	662±229b

Displayed are the means±standard errors of each treatment. Different letters within each column indicate significant difference after Tukey's test ($p < 0.05$; $n = 12$).

3.2.2. Near-range sensing of crop status

There was a correlation between the RCRR leaf symptom ratings (Fig. 3.3) and the NDVI data (Fig. 3.4) ($r = -0.61$, $p < 0.01$). The vegetation index demonstrated that plants inoculated concomitantly were affected most by the disease interaction. The NDVI values between 3 and 35 dpi of the concomitant treatments were the lowest and demonstrated a decrease in plant vitality (Fig. 3.4). Beet cyst nematode plants treated 14 dpi were not affected, because the disease complex had less time to develop and the plants were older than those for the simultaneous treatment.
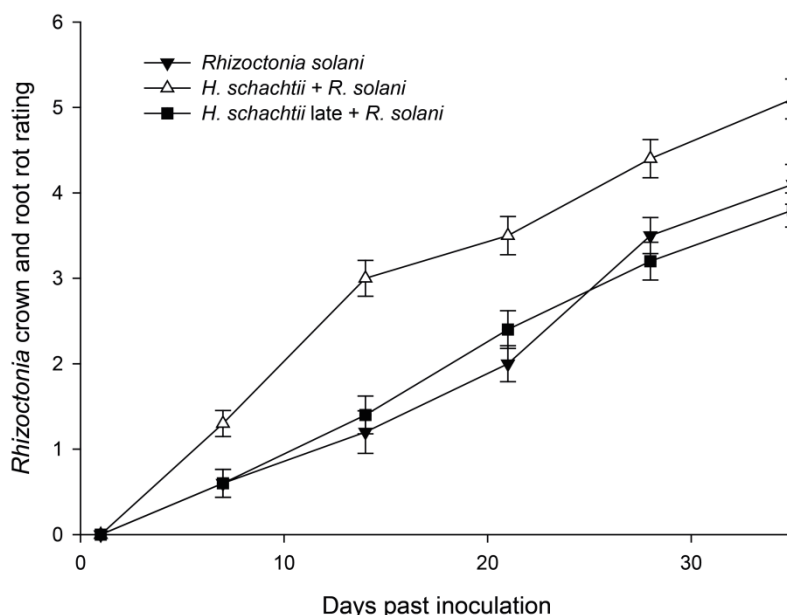

Figure 3.3 ***Rhizoctonia* crown rot and root rot rating of foliar leaf tissue of sugar beets cultivar Alyssa in a time series of 35 days past inoculation. Plants were inoculated simultaneous or sequential with *Heterodera schachtii* and *Rhizoctonia solani*. Bars represent standard error of the means (n = 12).**
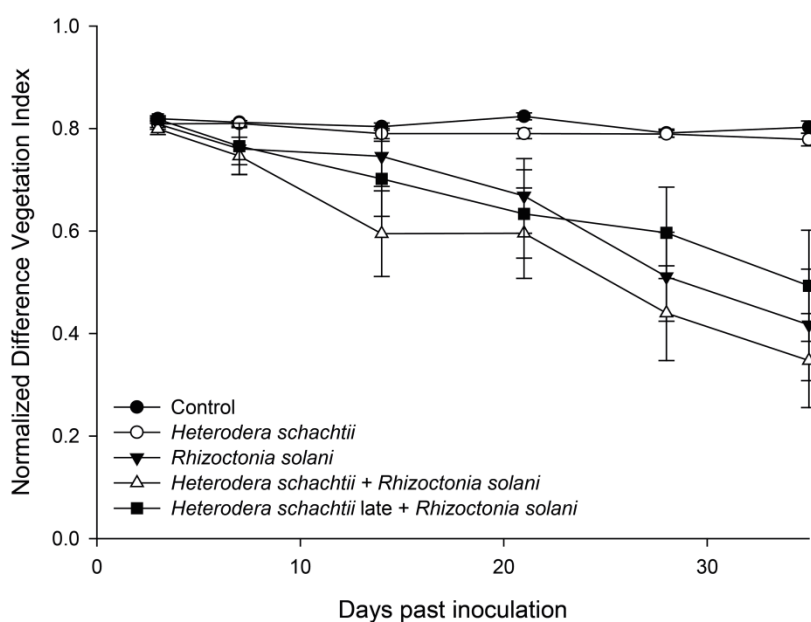
Figure 3.4 **Effect of *Heterodera schachtii*, *Rhizoctonia solani* and their sequential combination on NDVI values of sugar beet cultivar Alyssa in a time series of 35 days past inoculation. Bars represent standard error of the means (n = 12).**

4. DISCUSSION

4.1. Plant and pathogen

A statistically based synergistic interaction between BCN and RCRR caused by AG2-2 was detected for the first time on sugar beet cultivars that were susceptible, resistant or tolerant to one of the two disease agents. The results contrast those obtained earlier in a study by Polychronopoulos (1970) who demonstrated high levels of mortality in young sugar beet seedling inoculated with *H. schachtii* and *R. solani* at sowing. The mortality detected in the latter investigations indicates that the test was conducted with the AG 4 which causes damping-off and not crown and root rot (Herr, 1996). At the time of their work the use of anastomosis grouping was not yet developed. In the present studies the concomitant treatments with *R. solani* AG2-2 did not cause plant mortality at seedling stage. The results demonstrate that complex interactions can vary greatly with the virulence of the pathogen present in the field.

Root, beet and shoot growth of the susceptible cultivar Alyssa were synergistically reduced compared to the treatments with *H. schachtii* and *R. solani* alone or the control. The magnitude of plant damage in the concomitant treatments exceeded the sum of the growth responses caused by each pathogen alone. A statistically based multifactorial interaction was found for leaf and root weights in the concomitant treatments than when the pathogen was treated alone. The use of statistical and mathematical interaction analysis (Khan & Dasgupta, 1993) underscored the found synergistic interaction.

The cultivar Calida is moderately tolerant to RCRR (Rheinischer Rübenbauer Verband, 2008) and developed clear aboveground symptoms of RCRR in the concomitant treatments as well as with *R. solani* alone. A synergistic interaction was detected for shoot and root weight as well as for root length. Back et al. (2006) reported that the severity of *R. solani* infection increased with increasing population densities of *G. rostochiensis*. Tolerance, therefore, may completely break down in a tolerant sugar beet variety if inoculum densities are high. Sugar beet has minimum of two resistance genes (Hecker & Ruppel, 1975) and Lein et al. (2008) showed quantitative trait loci on three sugar beet chromosomes responsible for RCRR resistance and tolerance. Due to the polygenic nature of RCRR tolerance, phenological changes of sugar beet may have a strong influence on the characteristics of tolerance or resistance.

Synergistic interactions were not detected on the nematode resistant cultivar Sanetta. Plants inoculated concomitantly with *H. schachtii* and *R. solani* were less damaged by RCRR than sugar beet inoculated with *R. solani* alone. The juveniles of BCN can penetrate resistant plant roots thereby causing initial root damage. However, they cannot build syncytia and their life cycle is terminated (Cai et al., 1997). Plant defence mechanisms that affect nematode penetration, such as expression of an amino acid protein or a putative membrane stretch segment (Cai et al., 1997), also may retard the development of *R. solani* in the plant. *Rhizoctonia solani* alone did not activate resistance mechanisms in this cultivar, which was probably the reason for better development than in the combined inoculation with *H. schachtii* and *R. solani*.

The existence of a wound-based interaction between *R. solani* (AG 2-2) and *H. schachtii* under field conditions is questionable, because the two organisms infect the plant at different sites and times. *Heterodera schachtii* penetrates lateral roots behind the root tip, whereas, *R. solani* penetrates in the upper region of the beet body at the base of the petioles (Moriarty, 1964; Baker, 1970; Cooke, 1987; Herr, 1996). The results of the present experiments on sequential inoculation clearly demonstrated that young plants are initially damaged by RCRR regardless of whether the organisms are treated singly or staggered over time. However, the concomitant inoculation caused significantly higher levels of damage to the young plants, due to the fact that the root system was poorly developed and more susceptible to both organisms (Olthof, 1983; Berdugo, 2009). *Heterodera schachtii* final densities were lower when inoculated 14 dpi, which was probably related to initial RCRR damage and a poor food source for nematode development (Back et al., 2006).

4.2. Near-range sensing of crop status

The RCRR leaf symptom rating assessed the typical symptoms of yellowing, wilting and necrosis of leaves resulting from modifications in chlorophyll, carotenoid and water content of leaves. The significant differences between treatments obtained with NDVI confirmed its suitability as an indicator for disease development. NDVI was strongly correlated with the aboveground RCRR leaf symptom rating. The fact that NDVI and aboveground RCRR leaf symptom ratings were always correlated, as the aboveground RCRR rating with the *R. solani* beet rot rating, the suitability of sensors for assessing disease severity in the greenhouse and field was demonstrated (Hillnhütter & Mahlein, 2008). Heath et al. (2000) reported correlations between the number of juveniles of potato cyst nematodes in the roots of potato and NDVI of leaf reflectance measurements. In the present study it was not possible to discriminate between *H. schachtii* damage over the non-inoculated controls. Discrimination might be possible when: higher initial inoculum densities are used, in older beets when multiple generations have developed or under water and heat stress growing conditions when damage is greater.

5. CONCLUSIONS

The concomitant treatment of *H. schachtii* and *R. solani* caused synergistic levels of damage on the susceptible sugar beet cultivar. Shoot and root development of RCRR tolerant cultivar was also impacted synergistically in the concomitant treatments, but damage was less severe. On the BCN resistant cultivar the disease complex caused no synergistic damage and less than *R. solani* alone. Therefore, *H. schachtii* resistance in a cultivar is important for reduction of *R. solani* damage on sugar beet when the two organisms occur simultaneously in a field. The results clearly demonstrated that hyperspectral leaf reflectance can be used to quantify sugar beet cultivar resistance and to assess the RCRR disease development over time in a non-destructive manner. The use of hyperspectral leaf reflectance data could, therefore, be a cost effective and precise instrument for screening breeding lines for resistance or tolerance to RCRR.

CHAPTER 4: NUCLEAR MAGNETIC RESONANCE FOR NON-DESTRUCTIVE IMAGING OF ROOTS AND DAMAGE CAUSED BY DISEASE COMPLEX

1. INTRODUCTION

Belowground symptoms caused by *Heterodera schachtii* often include the development of compensatory secondary roots that result in the typical "bearded" root symptom as well as overall beet deformity and forking of the tuber can be seen following destructive removal of entire root systems from soil (Decker, 1969; Cooke, 1987). In addition, white to brown citrus shaped fourth stage juveniles, young females or cysts (Ø 2 mm) can be observed attached to the root surface. Brown decay or dry rot of the tissue is visible on the belowground beet and roots when the sugar beet is infected with RCRR caused by *Rhizoctonia solani* AG 2-2IIIB (Baker, 1970). Rotting beet tissue as well as deformation of the beet and development of compensatory roots change plant metabolism, which affects sugar and water content of the storage organ (Cooke, 1987; Bloch & Hoffmann, 2005).

The presence of *H. schachtii* is thought to support *R. solani* infection due to damage caused by the juvenile penetration and destruction of inter- and intra-cellular vascular tissue (Bergeson, 1972; Wyss, 1992). Furthermore, syncytia developed by nematodes are energy rich cell clusters which were reported as nutrient sources for *R. solani* (Back et al., 2006). Polychronopoulos et al. (1969) reported synergistic damage and direct interactions among *H. schachtii* and *R. solani* on young sugar beet seedlings. He used light microscope images to show the fungus colonizing penetration wounds made by the nematode. Their single experiment was conducted under sterile laboratory conditions in the absence of soil in petri dishes. Exposure of the roots growing on petri dishes to artificial light is known to cause shifts in phytohormones that can cause major changes to the plant tissue when growing under soilless conditions (Eliasson & Bollmark, 1988; Hummel et al., 2009). In the previous chapter synergistic damage of the disease complex of *H. schachtii* and *R. solani* to plants was demonstrated under greenhouse conditions in soil. Wound based stimulation of RCRR infection also is questionable due to different sites of infection of the two organisms

(chapter three). Thus, it remained unclear whether a direct or indirect interaction occurs between the two pathogens when the plant is growing in a natural soil environment.

Traditionally, destructive methods are used to extract tubers and roots from soil samples to construe plant pathogen interactions. Quantitative data are gained from weighing, counting or scanning and from parameters such as root weight, number of cysts, root length or percent surface rot (Nagel et al., 2009). Destructive methods often lead to loss of sensitive parts of the plants which then cannot be evaluated in more detail thereafter. Therefore, in this chapter non-invasive NMR imaging was tested to improve elucidation of plant-pathogen interrelationships. Information that is available on the use of NMRi techniques includes *in vivo* distribution of water flow in vascular conduits. Image contrast in this system can be highlighted to show water-binding, -distribution, -diffusion, and -transport patterns (MacFall et al., 1994; Köckenberger, 2001; Gossuin et al., 2010). Recently, high resolution NMR imaging (< 100 µm) for detailed and non-destructive examination of plant tissues has become available. Three dimensional images can be generated with a spatial resolution of up to 30 μm^3 per image pixel (Utsuzawa et al., 2005).

Jahnke et al. (2009) discussed the possibility of studying biotic interactions of roots of sugar beet, especially where nematodes or other soil-borne pathogens change the root structure. With a spatial resolution of 30 μm^3 it should be possible not only to detect changes in root geometry, but also visualize cysts or mature females and syncytia of *H. schachtii*. Detection of differences in water content of RCRR infested or healthy plant parts as belowground disease symptoms might also be possible to visualize with NMRi. Halloin et al. (1992) observed root rot caused by *R. solani* on sugar beet in a time series using NMRi, but the authors showed no results.

The objective of the experiment was to examine the potential use of NMRi for detection of biotic changes in sugar beet plants due to pathogen influence with special reference to the following aspects:

i.   define locus of penetration of *R. solani* and *H. schachtii*

ii.   investigate changes of root geometry due to BCN presence

iii.   visualize rotting symptoms caused by RCRR

iv.   detect cysts and syncytia on or in the roots

2. MATERIALS AND METHODS

2.1. Plant and pathogen evaluation

Seeds of sugar beet, cultivar Alyssa susceptible to *H. schachtii* and *R. solani* (KWS GmbH, Einbeck, Germany) were sown in Polyvinyl chloride (PVC) tubes with 54 mm inner diameter and 160 mm in depth. These tubes were specially modified with cables and loops to place them vertically into the NMRi system. Substrate in the tubes contained a 1:1 (v/v) mixture of sand (median grain size < 2 mm) and Cambisol that was steam-sterilized at 121 °C for 120 min one day before sowing. All ferrous particles from sand and soil were removed using a strong magnet to avoid disruptions during the MRI measurements (Jahnke et al., 2009). Temperature and light conditions for plant growth were as described in the general materials and methods section. The experiment consisted of four treatments: 1) non-treated control; 2) *H. schachtii*; 3) *R. solani*; 4) *H. schachtii* with *R. solani*. Each treatment had 5 plants.

The pathogens were added to the substrate 28 days after sowing. Treatments 2) and 4) were inoculated with 4000 J2 of *H. schachtii* and treatments 3) and 4) with *R. solani* following the methodology in chapter two.

The experiment was terminated six weeks after inoculation. The beet and lateral roots were washed free from soil (Fig. 4.1B - 4.4B) and the number of nematodes per plant was determined (see chapter two). Root, beet and shoot fresh weights were determined for each plant. Lateral roots were removed from the beet with a scalpel and root length measured with a root scanner (AGFA Snapscan 1236s™, Mortsel, Belgium) and the software WinRhizo Pro (Version 2004, Regent Instruments Inc., Quebec, Canada). Severity of *R. solani* beet rot was estimated as described in chapter two.

2.2. Nuclear magnetic resonance image acquisition

Twenty-eight days past inoculation, one plant from each treatment was evaluated in the NMR system. The images presented in figures 4.1A - 4.4A were collected at the ecoNMR facility of the Forschungszentrum Jülich (www.econmr.org) using a 4.7T/300 mm Varian VNMRS vertical wide-bore MRI system (Varian Inc., Oxford, UK). During MRI measurements, which took a maximum of 60 minutes, the plants were positioned in the borehole of the 4.7T MRI system at a controlled temperature of 18 °C. Images were recorded with a spatial resolution of 300 µm, using multi-slice spin echo techniques with sagital orientation. The *H. schachtii* infested plant was recorded using the same procedure, but 42 days past inoculation (Fig. 4.5).

Software VnmrJ™ (Varian Inc., Oxford, UK) was used to acquire and process images. Signal intensity (Fig. 4.1A - 4.4A) depends on several factors, but mainly on the water content of tissue and its relaxation times (MacFall et al., 1994). Different colours in the figures represent low, medium or high signal intensity or water content, respectively. Red equals low signal intensity, blue = medium and yellow to green = high signal intensity, which accordingly corresponds to the water content.

2.3. Statistical analysis

The statistical analysis included ANOVA and MANOVA of the plant variables, t-test for numbers of nematodes and *R. solani* beet rot rating. The synergy factor also was determined (see chapter 2). The analyses used are described in chapter two.

3. RESULTS

3.1. Destructive plant-pathogen evaluation

Significant differences in plant weights were observed among treatments (Tab. 4.1). Fresh leaf, beet and root weights were lowest in the treatment with concomitant presence of BCN

and RCRR. Root length also was lower in the treatment inoculated with both experimental organisms.

Table 4.1   **Influence of *Heterodera schachtii* and *Rhizoctonia solani* alone or in combination on plant fresh weights and root length of sugar beet 42 days past inoculation.**

Treatment	Leaf weight [g]	Root weight [g]	Beet weight [g]	Root length [cm]
Control	25.8±0.9a	6.5±0.7b	12.9±1.9a	2687±81 a
Heterodera schachtii	15.6±0.3ab	9.9±0.7a	5.6±0.3b	2786±191a
Rhizoctonia solani	9.8±6.7bc	1.7±1.1c	3.7±2.4b	35±4 b
H. schachtii + R. solani	0.3±0.1c	0.2±0.1c	0.4±0.1b	18±4 b

Displayed are the means±standard errors. Different letters indicate significant difference after Tukey's test ($p < 0.05$; $n = 5$).

A statistical interaction between *H. schachtii* and *R. solani* was only detected with root fresh weight ($F = 30.7$; df = 1; $p < 0.01$). Fresh leaf weight, root weight and root length were impacted synergistically according to the synergy factor (Tab. 4.2).

Table 4.2   **Effect of the disease complex on the synergy factor for leaf, root and beet fresh weight as well as root length 42 days past inoculation.***

Plant variable	*Synergy Factor*
Leaf fresh weight	1.1
Root fresh weight	1.3
Beet fresh weight	0.8
Root length	1.1

*Synergy factor above 1.0 indicates synergistic effects among organisms.

Numbers of BCN eggs and J2 per plant were significantly lower in the disease complex when compared to *H. schachtii* inoculated alone (Tab. 4.3). Conversely, the severity of *R. solani* rotting of the beets was more severe in the disease complex treatment than in the treatment with *R. solani* alone (Tab. 4.3).

Table 4.3   **Number of juveniles (J2) and eggs of *Heterodera schachtii* inoculated treatments, and *Rhizoctonia solani* caused beet rot rating of inoculated treatments 42 days past inoculation.**

Treatment	Number of eggs and J2	*R. solani* beet rot rating
Heterodera schachtii	10,249±208b	-
Rhizoctonia solani	-	2.45 ± 0.31a
H. schachtii + R. solani	4,438±116a	4.93 ± 0.21b

Displayed are the means±standard errors. Different letters indicate significant difference after t-test ($p < 0.05$; $n = 5$).

3.2. Non-destructive detection of the disease complex by nuclear magnetic resonance imaging

The highest signal intensity measurement was detected in the upper beet region (2 cm) as seen by the yellow-green colour in the non-inoculated healthy control (Fig. 4.1A). Less lateral roots were built and the water content and activity of plant tissue was higher in the control when compared to all other treatments.
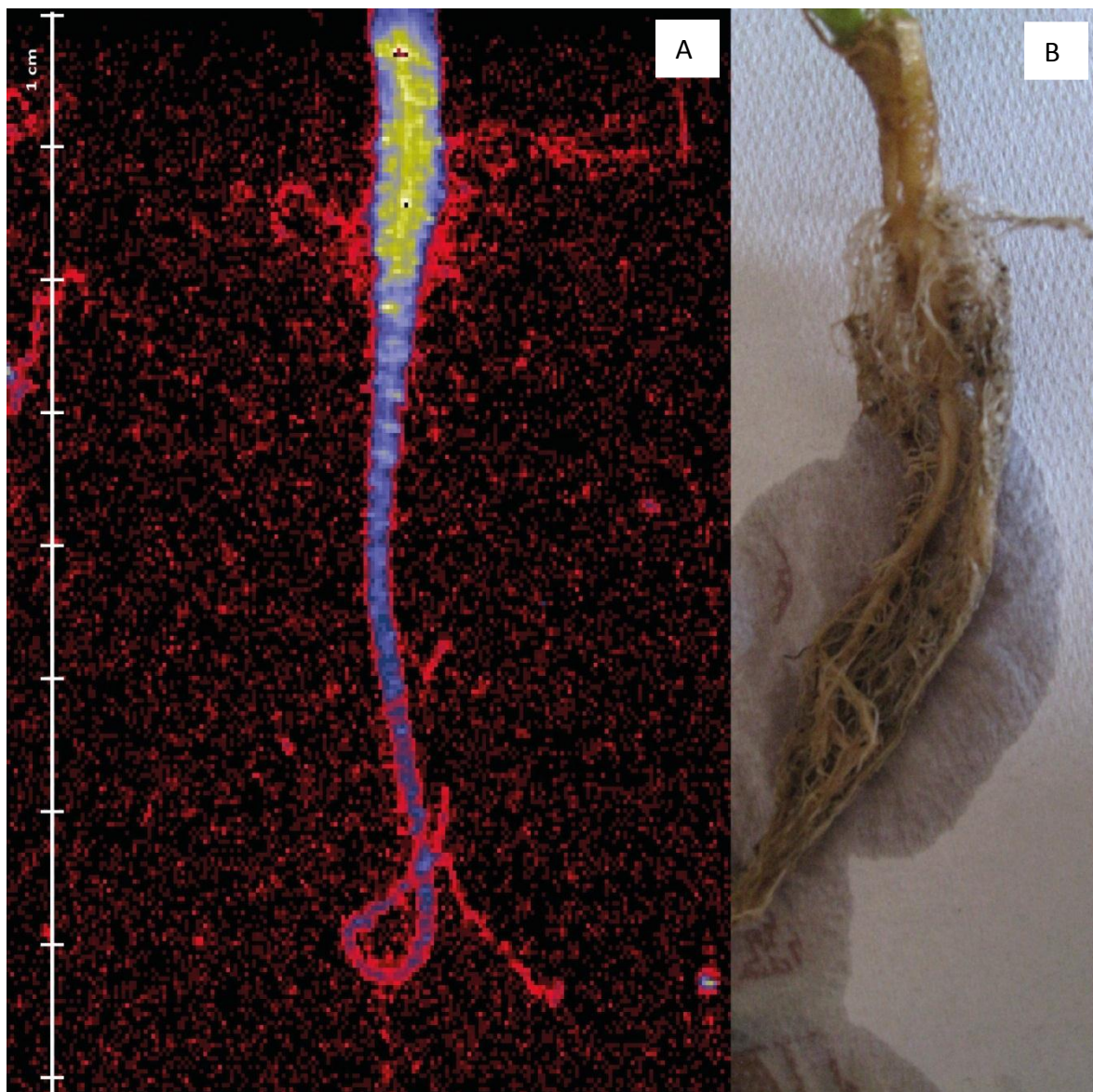

Figure 4.1   Nuclear magnetic resonance image of a non-inoculated sugar beet plant 28 days past inoculation (A), black = no signal; red = low signal intensity; blue = medium signal intensity; yellow-green = high signal intensity and (B) the same plant washed free of soil 14 days later.

The NMR image of the *H. schachtii* inoculated plant (Fig. 4.2A) showed evident differences in root and beet development compared to the control image. Considerably, more lateral roots were produced than in the control three centimetres below the surface of the soil following nematode infection (Fig. 4.2A). The beet was less developed and this resulted in only medium signal intensity, an indication of low water content. White females attached to the beet and roots were visible in the reference image (Fig. 4.2B). The three-dimensional image of the same plant 42 dpi verified clearly the increase in the number of lateral roots.
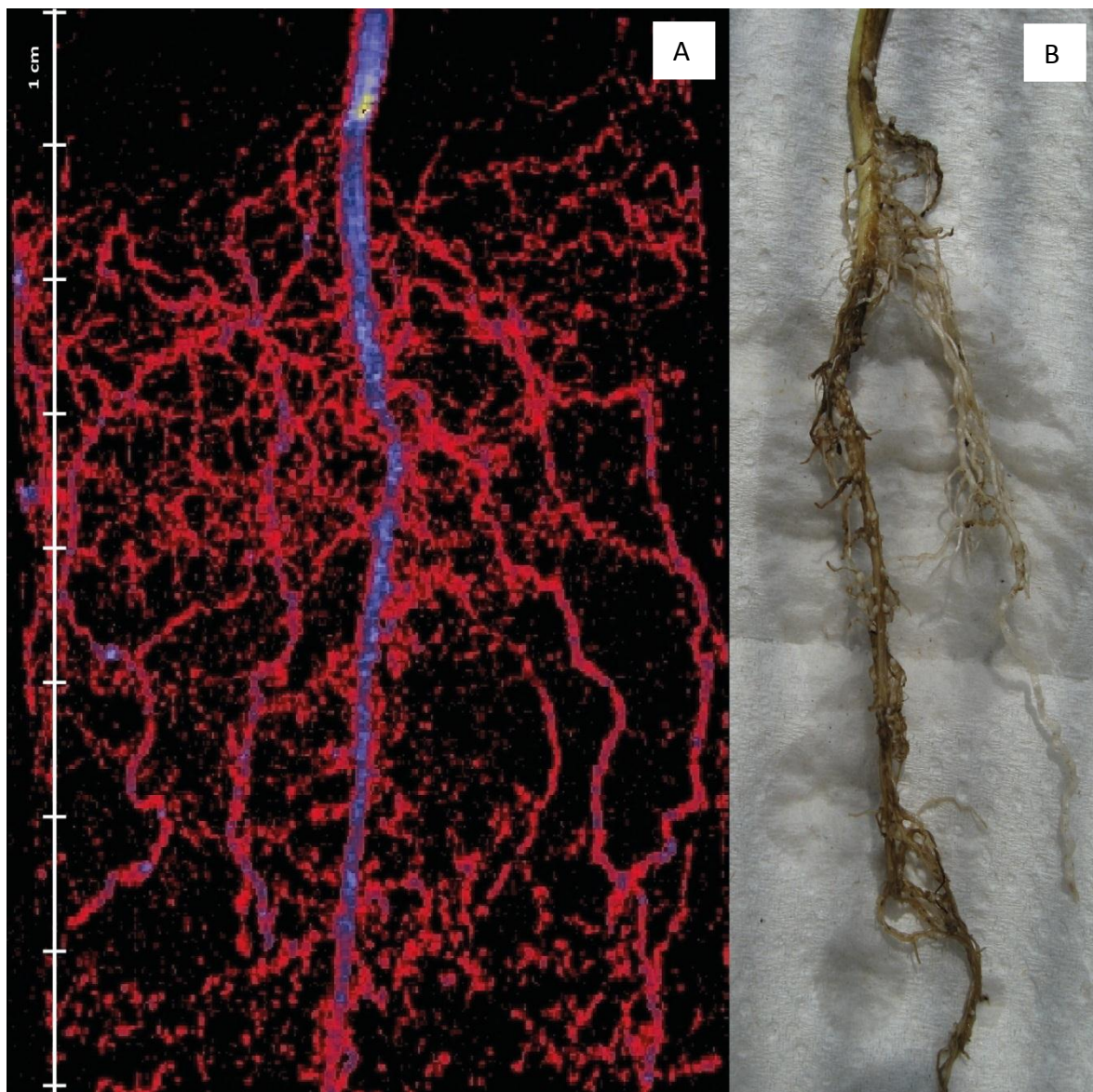

Figure 4.2 **Nuclear magnetic resonance image of a *Heterodera schachtii* inoculated sugar beet plant 28 days past inoculation (A), with black = no signal; red = low signal intensity; blue = medium signal intensity; yellow-green = high signal intensity and (B) the same plant washed free of soil 14 days later.**

There are also concentrated areas which seem to indicate the presence of the white females attached to the roots (Fig. 4.5).

A circular dump of high signal intensity was visible at a depth of 2 cm near the area where the *R. solani* inoculum was introduced into the soil four weeks earlier (Fig. 4.3A). Root rot was detected in the beet tissue 1 cm above the area of inoculation and is expressed in a decrease in signal intensity (Fig. 4.3A;B).
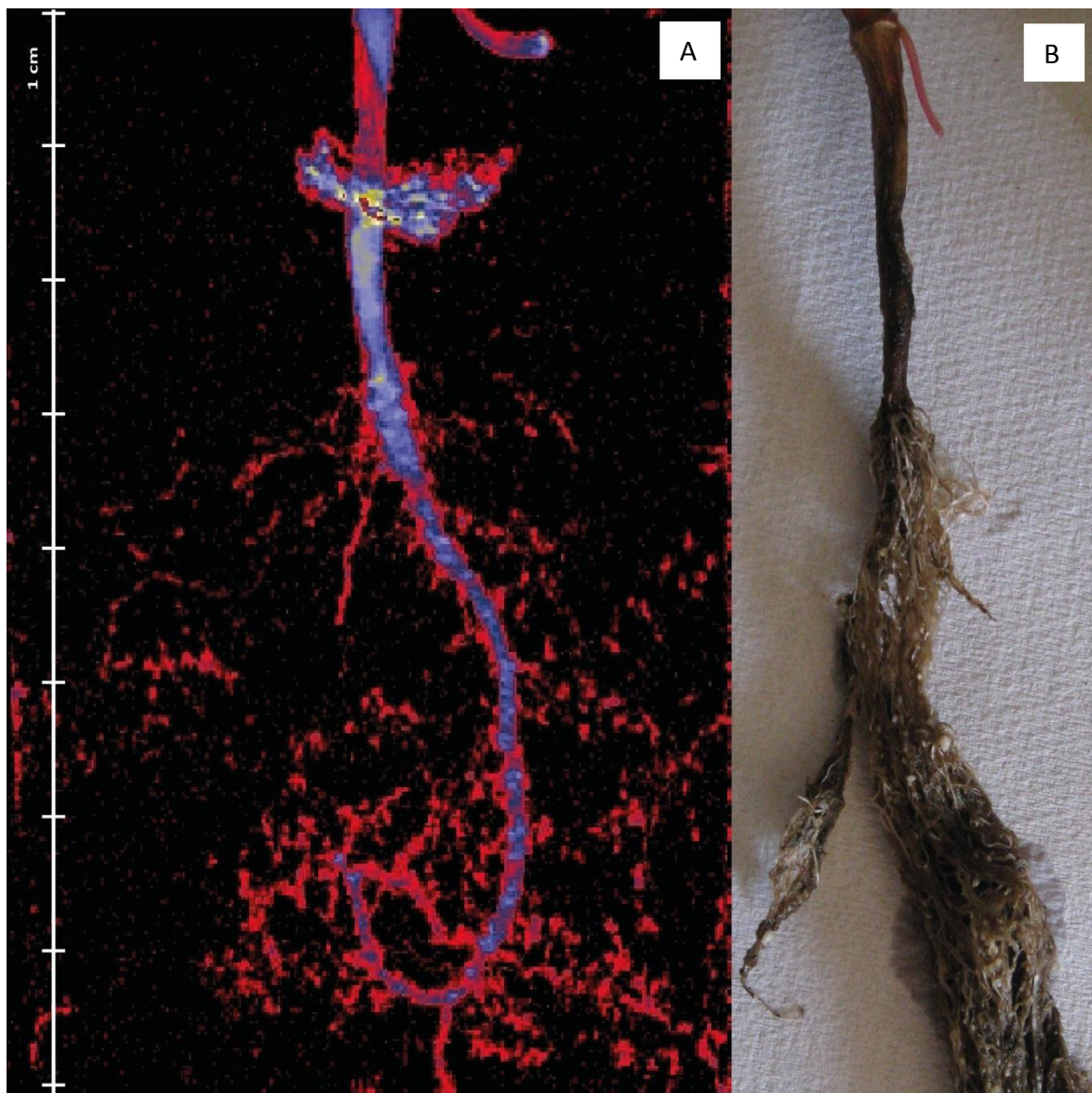
Figure 4.3   Nuclear magnetic resonance image of a *Rhizoctonia solani* AG 2-2IIIB inoculated sugar beet plant 28 days past inoculation (A), black = no signal; red = low signal intensity; blue = medium signal intensity; yellow-green = high signal intensity and (B) the same plant washed free of soil 14 days later.

Root rot and additional lateral roots were detected on the plant treated with *H. schachtii* and *R. solani* concomitantly (Fig. 4.4A;B). RCRR development was more severe in the dual treatments when compared to the RCRR control plant; whereas lateral root development was clearly lower than in the BCN control.
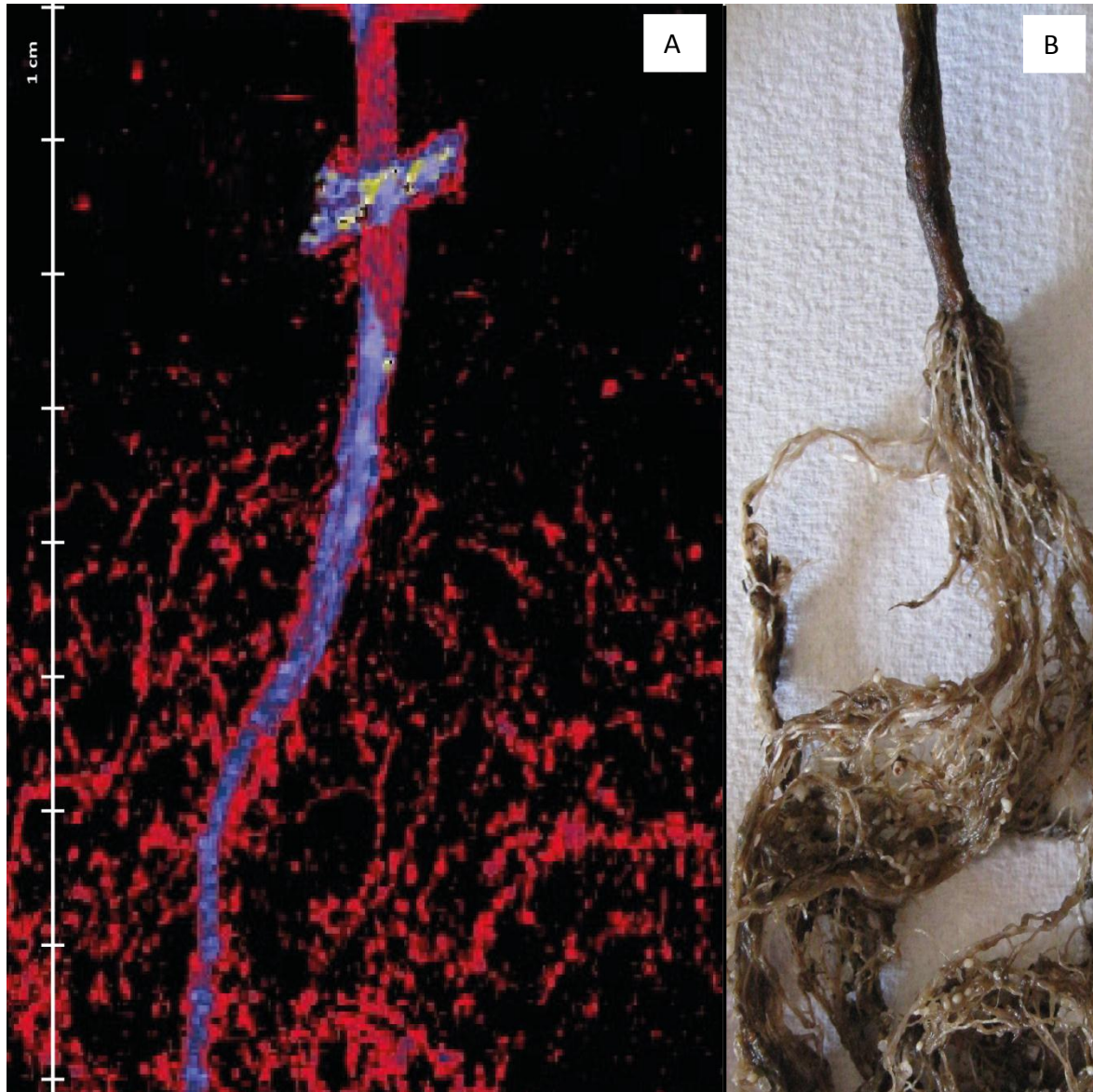

Figure 4.4 **Nuclear magnetic resonance image of a *Heterodera schachtii* and *Rhizoctonia solani* AG 2-2IIIB concomitantly inoculated sugar beet plant 28 days past inoculation (A), black = no signal; red = low signal intensity; blue = medium signal intensity; yellow-green = high signal intensity and (B) the same plant washed free of soil 14 days later.**

4. DISCUSSION

As reported in the previous experiments (chapter 3), synergistic damage was also detected in the concomitant treatments in this experiment. This is the first time that NMR imagery was used for non-destructive detection of symptoms caused by two plant pathogenic organisms, and therefore a synergistic interaction affecting the root system in a soil environment.
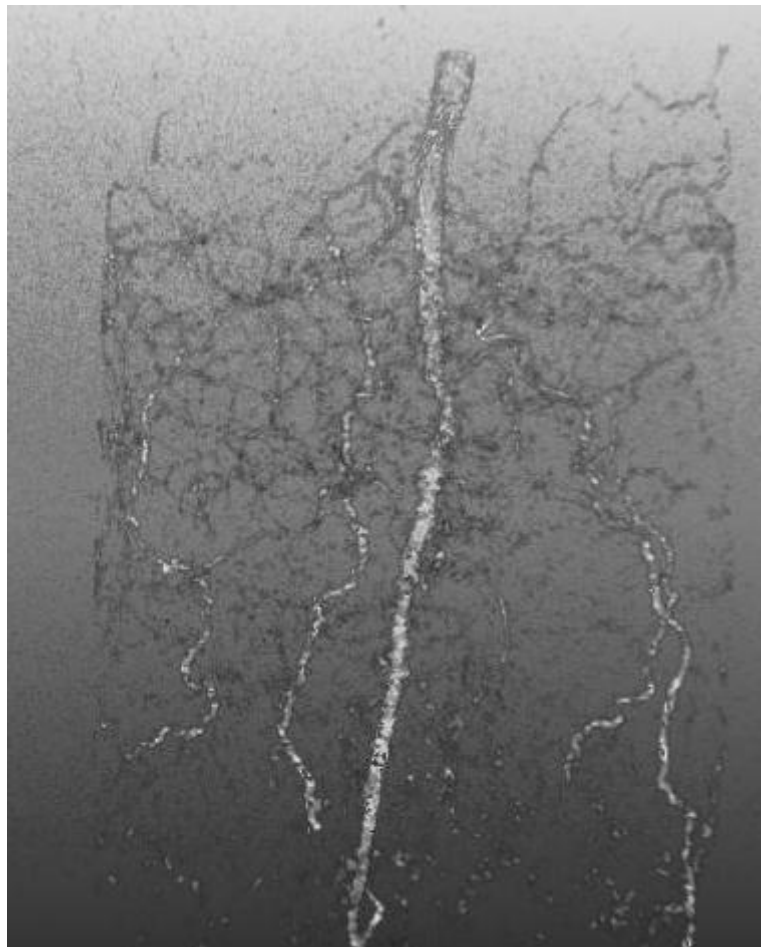
Figure 4.5   **A three-dimensional nuclear magnetic resonance image of a sugar beet root system inoculated with *Heterodera schachtii* 42 days past inoculation.**

The symptomatic production of the "bearded" root on sugar beet is reported to be responsible for *H. schachtii* damage to sugar beet, since most of these extra roots led to loss of resources and drain the plants off energy (Cooke, 1993). The first "bearded" or profusely branched lateral roots were detected at a depth of 3 cm on the NMR image or near the site of J2 inoculation. This finding contrasts those of Moriarty (1964) who reported that juveniles

46

only penetrate in the elongation zone behind the root tip. During the removal of the sugar beet plants from the PVC tubes used in this experiment, many of the tender lateral roots were inadvertently lost. The loss of these roots in normal experimentation leads to inexact data on root growth and the effects of pathogens and or nematodes on real root growth. It also underscores the advantage of using a non-destructive technique like NMR imagery to investigate soil-borne pathogens on plant root systems.

Rhizoctonia crown and root rot on the beet was detected on the NMR image of the *R. solani* alone inoculated plant belowground. Decay on the beet caused a decrease in water binding of the tissue and therefore decreased signal intensity.

Richards (1921) and Herr (1996) reported the initial invasion of RCRR into plants at the petioles. In the present investigation, when the fungal mycelium was used for inoculum it was placed 2 cm below the soil surface. *Rhizoctonia solani* infection was clearly shown to be initiated belowground and not aboveground on the obtained images.

The assumption that fungal penetration is stimulated by nematode root damage was confirmed with the NMR images on the concomitant inoculated plants. *Rhizoctonia* crown and root rot developed below and above the inoculation site. Signal intensity was lower and surface rot on the beet was higher when compared to the RCRR control. The distinct development of RCRR below the site of fungal inoculation seems to be correlated with the region of the root damaged by nematode penetration. Lower numbers of nematodes in the disease complex treatment could be explained by root rot and the decreased numbers of roots serving as host for the obligate parasite.

The fact that outer diameter of tubes used did not allow the maximum resolution of the MRI system (> 300 μm pixel^{-1}) prevented clear delineation of white females or cysts on the root surface. The adults are small, approximately 100 – 200 μm in diameter and require full resolution. The syncytia formed in the root by the juveniles and females were also not detectable with NMR.

5. CONCLUSIONS

This is the first report of the detection of damage caused by BCN and RCRR on sugar beet as well as the development of a synergistic disease complex by non-destructive NMRi. The results could be important for early detection of damage before visual symptoms are detectable when infection processes occur in the soil environment. The non-destructive nature of NMRi technology could give fundamental insight into the presence of cultivar resistance to soil-borne fungal pathogens and plant parasitic nematodes at different times after infection and allow protection of valuable germplasm. Experimentation is needed to increase the resolution of the system so that white females can be detected on the surface of the roots in a non-destructive system. Furthermore, research should look more closely at the development on RCRR in the beet prior to the set-in of the rotting process.

CHAPTER 5: INVESTIGATION OF COMPLEX DISEASE INTERACTIONS USING HYPERSPECTRAL LEAF REFLECTANCE ANALYSIS

1. INTRODUCTION

The potential of a non-imaging hyperspectral sensor and calculation of the NDVI was used in chapter three to assess symptoms caused by BCN and RCRR on sugar beet in greenhouse trials. Biotic stresses in the plant canopy, induced by nematode or soil-borne fungal root infection have been detected by non-imaging multi- and hyperspectral sensors (Hope et al., 1999; Heath et al., 2000; Nutter et al., 2002; Laudien et al., 2003). In this chapter an imaging hyperspectral sensor was used to detect symptoms caused by BCN and RCRR.

Comparing hyperspectral imaging used in this chapter to the non-imaging technique used in chapter three, imaging systems have several advantages (Kumar et al., 2001). Spatial resolution of non-imaging sensors is low and contains mixed information of plant material - diseased and non-diseased - and soil. The use of an imaging system, conversely, allow for the separation of this type of information (Bravo, 2006). Imaging spectroscopy is the fusion of imaging technology and spectroscopy, in which each pixel of the image is a vector of high resolution spectral information (Noble et al., 2003). Until recently this technology has been primarily used in remote sensing applications, but it has become available also for near-range hyperspectral imagery and has been identified as a tool with high potential for disease detection in crop production (Moshou et al., 2006).

For the detection of leaf pathogens by reflectance it is important to eliminate the influence of soil reflectance on spectral information in order to obtain more sensitive data. Threshold levels of NDVI are often used to discriminate leaf reflectance from soil reflectance (Moshou et al., 2006). The NDVI was shown to be a suitable parameter for the discrimination of vegetation from background (Rouse et al., 1974). For the assessment of damage caused by soil-borne pathogens like *H. schachtii* and *R. solani*, however, soil reflectance may be used for the quantification of disease incidence and plant biomass which decreases with disease severity while the proportion of the soil surface area increases due to added exposure.

Spectral vegetation indices are used routinely in remote sensing for the extraction of information from hyperspectral data. Several studies reported correlations of SVIs with nutrient supply, yield or damage by leaf pathogens under controlled and field conditions (Yang & Everitt, 2002; Bajwa et al., 2010; Mahlein et al., 2010). Because pigment content provides information on the physiological state of leaves, pigment-specific SVIs may be correlated to symptoms caused by BCN or RCRR. By calculating ratios from several bands at different ranges of the spectrum, SVIs result in a reduction of data dimension and may provide information on the content of pigments or water in the tissue, as well as on the tissue structure of leaves (Mahlein et al., 2010).

However, it also is possible that there is a loss of important information from parts of the spectrum through this reduction process. Hence, the use of a spectral analysis technique that takes advantage of spectral information of all bands, for example, the Spectral Angle Mapper (SAM) might be more advantageous for detection purposes (Yang et al., 2008). This method measures the similarity of image pixel spectra to reference spectra by calculating the angle between the spectra and treating them as vectors in a space which is dimensionality equal to the number of bands (Kruse et al., 1993). The SAM has been reported as a useful supervised classification method for a variety of hyperspectral remote and near-range sensing applications (Clark et al., 2005; Mundt et al., 2005; Qin et al., 2009; Feilhauer et al., 2010).

The objectives of these experiments were:

i.   to examine the potential of near-range hyperspectral imaging to detect and identify diseases caused by either BCN or RCRR alone, or both organisms in combination
ii. to use three different image processing approaches to determine the most sensitive data for disease discrimination
iii. to examine the use of a supervised classification on discrimination of symptoms caused by either organism alone or in combination

2. MATERIALS AND METHODS

2.1. Inoculation and plant-pathogen evaluation

Plants were sown in multipots as described in chapter two. After four weeks, plants were transplanted into boxes (1.2 × 0.8 × 0.25 m) containing 240 l substrate with sand and soil from the C- and A- horizon (plough-horizon) and Seramis (Mars GmbH, Mogendorf, Germany) in a ratio of 2 : 0.6 : 0.4 : 0.4 (v/v), respectively. Thirty-two plants were planted into each box with 0.15 m spacing between plants within rows and a row width of 0.2 m. Each box comprised of four rows with eight plants each. Plants were fertilized with 400 g long-term fertilizer Osmocote Plus per box (15 : 9 : 12, Scotts, Maysville, OH, USA).

Rhizoctonia solani sand-flour inoculum (see chapter 2 for production) at 2.5 g per plant was placed into 5 cm deep cavities in the soil of the boxes before transplanting the sugar beet seedlings into the inoculated cavities. After planting the cavities were filled up with the same substrate. Two thousand J2 were inoculated to each plant as described in chapter two.

The experiment included four treatments: 1) untreated control; 2) sugar beet inoculated with *H. schachtii* alone; 3) inoculated with *R. solani* alone; 4) inoculated with both organisms concomitantly. Each treatment consisted of 32 plants and the experiment was conducted twice.

The experiments were terminated nine weeks after inoculation. The number of eggs and J2 of *H. schachtii* were determined after harvest by sampling 100 ml of soil from the sites where sugar beet plants had grown. The number of nematodes and below- and aboveground leaf symptoms caused by RCRR were determined following the methodologies described in the general materials and methods in chapter 2.

2.2. Hyperspectral imaging

2.2.1. Data acquisition and pre-processing

Leaf reflectance of plants was recorded starting 5 to 64 dpi twice per week. Hyperspectral images were obtained by a line scanner (ImSpector V10E, Spectral Imaging Ltd., Oulu, Finland) in combination with a mirror scanner, which was mounted under a rack specially constructed for this sensor. Images were recorded in a dark room and the sensor was surrounded by six ASD Pro-Lamps (Analytical Spectral Devices Inc., Boulder, CO, USA) in order to provide optimum illumination. The ImSpector has a spectral range from 400 to 1000 nm and a spectral resolution of 2.8 nm. After focussing the camera using a black and white test target, the white reference (Spectral Imaging Ltd., Oulu, Finland) and the boxes with plants to be recorded were placed in exactly the same position to the camera for each measurement. Images were obtained from 1.5 m above canopy. The operator software SpectralCube (Spectral Imaging Ltd., Oulu, Finland) was used to record the images to the hard disc. Before the frame rate and the exposure time had to be optimized. A dark current image was taken by closing the shutter of the camera. Subsequently, the plants were recorded with the white reference and another image, with changed exposure time, without white reference.

The three images - dark current, white reference and raw image - obtained for each treatment were normalized using the program ENVI 4.6 + IDL 7.0 (ITT Visual Information Solutions, Boulder, CO, USA) by a special IDL tool. A normalized image was produced by comparing the raw image to the dark current image (minimum) and the white reference (maximum). The Savitzky-Golay smoothing filter (Savitzky & Golay, 1964) obtained from ITT Visual Information Solutions' Code Contribution Library was applied to the spectra of the normalized images. The filter was adjusted to the fifth node left and right and a polynomial of third order.

2.2.2. Soil exclusion and spectral vegetation indices

Three approaches were tested for data extraction. In approach I, the complete image was defined as a region of interest (ROI) and spectral data was extracted from all pixels, plants and soil reflectance. For approach II, a mask for plant biomass was created by calculating the NDVI (see Tab. 5.1) of the normalized image to exclude soil reflectance and to extract reflectance data of plant pixels only (NDVI > 0.5). The mask was applied to the normalized image and then reflectance was exported (Fig. 5.1A;B;C;D). For approach III, the margins of all leaves per plant were circumscribed manually by polygon-type ROIs and then the mean spectrum of each plant within an image was extracted (Fig. 5.1E). In contrast to approach II, this leaf approach was used to obtain spectral information for the leaves of plants only, excluding petiole and soil reflectance.
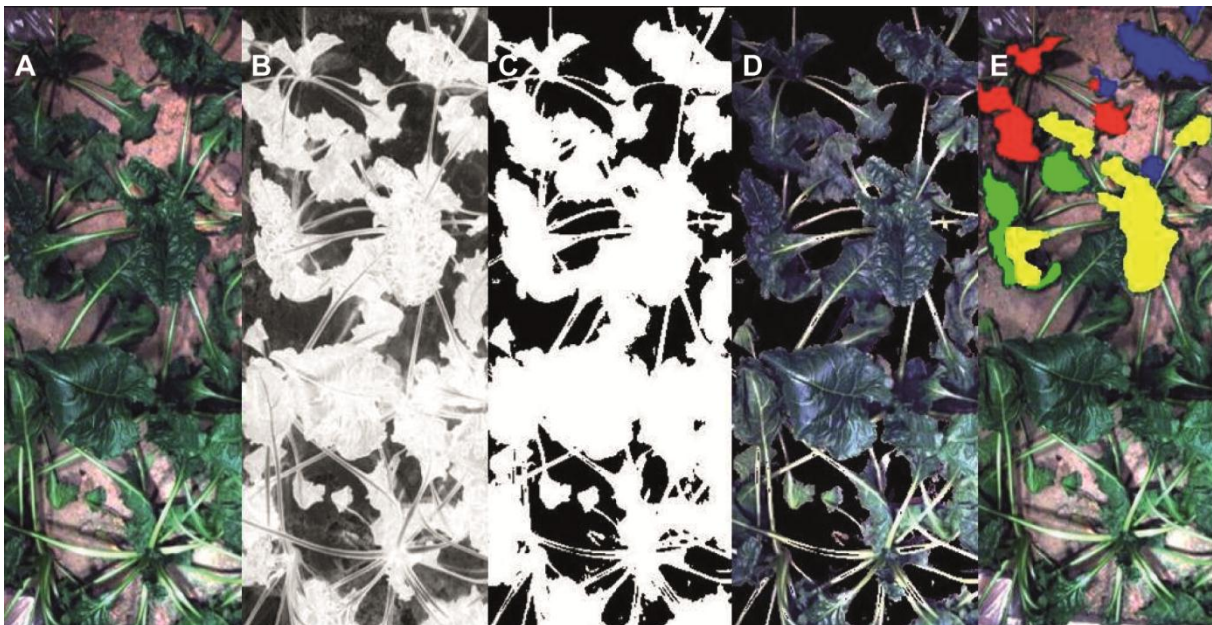
Figure 5.1 **Different stages of image processing: A = normalized image; B = NDVI transformed normalized image for creating a mask; C = binary mask created from image B; D = mask applied to the normalized image A; E = regions of interest (ROIs) on leaves.**

For each ROI the mean spectrum was calculated by ENVI and exported as ASCII file. This file was imported to MS Excel 2007 (Microsoft Corporation, Redmond, WA, USA) to calculate nine SVIs of spectra in a time series (Tab. 5.1). Spectral vegetation indices from remote sensing were tested for their correlation to ratings of aboveground disease symptoms depending on the method of image processing.

Table 5.1 Spectral vegetation indices used for correlation with leaf symptoms caused by *Rhizoctonia* crown and root rot.

Index	Equation	Reference
NDVI	$(R_{800}-R_{670})/(R_{800}+R_{670})$	Rouse et al. (1974)
Carter Index II	R_{695}/R_{760}	Carter et al. (1996)
Lichtenthaler Index I	$(R_{800}-R_{680})/(R_{800}+R_{680})$	Lichtenthaler et al. (1996)
OSAVI	$(1+0.16)\times(R_{800}-R_{670})/(R_{800}+R_{670}+0.16)$	Rondeaux et al. (1996)
mCAI	$(R_{545}+R_{752})/2\times(752-545)-\Sigma(R\times2.8)$	Laudien et al. (2003)
NDI	$(R_{750}-R_{705})/(R_{750}+R_{705})$	McNairn et al (1993)
SRPI	R_{430}/R_{680}	Penuelas et al. (1995)
WI	R_{900}/R_{970}	Penuelas et al. (1997)
PRI	$(R_{550}-R_{531})/(R_{550}+R_{531})$	Gamon et al. (1992)

2.2.3. Supervised classification

Hyperspectral images obtained by the pre-processing approach II were used for supervised classification within the program ENVI (Fig. 5.1D). Four classes were formed; class 1: healthy, class 2: wilting, class 3: yellowing, class 4: tissue necrotic and brown. For each class ROIs with 50 to 60 pixels were created in different images at locations with characteristic symptoms (n = 5). These classified ROIs were used to extract the pixels' mean spectra, which were saved as endmembers in a spectral library and used as references in the classification algorithm (Fig. 5.2).

The supervised classification method SAM was used, in which each pixel of the image was classified according to the endmembers spectra. For post classification a confusion matrix was applied to the classified image with five truth ROIs per class selected for validation of the classification result. The confusion matrix results in an overall accuracy by summing the number of pixels classified correctly, divided by the total number of pixels. Additionally, the kappa coefficient (κ) - a statistical measure of interrater agreement for qualitative items - was calculated; it is a more robust measure than simple percent agreement calculation since κ takes into account the agreement occurring by chance (Cohen, 1960).
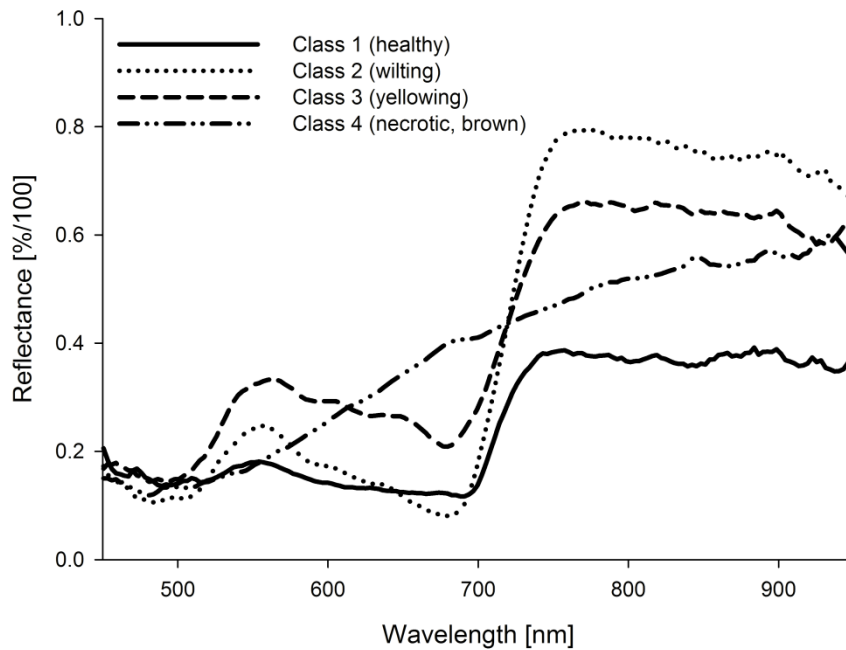
Figure 5.2   Spectral library of signatures of sugar beet leaves with four classes of leaf damage / disease symptoms.

2.3. Statistical analysis

Plant fresh weights were tested by ANOVA and MANOVA (see chapter two) at a probability level of 0.01. Beet and leaf weights were tested for correlation at a probability level of 0.01 by Pearson's correlation coefficient. Correlations between plant weights, RCRR leaf symptom rating, *R. solani* beet rot rating and NDVI values were also calculated. Nine SVIs were correlated to leaf symptom ratings using Spearman's rank correlation coefficient. Leaf symptom ratings for RCRR were compared for each date using t-test ($p < 0.05$). Also the *R. solani* beet rot rating and the number of eggs and J2 per plant were compared using the t-test ($p < 0.05$).

3. RESULTS

3.1. Visual development of plant-pathogen interactions

No differences were detected in plant development and leaf reflectance among treatments until 28 dpi. Neither *H. schachtii* nor *R. solani* produced visible aboveground symptoms at

55

this time. Leaf wilting became visible on BCN inoculated plants from 28 to 40 dpi. Wilted leaves were detected predominantly for plants inoculated with *H. schachtii* alone. These observations were in accordance with the higher number of eggs and J2 in boxes inoculated with BCN alone compared to the combined inoculation (Tab. 5.2).

Table 5.2 Influence of *Heterodera schachtii* and *Rhizoctonia solani* alone or in combination on the number of eggs and juveniles of *H. schachtii* and on the *Rhizoctonia solani* beet rot rating.

Treatment	Number of eggs and J2	RCRR beet rating
Heterodera schachtii	12,375 ± 408b	-
Rhizoctonia solani	-	2.97 ± 0.31a
H. schachtii + R. solani	5,987 ± 257a	5.13 ± 0.27b

Displayed are the means±standard errors. Different letters indicate significant difference after t-test ($p < 0.05$; $n = 32$).

The first leaf symptoms caused by RCRR became visible at the petioles of the oldest leaves 40 days past inoculation. Leaf symptom ratings showed significant differences between the *R. solani* inoculated treatments starting 47 dpi (Fig. 5.3). These symptoms were not visible until 50 dpi and 54 dpi in the closed canopy of plants inoculated with the combination of *H. schachtii* and *R. solani* and with *R. solani* alone, respectively.
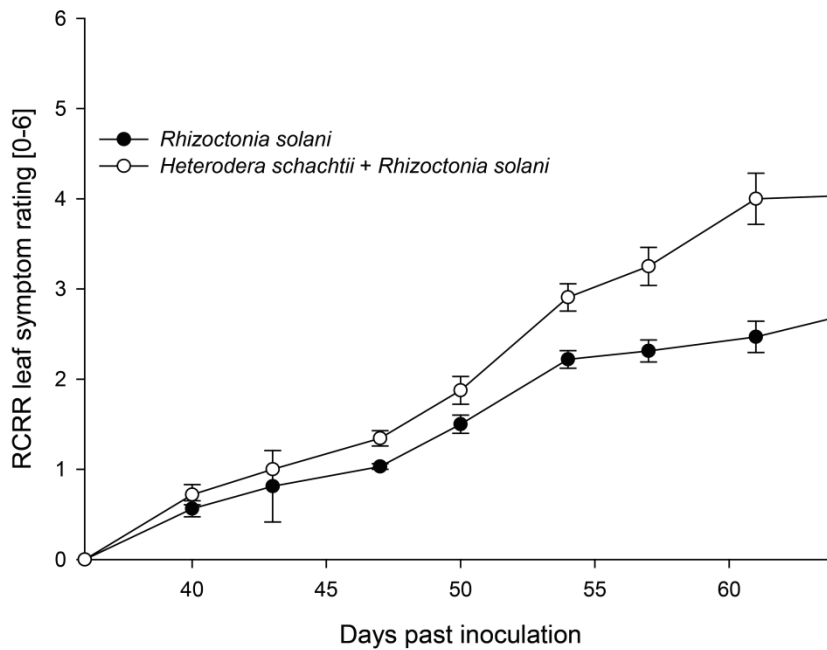

Figure 5.3 Effect of *Rhizoctonia solani* alone and in combination with *Heterodera schachtii* on the development of sugar beet leaf symptoms. Bars indicate standard error of the mean ($n = 32$).

The number of eggs and J2 of *H. schachtii* was significantly higher in the treatment with the nematode alone compared to the combined inoculation. Conversely, beet rot was significantly more severe in the dual inoculation when compared to plants inoculated with *R. solani* alone (Tab. 5.2).

Leaf weights were closely correlated to beet weights ($r = 0.83$, $p < 0.01$). Leaves and beets of plants inoculated with the combination of *R. solani* and *H. schachtii* had the lowest biomass of all treatments (Fig. 5.4). According to the synergy factor (*SF*) described in chapter two, leaf weight was impacted in an additive way by disease complex (*SF* = 1), whereas beet weight resulted in synergistic damage (*SF* = 1.2). Multivariate statistical analysis showed no interaction between *H. schachtii* and *R. solani* for leaf and beet fresh weights, respectively ($F = 0.01$, df = 2, $p = 0.98$ and $F = 0.68$, df = 2, $p = 0.40$).
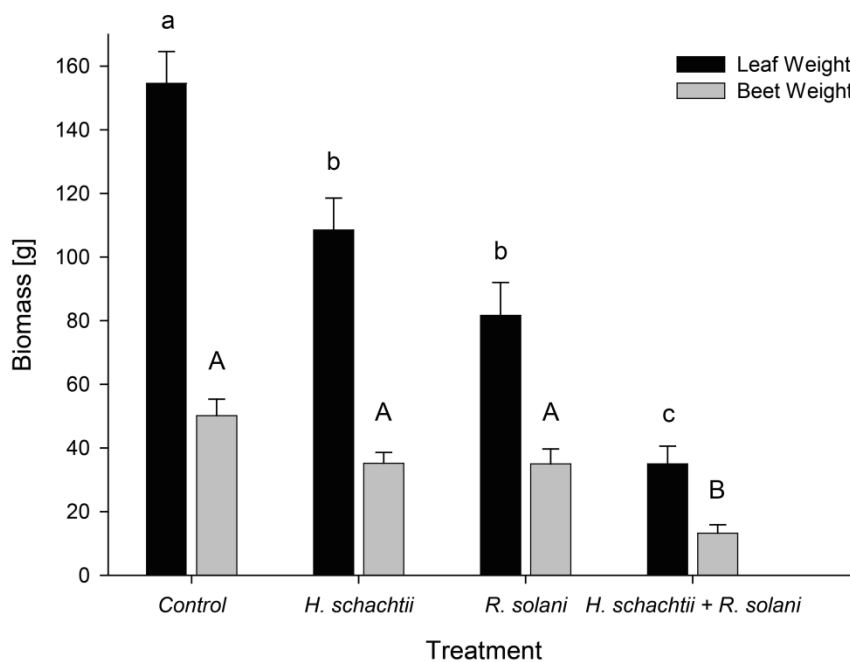

Figure 5.4 **Mean leaf and beet weight of sugar beet inoculated with *Heterodera schachtii* or *Rhizoctonia solani* alone or in combination. Error bars represent the standard error of the mean. Different letters indicate significant differences among treatments according to Tukey's test ($p < 0.01$, *n* = 32).**

3.2. Hyperspectral imaging

3.2.1.   Effect of image processing on information from hyperspectral reflectance

Three different approaches of image processing were tested for their suitability to monitor symptom development caused by *H. schachtii* or *R. solani* alone or in combination, respectively.

The NDVI was calculated as a parameter for biomass / leaf area index and plant vitality for complete images including soil reflectance (approach I), images without soil reflectance (approach II), and images with leaf tissue only (approach III).

Calculations of the average NDVI from complete images, in general, resulted in slightly lower values than for the other image processing methods (Fig. 5.5). Leaf wilting of plants inoculated with *H. schachtii* resulted in lower NDVI values from 28 to 40 dpi, for approach I (Fig. 5.5A). In contrast, methods excluding soil reflectance resulted in only marginal changes of NDVI. Forty days past inoculation the BCN inoculated plants recovered from wilting as demonstrated by NDVI values.

Starting 50 dpi, the NDVI of sugar beet inoculated with both pathogens decreased. This effect was detected by all processing approaches (Fig. 5.5A;B;C). Using approach I, the NDVI of canopies of non-inoculated plants was higher than that of sugar beet inoculated with *R. solani* alone 64 dpi and later (Fig. 5.5A). Image processing approach III - use of leaf pixels only - resulted in the discrimination between these treatments already 7 days earlier (Fig. 5.5C). Approach II - exclusion of soil reflectance - was less sensitive in the discrimination of leaf symptoms caused by the pathogens (Fig. 5.5B).

The leaf weight of sugar beets was correlated to the NDVI calculated from approach one (r = 0.61, p < 0.01). As leaf symptom ratings were related to RCRR beet rot rating (r = 0.93, p < 0.01), therefore the NDVI was also correlated to the RCRR beet rot rating (r = -0.84, p < 0.01).
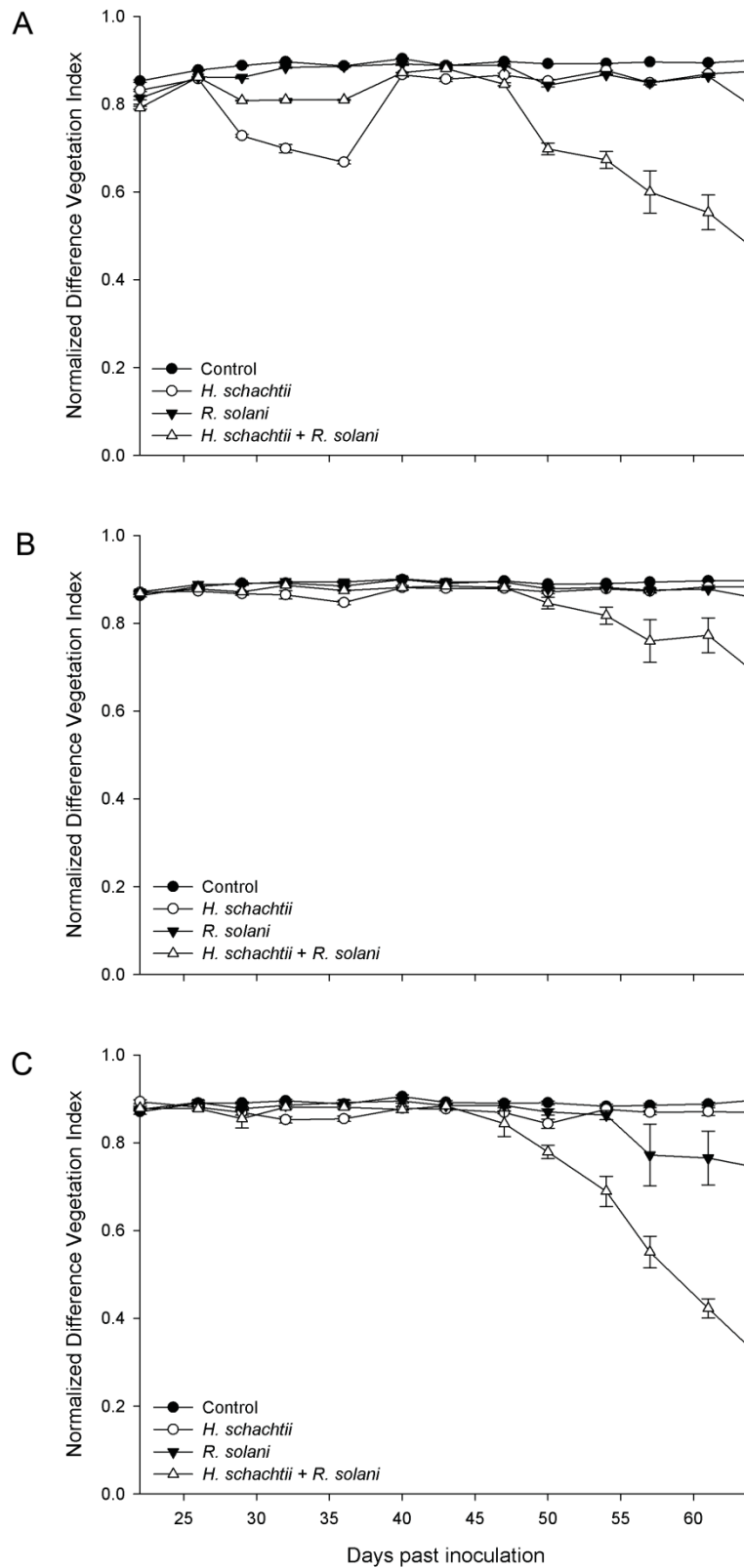
Figure 5.5 Influence of image processing (A = approach I [complete image]; B = approach II [soil reflectance excluded]; C = approach III [leaf reflectance only]) on NDVI calculated from spectra of sugar beet inoculated with *Heterodera schachtii* or *Rhizoctonia solani* alone or in combination. Error bars represent the standard error of the mean.

3.2.2.   Spectral vegetation indices

Nine SVIs were tested for their suitability to discriminate between healthy plants and sugar beet with BCN infection and RCRR, respectively. The SVIs calculated from reflectance spectra differed considerably in their correlation to leaf symptoms depending on the image processing approach. Approach I, which included soil reflectance, resulted in the highest correlation between leaf symptom rating and NDVI (Tab. 5.3). Approach II - exclusion of soil pixels - gave the highest correlations of pigment-specific SVIs to leaf symptom ratings. Especially indices related to photosynthesis - PRI, Lichtenthaler Index I, SRPI – yielded strong correlations to visual symptom ratings (r = -0.85 to -0.88). In contrast, NDVI and the water index (WI) had the lowest correlation coefficients when using the image processing approach II. The WI was the only SVI which showed a significantly better correlation to leaf symptom ratings when applying image processing approach III (Tab. 5.3).

Table 5.3   **Spearman's correlation coefficient for the relation between leaf symptoms caused by *Rhizoctonia* crown and root rot and nine vegetation indices depending on the pre-processing method for hyperspectral images from sugar beet plants ($p < 0.01$; n = 64).**

Index	Image processing approach		
	Complete image	Soil excluded	Leaves only
NDVI	-0.93	-0.69	-0.74
Carter Index II	0.73	0.71	0.73
Lichtenthaler Index I	-0.71	-0.86	-0.74
OSAVI	-0.73	-0.82	-0.69
mCAI	-0.71	-0.79	-0.65
NDI	-0.73	-0.80	-0.67
SRPI	-0.62	-0.85	-0.74
WI	0.34	0.09	0.32
PRI	-0.71	-0.88	-0.78

3.2.3.   Supervised classification

SAM classification was applied to images processed by approach II based on four classes of increasing leaf damage severity (Fig. 5.6). The confusion matrix of SAM results - comparison of classification to the four truth ROIs per class - indicated an overall accuracy of 79.4 %. With a Kappa coefficient of κ = 0.72, a substantial agreement was achieved. There was some misclassification when spectral library classification was compared to truth ROIs. When

comparing class 1 to class 2 it resulted in 30 % misclassification, because truth ROIs did not match with the spectral library classes (Tab. 5.4).
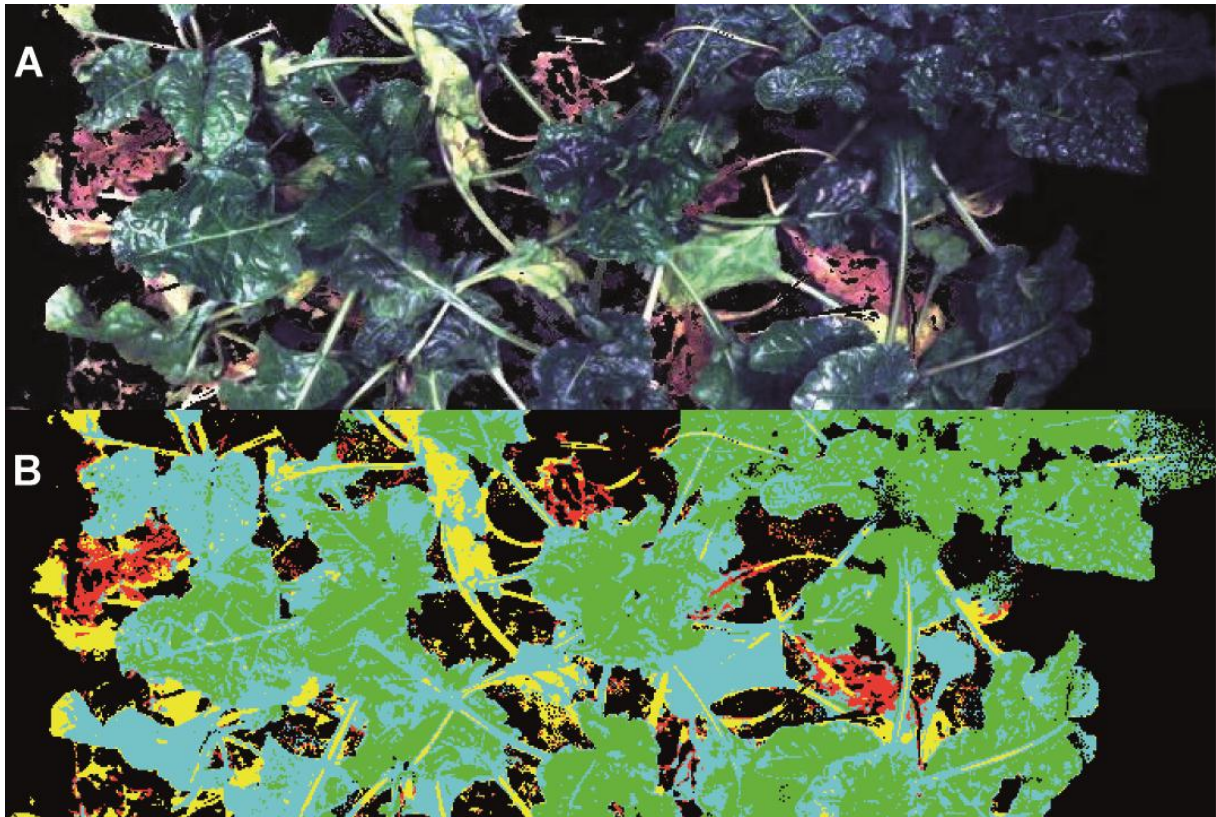
Figure 5.6   **Masked hyperspectral image (A) with different levels of damaged leaves and (B) the spectral angle mapper (SAM) classified image based on four classes (green = class 1, healthy; cyan = class 2, wilting; yellow = class 3, yellowing; red = class 4, necrotic brown) from spectral library.**

4. DISCUSSION

Nematode inoculated plants started to wilt after completion of the first generation due to damage caused by penetration of the second generation into the roots. The developmental stage of the nematodes at any time was calculated by the heat sum-model according to Čuri & Zmoray (1966), which in this case showed a relationship between the beginning of the second generation and initiation of wilt symptoms. When a heat sum of 465 °C was reached 32 dpi, the first wilt symptoms were detected. The plants recovered after about ten days due to the production of secondary roots associated with nematode infection, which lead to a reduction of leaf and beet biomass (Cooke, 1987).

Sugar beet inoculated with *H. schachtii* alone showed more severe wilting than plants inoculated with *R. solani* and *H. schachtii* together. As mentioned in chapters three and four, the activity of *R. solani* is likely to inhibit the development of *H. schachtii* due to damage to the root tissue and habitat disintegration of feeding sites for the obligate biotrophic nematode. In contrast, development of RCRR was faster and more severe in the presence of the nematode as compared to sugar beets attacked by *R. solani* alone. The fungal pathogen has been reported to be able to enter root tissue through *H. schachtii* penetration sites and then continue to effectively colonize the root tissue (Bergeson, 1972). Synergistic effects between the pathogens were not as clear as in chapters three and four and may have been due to differences in experimental set-up. Nevertheless, the synergy factor verified synergistic damage to beet weight in the concomitant treatments as observed in chapter three.

Significant correlations between the biomass of leaves and beets demonstrated the close interrelationship between leaves as the source of assimilates for beet development and the belowground plant organs for the uptake and allocation of water and nutrients. This balance between leaves and beets is the reason for the potential importance of NDVI measurements for the assessment of belowground damage of plants due to pathogens. Non-destructive hyperspectral sensing may be used in time series experiments on host-pathogen interactions as well as in screening systems for crop resistance to soil-borne pathogens and pests.

Table 5.4 **Confusion matrix of four classes ImSpector image of spectral library endmembers with ground truth data. Agreement and disagreement of class to class comparison are given in percent.**

| | | Ground truth | | | | |
	Class	Class 1	Class 2	Class 3	Class 4	Total
Spectral Library	Unclassified	0	0	10	1	3
	Class 1	71	0	0	0	22
	Class2	28	83	10	6	32
	Class 3	1	17	80	8	25
	Class 4	0	0	0	85	18
	Total	100	100	100	100	100

Three approaches of image processing were tested for their usefulness in assessing the development of sugar beet symptoms due to the infection of *H. schachtii* and *R. solani.* The NDVI confirmed to be a reliable indicator of ground cover and biomass of plants as reported

by Rouse et al. (1974). Sensitivity was suitable enough to detect the wilting of leaves due to the juvenile penetration of the second generation of *H. schachtii* into roots, as well as the transient recovery of plants. Typically, symptoms of the nematode include wilting due to drought stress and are induced by root damage (Cooke, 1987). Because the leaves of diseased plants do not cover the soil as extensively as leaves of healthy plants, increased soil reflectance decreased NDVI when approach I was used. This approach was similar to the non-imaging approach tested successfully in chapter three, which resulted in a spectral mixing of reflectance from crop and soil. In contrast, image processing approaches leading to pure plant reflectance resulted in only marginal changes of NDVI despite of considerable leaf wilting. The NDVI *per se* is not suitable to assess the water status of plant tissue. Spectral vegetation indices sensitive to drought stress, therefore, should be tested for the detection of spectral differences between nematode-infested and healthy plants.

Aboveground leaf symptoms of RCRR include yellowing of sugar beet leaves and the formation of a rosette of dying leaves on the soil in later stages (Herr, 1996). Leaf symptoms were closely correlated to NDVI obtained from image approach I, whereas image processing approaches eliminating the soil gave considerably weaker correlations. The NDVI proved to be highly sensitive to changes in soil crop cover. However, it seems not to be suitable for the detection of disease-specific modifications of plant tissue. Conversely, pure plant pixel approaches are not very suitable for the assessment of crop biomass, unless the pixels classified as biomass are quantified.

The SVIs tested besides NDVI are mainly pigment specific (Lichtenthaler Index I, Carter II, mCAI, NDI, OSAVI, PRI, SRPI) or give information on the water status of plants (WI). They are commonly used in remote sensing, but - similar to NDVI - largely lack specificity for the detection of plant diseases. Nevertheless, approach II with elimination of soil reflectance significantly increased their correlation to leaf symptom ratings. This approach has been used by Moshou et al. (2006) in order to remove soil reflectance for the discrimination of yellow rust from nutrient stress of wheat leaves. For RCRR leaf symptom ratings in sugar beet, the PRI had the highest correlation to leaf symptoms. It has been developed for tracking of photosynthetic light use efficiency (Gamon et al., 1992). The PRI proved to be more precise in the detection of physiological changes in leaves resulting from disease

development than the NDVI as reported by Gamon et al. (1992). Also the Lichtenthaler Index I, developed for the assessment of leaf fluorescence (Lichtenthaler et al., 1996) and the SRPI, related to carotenoids and chlorophyll a content of plant tissue (Penuelas et al., 1995) showed higher correlations to leaf symptoms.

The extraction of reflectance data by leaf-specific ROIs (approach III) gave the weakest correlations between SVIs and leaf symptoms incited by RCRR. This method was used by Rascher et al. (2007) for the assessment of leaf photosynthesis. The authors discussed it's usefulness because of the manual selection of leaf area by ROIs and the non-normal distribution of data. Furthermore, manual selection is more time consuming than the use of a mask based on NDVI threshold values. Correlations between leaf symptoms and NDVI, Carter Index, and WI were higher in approach III than in the approach excluding soil only. This may be due to omitting the beet crown and petioles in ROIs. In addition, dead leaves selected by ROIs had spectral properties similar to the soil and contributed to the assessment of necrotic plant tissue as a leaf symptom of RCRR. A differentiation between BCN- and RCRR-affected sugar beet plants actually is only possible by taking into account the differences in the time of appearance of shoot symptoms.

Due to the lack of specificity of SVIs to characterize leaf symptoms of different diseases, a supervised classification method was tested. The SAM was useful in classifying different states of leaf disease. A substantial interrater agreement shows the applicability of imaging sensor systems for disease symptom ratings. The spatial resolution of hyperspectral images in combination with the classification applicability is an enormous advantage to non-imaging sensors. Hyperspectral imaging in combination with SAM classification has been used successfully for quality management in fruits (Qin et al., 2009) and could also be a useful tool for sugar beet breeders. Furthermore, the SAM method could be used for the differentiation between aboveground symptoms of BCN and RCRR and also for the quantification of RCRR severity from aerial field data as will be discussed in the next chapter.

5. CONCLUSIONS

Unprocessed images of sugar beet canopies allowed the assessment of differences in plant biomass as measured by NDVI. The elimination of pixels representing the soil or non-relevant plant tissue enabled the use of pigment-specific SVIs for the detection of physiological changes in plant tissue due to the presence of root diseases. Therefore, leaf symptoms caused by root damage caused by either BCN or RCRR have to be investigated more in detail at tissue level for characteristic differences in spectral reflectance. Disease-specific SVIs and/or combinations of existing SVIs may be applied in hyperspectral imaging of plant diseases in order to identify the presence of diseases, improve quantification of disease and allow for earlier detection of symptoms. The SAM classification seems to be a promising tool for the discrimination and quantification of diseases in the field. Furthermore, this sensor technology in combination with leaf symptom classification can be effectively used by breeding companies for resistance tests.

CHAPTER 6: TRANSFER OF NON-DESTRUCTIVE TECHNOLOGY TO THE FIELD FOR THE ANALYSIS OF COMPLEX DISEASES

1. INTRODUCTION

Due to economic losses caused by BCN and RCRR to sugar beet and the high costs of treating entire field for example with pesticides for their successful management, new methods are needed for site-specific detection and quantification of damage. A basic principle of precision agriculture is that the presence, distribution and intensity of a specific yield-reducing factor within a field must be identifiable (Melakeberhan, 2002). The patchy appearance of aboveground symptoms in the canopy and low mobility of *H. schachtii* and *R. solani* makes them suitable targets for application of precision agriculture tools, like non-invasive sensors, information and management systems. Geographic information systems (GIS) that can accurately locate and precisely map variations in crop status can then be used to display georeferenced ground truth data and to correlate this with remote sensing data (Hillnhütter & Mahlein, 2008). This information then allows accurate treatment of a field with pesticide, the planting of resistant cultivars or the use of green manure for effective and economically acceptable management.

In addition to the spatial variation of the two organisms in a field, temporal shifts in disease symptom development should be taken into account, because temporal variation at the onset of stress symptoms is an important diagnostic feature (Nutter et al., 2002). Stunted growth caused by the BCN occurs in the beginning of the cropping season (growth stage 10 - 35), whereas yellowing of leaves caused by RCRR only starts late in the cropping season (growth stage 40 - 49). Consequently, the temporal pattern of near-range and remotely sensed data obtained over time may provide a useful means to accurately differentiate between these two biotic stresses that often occur simultaneously in the same field. Therefore, remote measurements of canopy reflectance coupled with GIS are technologies that may allow exact detection of BCN and RCRR due to their spatio-temporal pattern of plant stress (Wyse-Pester et al., 2002).

66

In chapters three and five hyperspectral sensor technologies were tested under controlled conditions for assessment of symptoms caused by BCN and RCRR alone or in combination. In chapter three the potential of a non-imaging spectroradiometer was demonstrated in combination with the calculation of the NDVI. In chapter five, imaging spectrometry resulted in detection of symptoms caused by BCN and RCRR. It was also shown that it is possible to classify leaf symptoms by hyperspectral supervised classification. However, the methods used were not tested under field conditions for detection of BCN and RCRR.

Spectral vegetation indices were correlated to yield, nutrient supply or damage by pathogens as reported by Yang & Everitt (2002), Bajwa et al. (2010) and Mahlein et al. (2010). They are the standard tool for analysis of remote sensing data in crop management and were effectively used in the previous chapters to discriminate stresses caused by BCN and/or RCRR.

The supervised classification SAM was tested successfully on discrimination of leaf symptoms in chapter five.

Therefore, supervised classification of aerial hyperspectral images with SAM could be used to create digital maps illustrating healthy plant sites in the field and areas with symptoms affected by BCN or RCRR.

The objectives were to:

i.   detect and discriminate canopy symptoms caused by BCN and RCRR with hyperspectral canopy reflectance measurements in combination with SVIs and supervised classification

ii.   validate the hyperspectral measurements with ground truth data of BCN and RCRR infestation and plant status

iii.   geographically reference and display this data by GIS in digital maps

2. MATERIALS AND METHODS

2.1. Test site and plant cultivation

The field site "Meckenheim Scheune" of INRES-Phytomedicine of the Faculty of Agriculture of the University of Bonn is located at 50°37'N, 6°59'E at an altitude of 170 m above sea level. The field has a loamy-silt soil classified after the World Reference Base for Soil Resources as Luvisol (FAO, 2007). The annual mean temperature is 9.2 °C with 600 mm rainfall and 1530 sun hours per year (Franke & Menz, 2007). The 0.65 ha test site was chosen based on its natural infestation with both *H. schachtii* and *R. solani* and because of its homogenous topography.

In the first week of April 90 kg ha^{-1} nitrogen-fertilizer (Ammonium nitrate 75 %, Kalkamonsalpeter Rieselkorn 27, fertiva GmbH, Mannheim, Germany) was applied before sowing. In the last week of June 20 l ha^{-1} NPK (12:4:6) liquid leaf fertilizer (Blattflüssigdünger, Caspar Berghoff KG, Warstein, Germany) was applied. Sugar beet plants, cultivar Beretta (KWS GmbH, Einbeck, Germany) susceptible to BCN and RCRR and tolerant to rhizomania were sown in the first week of April 2009. In the second week of May and the first week of June herbicides were applied to reduce the influence of weeds on sugar beet plant growth and canopy reflectance (May: 0.7 l ha^{-1} Powertwin Plus + 1.5 l ha^{-1} Goltix, Feinchemie Schwebda GmbH, Eschwege, Germany + 1 l ha^{-1} Fusilade Max, Syngenta AG, Basel, Switzerland; June: 1.7 l ha^{-1} Betanal, Bayer Cropscience, Monheim, Germany + 2.0 l ha^{-1} Goltix, Feinchemie Schwebda GmbH, Eschwege, Germany + 0.9 l ha^{-1} Spectrum, BASF, Ludwigshafen, Germany). To avoid fungal leaf pathogens and insects two fungicides and one insecticide were applied in the first week of July (1.2 l ha^{-1} Opus Top, BASF, Ludwigshafen, Germany + 0.075 l ha^{-1} Karate Zeon, Syngenta AG, Switzerland); and in the last week of July (1.0 l ha^{-1} Juwel, BASF, Ludwigshafen, Germany), respectively. The sugar beets were harvested on 15th of October 2009. Workflow during the field experiment is summarized chronologically in table 6.1.

2.2. Pathogen and plant evaluation

Plant growth stages (GS) were defined according to the BBCH scale (Meier et al., 1993). At 31 geo-referenced and randomized points in the field, five samples for each of the following variables were determined:

- BCN juvenile root invasion

- final BCN population density (Pf)

- *Rhizoctonia* crown and root rot rating of foliar disease symptoms (RCRR rating)

- leaf and beet fresh weights

- and hyperspectral near-range reflectance measurements

Table 6.1   Workflow during the field experiment in 2009.

Date	Performed activity in field
March 15th 2009	soil sampling for initial nematode population determination
April 1st 2009	application of granular nitrogen fertilizer
April 3rd 2009	sowing of sugar beet cultivar Beretta
May 11th 2009	herbicide application
June 3rd 2009	herbicide application
June 17th 2009	AISA flight campaign; near-range ASD measurements; RCRR rating; determination of penetration of nematodes in the roots and leaf weight
June 30th 2009	leaf fertilizer application
July 2nd 2009	fungicide + insecticide application
July 29th 2009	fungicide application
August 28th 2009	HyMap flight campaign; near-range ASD measurements; RCRR rating; leaf and beet weight determination
October 9th 2009	harvest of sugar beets
October 15th 2009	soil sampling for final nematode population determination

The initial population density (Pi) of BCN eggs and infective juveniles (J2) was assessed at the time of planting (Tab. 6.1). Ten soil cores (∅ 2 cm, depth 30 cm) were collected at each point of a 5 × 5 m geo-referenced grid in the field. The soil samples for Pi and also Pf were stored at 4 °C until cyst extraction and nematode counting was done as described in chapter two.

J2 root penetration at GS 31 was determined by removing soil cubes of 30 × 30 × 30 cm with roots and beet from the field and separating the roots by washing with tap water. The roots were then blotted on tissue paper and weighed. Nematode penetration was determined by staining the roots in a 0.1 % acid fuchsin. Excess stain on the roots was washed with tap water and the roots macerated twice at high speed in water in a blender (Waring products,

Torrington, CT, USA) for 10 seconds. The nematodes in two 10 ml aliquots were counted and the total number of nematodes 100 g^{-1} root was calculated (Dababat & Sikora, 2007).

A RCRR leaf symptom rating of disease symptoms (Zens et al., 2002) was conducted twice during the cropping season at GS 31 (17th of June) and GS 39 (28th of August) following the description of chapter two.

2.3. Map computation

Maps depicting within-field variation of initial or final BCN population densities, juvenile root invasion and the Pf/Pi-index were constructed with the GIS software program ArcMap 9.2 (ArcGIS, ESRI Inc., Redlands, CA, USA) and were displayed as geo-referenced maps using Inverse Distance Weighting (IDW) interpolation method (Shepard, 1968; Gotway et al., 1996). Maps were also constructed for RCRR leaf symptom ratings at GS 31 and GS 39 and for beet and leaf fresh weights by IDW, respectively.

2.4. Hyperspectral leaf reflectance measurements

When the plants reached GS 31 (17th of June 2009) the experimental field was aerial photographed with the Airborne Imaging Spectroradiometer for Applications (AISA Dual, Spectral Imaging Ltd, Oulu, Finland). The AISA provides 481 spectral bands per pixel between 400 nm and 2500 nm. Data was collected at an altitude of 1300 m resulting in 1.5 m spatial resolution. After radiometric and geometric calibration using CaliGeo 4.9.7 (Spectral Imaging Ltd., Oulu, Finland), the data was atmospherically corrected using ATCORR 4 (R. Richter, German Aerospace Centre, Wessling, Germany). Parallel to the flight campaign, near-range hyperspectral reflectance measurements were recorded at a height of one meter above canopy with a handheld non-imaging spectroradiometer (ASD FieldSpec Pro spectrometer, Analytic Spectral Devices, Boulder, CO, USA) fitted with a 25° field of view fore-optic, covering a ground area of 0.16 m^2. The spectral range was 400 to 1050 nm. Instrument optimization and reflectance calibration were performed prior to sample acquisition. An average of 50 dark current measurements was calibrated to the average of 50 barium sulphate white reference (Spectralon, Labsphere, North Sutton, NH, USA) measurements.

Final reflectance spectra were obtained by determining the ratio of data acquired for a sample related to data acquired for the white reflectance standard. Each sample scan represented an average of 20 reflectance spectra.

At GS 39 on 28th of August 2009, a second flight campaign was conducted with the HyMap (Integrated Spectronics, Sydney, Australia) hyperspectral imaging sensor. HyMap is an aircraft-mounted hyperspectral sensor providing 126 spectral bands between 450 and 2500 nm. The data was collected at an altitude of 2000 m and resulted in a spatial resolution of 4 m. At the same time, near-range hyperspectral reflectance measurements were conducted with ASD FieldSpec Pro FR spectrometer. The spectroradiometer calibration and scans followed the procedure described above.

2.4.1. Spectral vegetation indices

Out of 41 computed SVIs, the five most significant for this chapter are described in table 6.2. Spectral vegetation indices were computed from the near-range hyperspectral reflectance measurements taken at GS 31 and 39, respectively. In addition, SVIs from airborne sensor images were calculated and correlated to pathogen ratings.

Table 6.2   Spectral vegetation indices used with equations and references.

Spectral Vegetation Index	Equation	Reference
NDVI	$(R_{800}-R_{670})/(R_{800}+R_{670})$	Rouse et al. (1974)
WI	R_{900}/R_{970}	Penuelas et al. (1997)
SIPI	$(R_{800}-R_{445})/(R_{800}-R_{680})$	Penuelas et al. (1995)
AOKI	R_{550}/R_{800}	Aoki et al. (1981)
SRPI	R_{430}/R_{680}	Penuelas et al. (1995)

A number of indices were used in the study. The NDVI was explained in chapter three and is the most often used vegetation index in remote sensing (Rouse et al., 1974). Penuelas et al. (1997) developed the Water Index (WI), which is related to water content of plants. The Structural Independent Pigment Index (SIPI) gives information on the ratio of carotenoids to chlorophyll *a* and is independent of the leaf structure by including the near-infrared into equation (Penuelas et al., 1995). The SRPI was described in chapter five and calculates the ratio of carotenoids to chlorophyll *a* content (Penuelas et al., 1995). The ratio of R_{550}/R_{800}

was reported to be highly correlated to the total chlorophyll content of several plants (Aoki et al., 1981).

2.4.2. Supervised classification

Hyperspectral aerial images obtained by AISA and HyMap sensors were analysed by supervised classification using ENVI 4.6 (Research Systems Inc., Boulder, CO, USA). Five classes were built: 1. healthy; 2. Pf < 1000 eggs and J2 100 ml^{-1} soil; 3. Pf > 1000 eggs and J2 100 ml^{-1} soil; 4. RCRR rating ≤ 3 and 5. RCRR rating > 3. For each class, five regions of interest (ROIs) with one pixel were set in the image at a location with known disease status of the plants. These classified ROIs were used to extract the pixels' mean spectra, which were saved as endmembers in a spectral library. The supervised classification method SAM was used to classify each pixel in the image according to the endmember spectra (Kruse et al., 1993). For post classification, a confusion matrix was applied to the classified images which resulted in overall accuracy and kappa coefficient (Cohen, 1960).

2.5. Statistical data analysis

The computed SVIs of reflectance at GS 31 were tested on Spearman's rank correlation coefficient at a probability level of 0.01 for the Pi, juvenile root invasion, RCRR leaf symptom rating and leaf fresh weight. Similarly, SVIs calculated from reflectance at GS 39 were correlated to Pf, RCRR rating and to beet and leaf weight data. The comparability of near-range with aerial SVIs data was tested by Pearson's correlation coefficient at a probability level of 0.01. Plant masses were analysed by ANOVA, MANOVA and synergy factor following descriptions in chapter two.

3. RESULTS

3.1. Spatial pathogen distribution

GIS spatial maps were constructed that depicted quantitative information concerning initial BCN population densities (Fig. 6.1A), final population densities (Fig. 6.1B) and nematode root

penetration (Fig. 6.1D). Initial BCN population densities ranged from zero to 2504 eggs and J2 100 ml^{-1} soil and final BCN populations from zero to 4462 eggs and J2 100 ml^{-1} soil. Juvenile root penetration at GS 31 ranged from zero to 1096 juveniles 100 g^{-1} root. The BCN were not homogenously distributed in the field. The population was especially clustered in the eastern part of the test site. The reproduction index (Pf/Pi-index ± STD) resulted in a mean of 2.1 ± 0.25 over all soil samples (Fig. 6.1C).
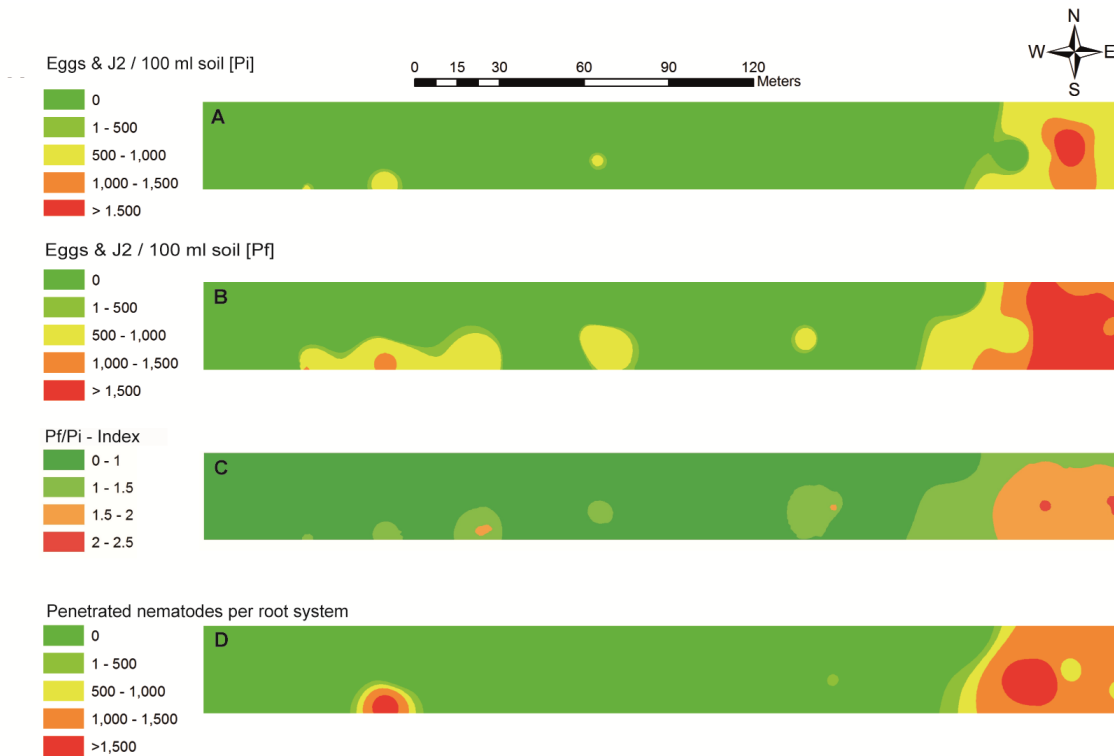

Figure 6.1 **Maps of (A) initial *Heterodera schachtii* population densities (Pi), (B) final population densities (Pf), (C) Pf/Pi-index values depending on the population development between March and October and (D) root invasion (juveniles 100 g^{-1} root) at GS 31. The dimension of the field was 215 × 30 m.**

Spatial maps on the RCRR leaf rating at GS 31 (Fig. 6.2A) and GS 39 (Fig. 6.2B) were created. The RCRR leaf rating ranged from zero to three at GS 31 and from zero to five at GS 39. *Rhizoctonia* crown and root rot developed in patches in the field with the main symptoms detected late in the cropping season. In the eastern part of the test site, RCRR and BCN infestation overlapped spatially, but it did not overlap in the rest of the field.

73

3.2. Influence of BCN and RCRR on plant development

The same method used for BCN and RCRR distribution, was used for construction of plant fresh weight GIS distribution maps (Fig. 6.3).

Significant differences in plant fresh weights were observed between the control, BCN, RCRR and concomitant BCN/RCRR infested plants (Tab. 6.3). The modified Abbott formula (see chapter two) gained a synergy factor for leaf weight of 0.94 at GS 31 and at GS 39 of 0.44 or 0.69 for beet and leaf weight, respectively. A moderate statistical interaction was obtained
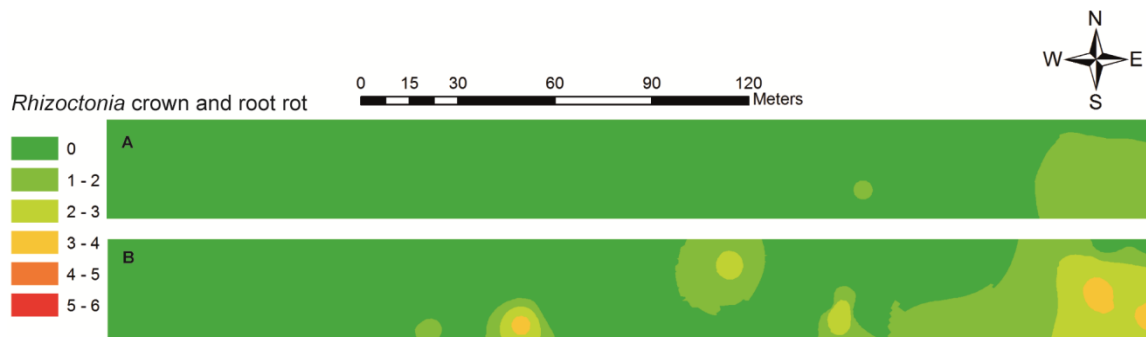

Figure 6.2 **Map of (A) *Rhizoctonia* crown and root rot (RCRR) disease severity of the foliar at growth stage 31 and (B) growth stage 39.**

for leaf fresh weight at GS 39 (F = 4.57, df = 1, p = 0.035). Plants infested with both organisms concomitantly had lower fresh weights compared to plants infested with one of the organisms or the uninfested plants.

Table 6.3 **Effect of *Heterodera schachtii* and *Rhizoctonia solani* infestation on beet and leaf fresh weight of sugar beet at GS 31 and 39.**

Infestation	Leaf weight GS 31	Beet weight GS 39	Leaf weight GS 39
Healthy control	137.9±8.4 a	403.4±44.0a	303.4±22.9a
Heterodera schachtii	46.6±10.8bc	160.3±34.3ab	72.4±12.4b
Rhizoctonia solani	104.1±18.3ab	220.7±43.3ab	130.9±18.5b
H. schachtii + R. solani	20.3±3.4 c	18.5±2.6 b	21.7±1.5 b

Displayed are the means ± standard errors of each treatment. Different letters within each column indicate significant differences after Tukey's test (p < 0.05; n = 155)

A negative correlation was obtained between J2 penetration at GS 31 and leaf weight (r = -0.72; $p < 0.01$, n = 155). At GS 39, leaf weights were negatively correlated with RCRR ratings (r = -0.72) and also with J2 penetration (r = -0.48) at a probability level of 0.01.

3.3. Relationship of SVIs with ground truth data

The five best correlated SVIs to plant fresh weights; BCN populations and RCRR leaf symptom ratings are presented in table 6.4; 6.5 and 6.6, respectively. All SVIs were significantly correlated with shoot and beet fresh weights (Tab. 6.4).

Table 6.4 Spearman's correlation coefficient for the relation between spectral vegetation indices from reflectance at GS 39 with fresh weights of beet and leaf. Bold numbers indicate highest correlation coefficient per column ($p < 0.01$, n= 155).

Spectral vegetation index	Beet fresh weight	Leaf fresh weight
NDVI	0.58	0.56
WI	**-0.59**	**-0.59**
SIPI	0.50	0.53
AOKI	0.58	0.53
SRPI	-0.56	-0.56

SVIs were correlated with Pi and root invasion of juveniles at GS 31 (Tab. 6.5). The NDVI obtained from AISA aerial data had the lowest correlation coefficient (r = -0.54, $p < 0.01$) with the Pi density compared to NDVI from near-range data (Tab. 6.5). In general, higher correlations between BCN populations and SVIs were obtained at GS 31, when compared to these at GS 39 (Tab. 6.5).

Table 6.5 Spearman's correlation coefficient for the relation between spectral vegetation indices from GS 31 with initial BCN population densities (Pi) and juvenile root invasion and spectral vegetation indices from GS 39 with the final BCN population densities (Pf). Bold numbers indicate highest correlation coefficient per column ($p < 0.01$, n= 155).

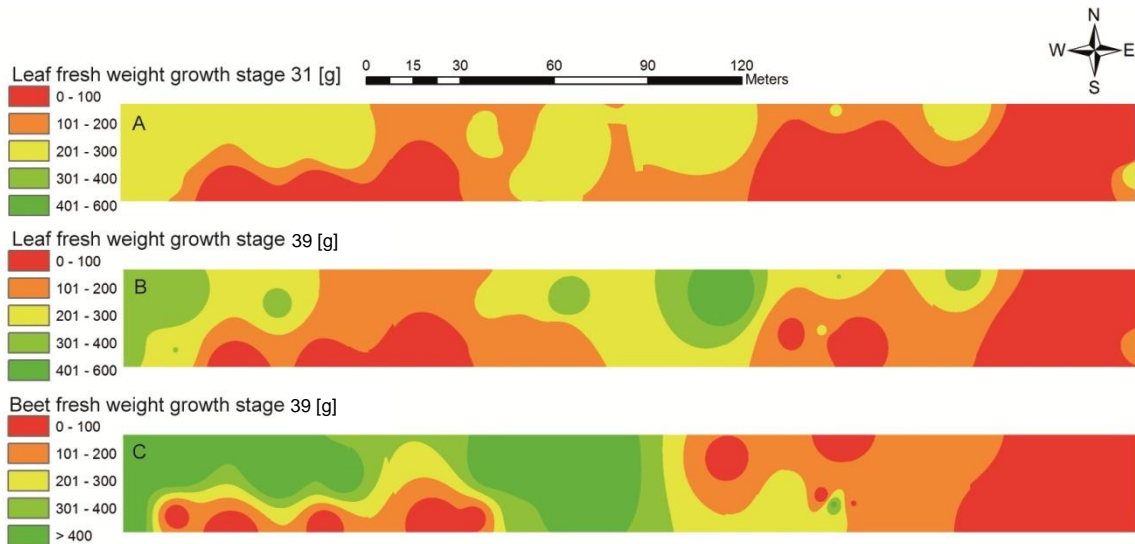| Spectral Vegetation Index	Pi	Juvenile root invasion	Pf
NDVI	**-0.74**	-0.62	**-0.22**
WI	0.70	0.63	0.21
SIPI	0.73	**0.66**	0.16
AOKI	-0.55	0.63	-0.14
SRPI	-0.68	-0.63	-0.12

75

Figure 6.3 **Effect of *Heterodera schachtii* and *Rhizoctonia solani* infestation on leaf fresh weight at GS 31 (A), and leaf and beet fresh weights at GS 39 (B, C) on the entire plot.**

Contrary to the correlations of SVIs with BCN, coefficients of the RCRR ratings with SVIs were lower at GS 31 when compared to those at GS 39 (Tab. 6.6). NDVI computed from AISA airborne data resulted in the highest correlation with the RCRR rating at GS 31 (r = -0.51, $p <$ 0.01). Conversely at GS 39, the aerial HyMap NDVI correlation with the RCRR leaf symptom rating was lowest (r = -0.37, $p <$ 0.01).

Table 6.6 **Spearman's correlation coefficient for the relation between spectral vegetation indices from reflectance at GS 31 and 39 with foliar symptom rating caused by *Rhizoctonia* crown and root rot. Bold numbers indicate highest correlation coefficient per column ($p <$ 0.01, n= 155).**

Spectral Vegetation Index	RCRR rating GS 31	RCRR rating GS 39
NDVI	-**0.48**	-0.78
WI	0.29	0.78
SIPI	0.32	-0.77
AOKI	0.34	-0.73
SRPI	-0.26	**-0.79**

Because of the inconsistency of correlations among the near-range and aerial sensed SVIs, correlation coefficients between them were calculated. Unexpectedly, only two near-range SVIs were significantly correlated with their aerial pendant (Tab. 6.7).

Table 6.7 **Pearson's correlation coefficient for the relation between near-range computed spectral vegetation indices with AISA airborne and HyMap airborne computed spectral vegetation indices obtained at GS 31 and 39, respectively. Asterix denotes significant correlations ($p < 0.01$, $n = 155$).**

Spectral Vegetation Index	AISA SVI	HyMap SVI
NDVI	0.62*	0.32
WI	0.18	0.07
SIPI	0.07	0.07
AOKI	0.66*	0.13
SRPI	0.41	0.21

3.4. Accuracy of SAM supervised classification for symptoms caused by BCN and RCRR

The SAM classification of the AISA aerial image at GS 31 resulted in an overall accuracy of 78.3 % and a kappa coefficient of $\kappa = 0.73$. The post classification demonstrated error classifications among the class Pf < 1000 J2 & eggs and the two RCRR rating classes (Tab. 6.8). There was 100 percent accuracy between healthy plants and those affected with BCN or RCRR. Supervised classification at GS 39 using HyMap aerial data resulted in an overall accuracy of 62 % and moderate agreement by kappa coefficient of $\kappa = 0.54$ and did not distinguish between pixels with healthy plants and pixels containing reflectance of plants with low nematode infection (Tab. 6.9).

Table 6.8 **Confusion matrix of five classes of SAM AISA image with ground truth pixels at GS 31. Agreement and disagreement of class to class comparison are given in percent.**

| Class | Healthy | Ground truth | | | |
		Pf < 1000 J2&eggs	Pf > 1000 J2&eggs	RCRR rating < 3	RCRR rating > 3
Unclassified	0	0	0	0	0
Healthy	100	0	0	0	0
Pf < 1000 J2&eggs	0	66	25	0	0
Pf > 1000 J2&eggs	0	0	75	0	25
RCRR rating ≤ 3	0	16	0	75	0
RCRR rating > 3	0	16	0	25	75
Total	100	100	100	100	100

4. DISCUSSION

The results of this study demonstrated that detection, mapping and quantification of BCN and RCRR infestation in sugar beet fields by GIS in combination with near-range and remote

sensed canopy reflectance data is possible. These precision tools, therefore, could develop into valuable techniques for use in long term nematode management in sugar beet.

Table 6.9   Confusion matrix of five classes SAM HyMap image with ground truth pixels at GS 39. Agreement and disagreement of class to class comparison are given in percent.

| | Ground truth | | | | |
Class	Healthy	Pf < 1000 J2&eggs	Pf > 1000 J2&eggs	RCRR rating < 3	RCRR rating > 3
Unclassified	0	0	0	0	0
Healthy	50	0	0	0	0
Pf < 1000 J2&eggs	50	75	0	50	0
Pf > 1000 J2&eggs	0	0	100	0	0
RCRR rating ≤ 3	0	25	0	50	50
RCRR rating > 3	0	0	0	0	50
Total	100	100	100	100	100

Damage to sugar beets caused by BCN or RCRR resulted in pathogen specific symptoms, such as differences in plant weight and canopy development as reported by Cooke (1987) and Herr (1996). However, synergistic effects of concomitant infection of sugar beet plants with BCN and RCRR which were found in chapters three, four and five could not be detected in this field experiment. Leaf weight, measured late in the cropping season, was the only parameter that gave an indication of a statistical interaction between the two organisms, comparable to that seen in chapter three.

The high correlation among plant fresh weights and spatial incidence of the two pathogens illustrated the potential of hyperspectral leaf reflectance for detection of the two pathogens in the same field. The suitability of canopy reflectance with the use of SVIs to determine plant biomass has been reported earlier (Tucker et al., 1985; Wiegand et al., 1991), and these results were confirmed in the present chapter by the correlations obtained between plant masses and SVIs.

Correlations between SVIs with BCN populations and RCRR disease severity at different times in the cropping season were evident due to the intimate relationship between plant weight and pathogen incidence but also plant weight with SVIs. Similar findings were reported by Heath et al. (2000) who detected correlations of NDVI, taken early in the cropping season, with the number of potato cyst nematodes *Globodera pallida* and *G.*

rostochiensis in potato roots. Several SVIs calculated from near-range and remote sensed data, resulted in detection of RCRR damage late in the cropping season in sugar beet fields (Hope et al., 1999; Laudien et al., 2003).

Symptoms caused by BCN can develop early in the season due to early infection damage to the young developing root. Subsequent infection cycles then constantly weaken the young growing plant as the season progresses (Cooke, 1987). Conversely, symptoms of RCRR develop late in the cropping season (Herr, 1996). Due to the temporal shift in symptom development patterns of the two organisms, it was hypothesis that SVIs obtained at GS 31 would be highly correlated with BCN populations when compared to the coefficients of SVIs for the RCRR rating at this growth stage. Conversely, indices obtained at GS 39 would be closely correlated to the RCRR ratings.

Symptoms related to BCN, including drought stress-induced wilting of the canopy could be confused with RCRR symptoms. However, the typical BCN wilt symptoms were not observed in this study, due to development of compensatory secondary roots by the plants. Nematode-induced wilting may need consideration when using remote sensing in hot dry seasons in non-irrigated conditions. Nutter et al. (2002) demonstrated in field studies that the onset of disease is an important diagnostic feature.

In the present study symptoms caused by BCN or RCRR could be discriminated by correlations with SVIs at different times in the cropping season.

Irrespective of the temporal aspect for disease discrimination, some SVIs were clearly correlated to BCN populations or RCRR leaf symptom ratings. Only a limited number of studies have been conducted on changes of specific pigment concentrations in the leaves of sugar beet due to BCN or RCRR infestation. Schmitz et al. (2006) reported a decrease in chlorophyll content in leaves due to BCN infestation. This could be a reason for correlations between nematode penetration with carotenoids / chlorophyll *a* dependent SIPI at GS 31. Yellowing of leaves due to RCRR disease development reflects a decrease in chlorophyll and could explain the correlation between *R. solani* infested plants and the chlorophyll /

carotenoids dependent SRPI at GS 39. These results were supported by the correlations of SRPI with RCRR leaf symptoms as outlined in chapter five.

Due to disparities in spectral resolution of the sensors used, it was difficult to obtain consistent and repeatable data sets. The near-range sensor used had a very high spectral resolution, followed by the AISA aerial sensor, whereas the aerial HyMap sensor had the lowest spectral resolution. Due to these disparities in resolution some SVIs had to be computed from non-optimal bands, which could be a reason for the low and inconsistent correlation results between SVIs and pathogens. Similarly, low correlation coefficients between the near-range sensor and the two aerial sensors demonstrated the problem of comparability.

In addition to disparities in spectral resolution, distinctions between sensors in spatial resolution were given. This could be another reason for the inconsistent results among different levels in SVI correlations and also differences in SAM classification accuracy. Aerial sensors had a lower spatial resolution than near-range sensors and the accuracy decreased with resolution. This is due to the fact that mixed pixels were obtained with reflectance of different degrees of infested or healthy plants.

Spectral vegetation indices were used to obtain a reduction of data dimension for less labour intense and faster analysis. However, as mentioned in chapter five, SVIs can cause a loss of important segments of information of the spectrum. For more precise analysis of spectral data and discrimination of pathogens; a high spectral and spatial resolution is needed. The use of an extended range of bands for analysis of data is required. Therefore, the SAM classification was used in this study. This method yielded promising results and illustrated the high potential of using hyperspectral imagery for the generation of detailed maps of diseased fields. Besides symptom discrimination, disease quantification was possible. Another advantage of SAM for multi-temporal monitoring of crop canopies is that variable illumination conditions due to day-dependent variation in sunlight intensity or field topography were attenuated. Since the analysed spectra are transferred as vectors, darker pixels will be plotted along the same vector, but closer to the origin (Kruse et al., 2003). The SAM classification could prove to be a new tool for generating digital maps of management

zones with soil-borne nematodes and pathogens, with a reduction of sampling points for ground truth data accumulation and thereby reduce the cost of assessment. SAM was used in field experiments for yield prediction in sorghum (Yang et al., 2008) and physiological properties in rice (Shwetank & Bahia, 2010) and also was suitable for plant disease symptom classification as described in chapter five and above in this chapter. However, in the present study the sensors, which had a lower spatial and spectral resolution, gave poorer results in classification accuracy. Therefore, sensors with high spatial and spectral resolution should be chosen for SAM classification.

5. CONCLUSIONS

The preparation of digital maps with GIS by the IDW interpolation method is a strong tool that can be used to simultaneously discriminate and depict the spatial distribution of pathogens in a field. The use of canopy reflectance gave promising results for localization of both BCN and RCRR in the same field over time. Canopy reflectance computed SVIs demonstrated significant correlations with symptoms caused by the two pathogens in the same field. However, inconsistency of detection by the different sensor systems was observed and is probably related to disparities in spectral and spatial resolution. The supervised classification with SAM gave good results for both diseases.

SUMMARY:

Little is known concerning the complexity of sugar beet disease when *Heterodera schachtii* and *Rhizoctonia solani* infect the plant simultaneously. Similarly the use of non-destructive analysis of symptoms caused by soil-borne organisms is in its infancy. Therefore, the findings of the present research are particularly important and can be summarized as follows:

Disease complex:

- under controlled conditions in pot experiments synergistic damage was found on susceptible and RCRR tolerant sugar beet cultivars
- RCRR development was faster and more severe when the nematode was present
- nematode development was supressed in presence of the fungus
- the fungus was able to take advantage of wounds caused by nematode penetration to more effectively enter the plant
- under field conditions, the disease complex had a negative influence on plant growth, but synergistic effects were not detected
- synergistic interactions may occur as initial inoculum densities of either of the organisms increases
- experiments have to be conducted in the future to investigate the influence of infection of each organism alone or in combination on the composition of root exudates

Non-destructive techniques:

- this is the first report of the use of nuclear magnetic resonance imaging for detection and discrimination of belowground symptoms caused by a plant parasitic nematode
- this technique has the ability to detect and discriminate between symptoms caused by *H. schachtii* and *R. solani*
- NMRi can be a useful tool for breeding companies to test cultivars for resistance to soil-borne pathogens

- experiments with NMRi have to be conducted in the future with higher spatial resolution to detect syncytia and cysts in and on the roots

- hyperspectral leaf reflectance was suitable to detect and also discriminate symptoms caused by the nematode and/or the fungus

- several vegetation indices were calculated from leaf reflectance and were highly correlated to symptom ratings

- supervised classification techniques showed promising results for discrimination, as well as quantification of symptoms caused by the experimental organisms

REFERENCES:

Abbott, W.S. (1925). A method of computing the effectiveness of an insecticide. *Journal of Economic Entomology* 18: 265-267.

Amin, M.H.G., Hall, L.D., Chlorey, R.J., Carpenter, T.A., Richards, K.S. and Bache, B.W. (1994). Magnetic resonance imaging of soil-water phenomena. *Magnetic resonance imaging* 12: 319-321.

Aoki, M., Yabuki, K. and Totsuka, T. (1981). An evaluation of use of a green channel in remote sensing of vegetation from chlorophyll content of leaves based on the spectral reflectivity in several plants. *Research Report from the National Institute for Environmental Studies Japan* 66: 125-130.

Atkinson, G.F. (1892). Some diseases of cotton. Bulletin No. 41, Alabama Polytechnical Institute Agricultural Experiment Station, Auburn, USA, pp. 64-65.

Avendano, F., Pierce, F. J., Schabenberger, O. and Melakeberhan, H. (2004). The spatial distribution of soybean cyst nematode in relation to soil texture and soil map unit. *Agronomy Journal* 96: 181-194.

Ayoub, S.M. (Ed). (1980). Plant Nematology - an agricultural training aid. NemaÁid Publication, Sacramento, USA, p. 195.

Back, M.A., Haydock, P.P.J. and Jenkinson, P. (2002). Disease complexes involving plant parasitic nematodes and soilborne pathogens. *Plant Pathology* 51: 683-697.

Back, M.A., Haydock, P.P.J. and Jenkinson, P. (2006). Interactions between the potato cyst nematode *Globodera rostochiensis* and diseases caused by *Rhizoctonia solani* AG3 in potatoes under field conditions. *European Journal of Plant Pathology* 114: 215-223.

Bajwa, S.G., Mishra, A.R. and Norman, R.J. (2010). Canopy reflectance response to plant nitrogen accumulation in rice. *Precision Agriculture* 11: 488-506.

Baker, K.F. (1970). Types of *Rhizoctonia* diseases and their occurrence. In: Parmeter, J.R. (Ed). Rhizoctonia solani*: Biology and pathology*. University of California Press, Los Angeles, USA, pp. 125-148.

Baker, C.J. and Bateman, D.F. (1978). Cutin degradation by plant pathogenic fungi. *Phytopathology* 68: 1577-1584.

Barker, K.R. and McGawley, E.C. (1998). Interrelations with other microorganisms and pests. In: Sharma, S.B. (Ed). *The Cyst Nematodes*. Kluwer Academic Publishers, Dordrecht, Netherlands, pp. 266-292.

Berdugo, C.A. (2009). Establishment of a screening test for resistance of sugar beet to *Rhizoctonia solani* AG 2-2IIIB and AG 4. MSc Thesis University of Bonn, Germany, p. 51.

Berdugo, C.A., Hillnhütter, C., Oerke, E-.C. and Sikora, R.A. (2010). Evaluation of inoculation techniques for screening sugar beet varieties for resistance to *Rhizoctonia solani*. *Proceedings 62nd International Symposium on Crop Protection*. May 18th 2010, Ghent, Belgium. [Abstr.]

Bergeson, B.B. (1972). Concepts of nematode-fungus associations in plant disease complexes: A review. *Experimental Parasitology* 32: 301-314.

Bleve-Zachero, T. and Zachero, G. (1987). Cytological studies of the susceptible reaction of sugar beet roots to *Heterodera schachtii*. *Physiological and Molecular Plant Pathology* 30: 13-25.

Bloch, D. and Hoffmann, C. (2005). Seasonal development of genotypic differences in sugar beet (*Beta vulgaris* L.) and their interaction with water supply. *Journal of Agronomy & Crop Science* 191: 263-272.

Börner, H. (Ed). (1990). Pflanzenkrankheiten und Pflanzenschutz. Eugen Ulmer, Stuttgart, Germany, p. 268-281.

Boosalis, M.G. and Scharen, A.L. (1959). Methods for microscopic detection of *Aphanomyces euteiches* and *Rhizoctonia solani* and for isolation of *Rhizoctonia solani* associated with plant debris. *Phytopathology* 49: 192-198.

Bottomley, P.A., Rogers, H.H. and Prior, S.A. (1993). NMR imaging of root water distribution in intact *Vicia faba* L. plants in elevated atmospheric CO_2. *Plant, Cell and Environment* 16: 335-338.

Buhre, C., Kluth, C., Bürcky, K., Märländer, B. and Varrelmann, M. (2009). Integrated control of root and crown rot in sugar beet: Combined effects of cultivar, crop rotation, and soil tillage. *Plant Disease* 93: 155-161.

Büttner, G., Pfähler, B. and Märländer, B. (2004). Greenhouse and field techniques for testing sugar beet for resistance to *Rhizoctonia* root and crown rot. *Plant Breeding* 123: 158-166.

Bravo, C. (2006). Automatic foliar disease detection in winter wheat. PhD Thesis University Leuven, Belgium, p. 258.

Cai, D., Kleine, M., Kifle, S., Harloff, H.J., Sandal, N.N., Marcker, K.A., Klein-Lankhorst, R.M., Salentijn, E.M.J., Lange, W., Stiekema, W.J., Wyss, U., Grundler, F.M.W. and Jung, C. (1997). Positional cloning of a gene for nematode resistance in sugar beet. *Science* 275: 832-834.

Carling, D. E., Baird, R.E., Gitaitis, R.D., Brainard, K.A. and Kuninaga, S. (2002). Characterization of AG-13, a newly reported anastomosis group of *Rhizoctonia solani. Phytopathology* 92: 893-899.

Carter, G.A., Dell, T.R. and Cibula, W.G. (1996). Spectral reflectance characteristics and digital imagery of a pine needle blight in the southern United States. *Canadian Journal of Forest Research* 26: 402-407.

Clark, M.L., Roberts, D.A. and Clark, D.B. (2005). Hyperspectral discrimination of tropical rain forest tree species at leaf to crown scales. *Remote Sensing of the Environment* 96: 375-398.

Cohen, J. (1960). A coefficient of agreement for normal scales. *Educational and Psychological Measurement* 20: 37-46.

Cook, C.G., Escobar, D.E., Everitt, J.H., Cavazos, I., Robinson, A.F. and Davis, M.R. (1999). Utilizing airborne video imagery in kenaf management and production. *Industrial Crop Production* 19: 205-210.

Cooke, D.A. (1984). The relationship between numbers of *Heterodera schachtii* and sugar beet yields on a mineral soil, 1978-81. *The Annals of Applied Biology* 104: 121-129.

Cooke, D.A. (1987). Beet cyst nematode (*Heterodera schachtii* Schmidt) and its control on sugar beet. *Agricultural Zoology Reviews* 2: 135-183.

Cooke, D.A. (1993). Nematode parasites of sugarbeet. In: Evans, K., Trudgill, D.L. & Webster, J.M. (Eds). *Plant parasitic nematodes in temperate agriculture*. CABI Publishing, Wallingford, UK, pp. 133-170.

Cubeta, M.A. and Vigalys, R. (1997). Population biology of the *Rhizoctonia solani* complex. *Phytopathology* 87: 480-484.

Čuri, J. and Zmoray, I. (1966). The relation of climatic factors to the duration of the development of *Heterodera schachtii* in Slovakia (ČSSR). *Helminthologica* 7: 49-63.

Dababat, A. and Sikora, R.A. (2007). Importance of application time and inoculum density of *Fusarium oxysporum* 162 for biological control of *Meloidogyne incognita* on tomato. *Nematropica* 37: 267-275.

Decker H. (Ed). (1969). Phytonematologie - Biologie und Bekämpfung pflanzenparasitärer Nematoden. Deutscher Landwirtschaftsverlag, Berlin, Germany, pp. 231-239.

Duggan, J.J. (1959). On the number of generations of beet eelworm, *Heterodera schachtii* Schmidt, produced in a year. *Nematologica* 4: 241-244.

Eliasson, L. and Bollmark, M. (1988). Ethylene as a possible mediator of light-induced inhibition of root growth. *Physiologia Plantarum* 72: 605-609.

Elliot, M.C. and Weston, G.D. (1993). Biology and physiology of the sugar beet plant. In: Cooke, D.A. & Scott, R.K. (Eds). *The sugar beet crop*. Chapman & Hall, London, UK, p. 37-66.

Engelkes, C.A. and Windels, C.E. (1994). Relationship of plant age, cultivar, and isolate of *Rhizoctonia solani* AG 2-2 to sugar beet root and crown rot. *Plant Disease* 78: 685-689.

Evans, K., Webster, R.M., Halford, P.D., Barker, A.D. and Russel, M.D. (2002). Site-specific management of nematodes - pitfalls and practicalities. *Journal of Nematology* 34: 194-199.

FAO (2007). IUSS Working Group WRB. World Reference Base for Soil Resources 2006, first update 2007. World Soil Resources Reports No. 103. FAO, Rome. Internet source accessed on 16.10.2010. [http://www.fao.org/nr/land/soils/soil/wrb-documents/en/].

FAO (2010). FAOstat. Internet source accessed on 30.08.2010. [http://faostat.fao.org/].

Feilhauer, H., Oerke, E.-C. and Schmidtlein, S. (2010). Quantifying empirical relations between planted species mixtures and canopy reflectance with PROTEST. *Remote sensing of the Environment* 114: 1513-1521.

Franke, J. and Menz, G. (2007). Multi-temporal wheat disease detection by multi-spectral remote sensing. *Precision Agriculture* 8: 161-172.

Franke, W. (Ed).(1997). Nutzpflanzenkunde: nutzbare Gewächse der gemäßigten Breiten, Subtropen und Tropen. Thieme, Stuttgart, Germany, p. 120.

Franklin, M.T. (1972). CIH descriptions of plant parasitic nematodes Set 1, No. 1. CABI Publishing, Wallingford, UK.

Gamon, J.A., Penuelas, J. and Field, C.B. (1992). A narrow-waveband spectral index that tracks diurnal changes in photosynthetic efficiency. *International Journal of Remote Sensing* 41: 35-44.

Gausman, H.W., Heald, C.M. and Escobar, D.E. (1975). Effect of *Rotylenchulus reniformis* on reflectance of cotton plant leaves. *Journal of Nematology* 7: 368-374.

Gierth, K. (2004). Pflanzenmorphologische und physiologische Untersuchungen zur Toleranz in der Wirt-Parasit-Interaktion *Beta vulgaris – Heterodera schachtii*. PhD Thesis University of Bonn, Germany, p. 113.

Glenn, O.F. and Sivasithamparam, K. (1990). The effect of soil compaction on the saprophytic growth of *Rhizoctonia solani*. *Plant and Soil* 121: 282-286.

Goffart, H. (Ed). (1951). Nematoden der Kulturpflanzen Europas. Paul Parey, Berlin, Germany, p. 144.

Gossuin, Y., Hocq, A., Gillis, P. and Vuong, Q.L. (2010). Physics of magnetic resonance imaging: from spin to pixel. *Journal of Physics D: Applied Physics* DOI: 10.1088/0022-3727/43/21/213001.

Gotway, C.A., Ferguson, R.B., Hergert, G.W. and Peterson, T.A. (1996). Comparison of kriging and inverse-distance methods for mapping soil parameters. *Soil Science Society of America Journal* 60: 1237-1247.

Halloin, J.M., Cooper, T.G. and Potchen, E.J. (1992). A study of disease development in *Rhizoctonia solani*-infected sugarbeets using magnetic resonance imaging. *Phytopathology* 82: 1160. [Abstr.]

Harveson, R.M. (2008). *Rhizoctonia* root and crown rot of sugar beet. Published by University of Nebraska-Lincoln Extension, Institute of Agriculture and Natural Resources. Internet source accessed on 18.10.2010. [http://elkhorn.unl.edu].

Harikrishnan, R. and Yang, B. (2004). Recovery of Anastomosis Groups of *Rhizoctonia solani* from different latitudinal positions and influence of temperatures on their growth and survival. *Plant Disease* 88: 817-823.

Heath, W.L., Haydock, P.P.J., Wilcox, A. and Evans, K. (2000). The potential use of spectral reflectance from the potato crop for remote sensing of infection by potato cyst nematodes. *Aspects of Applied Biology* 60: 185-188.

Hecker, R.J. and Ruppel, E.G. (1975). Inheritance of resistance to *Rhizoctonia* root rot in sugar beet. *Crop Science* 15: 487-490.

Henis, Y., Ghaffar, R., Baker, R. and Gillespie, S.L. (1978). A new pellet soil-sampler and its use for the study of population dynamics of *Rhizoctonia solani* in soil. *Phytopathology* 68: 371-376.

Herr, L.J. (1996). Sugar beet diseases incited by *Rhizoctonia* species. In: Sneh, B., Jabaji-Hare, S., Neate, S. & Dijst, G. (Eds). Rhizoctonia *species: Taxonomy, molecular biology, ecology, pathology and disease control*. Kluwer Academic Publishers, Dordrecht, Netherlands, pp. 341-349.

Herzog, W. and Wartenberg, H. (1958). Untersuchungen über die Lebensdauer der Sklerotien von *Rhizoctonia solani* im Boden. *Phytopathologische Zeitschrift* 33: 291-315.

Hillnhütter, C. and Mahlein, A.K. (2008). Early detection and localization of sugar beet diseases: new approaches. *Gesunde Pflanzen* 60: 143-149.

Hooper, D.J., Hallmann, J. and Subbotin, S. (2005). Methods for extraction, processing and detection of plant and soil nematodes. In: Luc, M., Sikora, R.A. & Bridge, J. (Eds). *Plant Parasitic Nematodes in Subtropical and Tropical Agriculture*. CABI Publishing, Wallingford, UK, pp. 53-86.

Hope, A., Coulter, L., Stow, D., Peterson, S., Service, D., Telk, A. and Melin, D. (1999). Root rot detection in sugar beet using digital multispectral video. *Proceedings Asian Association on Remote Sensing, 20th Asian Conference on Remote Sensing*, November 22.-25., 1999, Hong Kong, China.

Hummel, G.M., Schurr, U., Baldwin, I.T. and Walter, A. (2009). Herbivore-induced jasmonic acid bursts in leaves of *Nicotiana attenuata* mediate short-term reductions in root growth. *Plant, Cell & Environment* 32: 134-143.

Hyakumachi, M. and Ui, T. (1982). The role of overwintered plant debris and sclerotia as inoculum in the field occurred with sugar beet root rot. *Annals of the Phytopathological Society of Japan* 48: 628-633.

Jahnke, S., Menzel, M.I., van Dusschoten, D., Roeb, G.W., Bühler, J., Minwuyelet, S., Blümler, P., Temperton, V.M., Hombach, T., Streun, M., Beer, S., Khodaverdi, M., Ziemons, K., Coenen, H.H. and Schurr, U. (2009). Combined MRI-PET dissects dynamic changes in plant structures and functions. *The plant journal* 59: 634-644.

Jenkins, W.R. and Taylor, D.P. (Eds). (1967). Plant Nematology. Reinhold Publishing Corporation, New York, USA, pp. 47-57.

Jones, F.G.W. (1980). Some aspects of the epidemiology of plant-parasitic nematodes. In: Palti J. & Kranz J. (Eds). *Comparative epidemiology: A tool for better disease management*. Pudoc, Wageningen, Netherlands, pp. 71-92.

Kahn, M.W. (Ed). (1993). Nematode interactions. Chapman and Hall, New York, USA, p. 377.

Kahn, M.W. and Dasgupta, M.K. (1993). The concept of interaction. In: Kahn, M.W. (Ed). *Nematode interactions*. Chapman and Hall, New York, USA, pp. 42-54.

Köckenberger, W. (2001). Functional imaging of plants by magnetic resonance experiments. *Trends in Plant Science* 6: 286-292.

Köckenberger, W., De Panfilis, C., Santoro, D., Dahiya, P. and Rawsthorne, S. (2004). High resolution NMR microscopy of plants and fungi. *Journal of Microscopy* 214: 182-189.

Kohonen, T. (1998). The self-organizing map. *Neurocomputing* 21: 1-6.

Kruse, F.A., Lefkoff, A.B., Boardman, J.W., Heidebrecht, K.B., Shapiro, A.T., Barloon, J.P. and Goetz, A.F.H. (1993). The spectral image processing system (SIPS): Interactive visualization and analysis of imaging spectrometer data. *Remote Sensing of the Environment* 44: 145-163.

Kruse, F.A., Boardman, J.W. and Huntington, J.F. (2003). Comparison of airborne hyperspectral data and EO-1 Hyperion for mineral mapping. *IEEE Geosciences and Remote Sensing* 41: 1388-1400.

Kumar, L., Schmidt, K. S., Dury, S. and Skidmore, A. K. (2001). Imaging spectrometry and vegetation science. In: van der Meer, F. & de Jong, S. M. (Eds). *Imaging spectrometry*. Kluwer Academic Publishers, Dordrecht, Netherlands, pp. 111-115.

Laudien, R.K., Bareth, G. and Doluschitz, R. (2003). Analysis of hyperspectral field data for detection of sugar beet diseases. *Proceedings of the EFITA Conference*, July 5.-9., 2003, Debrecen, Hungary.

Laudien, R., Bareth, G., Doluschitz, R. (2004). Comparison of remote sensing based analysis of crop diseases by using high resolution multispectral and hyperspectral data – case study: *Rhizoctonia solani* in sugar beet. *Proceedings of the 12th International Conference on Geoinformatics* June 7.-9., 2004, Gävle, Sweden.

Lauterbur, P.C. (1973). Image formation by induced local interactions: examples employing nuclear magnetic resonance. *Nature* 242: 190.

Lawrence, G.W., Kelley, A.T., King, R.L., Vickery, J., Lee, H.-K. and McLean, K.S. (2004). Remote sensing and precision nematicide applications for *Rotylenchulus reniformis*

management in cotton. In: Cook, R. & Hunt, D.J. (Eds). *Nematology monographs and perspectives*. Brill, Leiden, Netherlands, pp. 13-21.

Lawrence, G.W., Doshi, R.A., King, R.L., Lawrence, K.L. and Caceres, J. (2007). Nematode management using remote sensing technology, self-organized maps and variable rate nematicide applications. *Proceedings World Cotton Research Conference.* September 10.-14., 2007. Internet source accessed on 11.10.2010. [http://wcrc.confex.com].

Lees, A.K., Cullen, D.W., Sullivan, L. and Nicolson, M.J. (2002). Development of conventional and quantitative real-time PCR assays for the detection and identification of *Rhizoctonia solani* AG-3 in potato and soil. *Plant Pathology* 51: 293-302.

Lein, J.C., Sagstetter, C.M., Schulte, D., Thurau, T., Varrelmann, M., Saal, B., Koch, G., Borchardt, D.C. and Jung, C. (2008). Mapping of *Rhizoctonia* root rot resistance genes in sugar beet using pathogen response-related sequences as molecular markers. *Plant Breeding* 127: 602-611.

Lichtenthaler, H.K., Lang, M., Sowinska, M., Heisel, F. and Miehe, J.A. (1996). Detection of vegetation stress via a new high resolution fluorescence imaging system. *Journal of Plant Physiology* 148: 599-612.

MacFall, J.S., Spaine, P., Doudrick, R. and Johnson, G.A. (1994). Alterations in growth and water-transport processes in fusiform rust galls of pine, determined by magnetic resonance microscopy. *Phytopathology* 84: 288-293.

Mahlein, A.-K., Steiner, U., Dehne, H.-W. and Oerke, E.-C. (2010). Spectral signatures of sugar beet leaves for the detection and differentiation of diseases. *Precision Agriculture* 11: 413-431.

McNairn, H. and Protz, R. (1993). Mapping Corn Residue Cover on Agricultural Fields in OxfordCounty, Ontario, Using Thematic Mapper. *Canadian Journal of Remote Sensing* 19: 152-159.

Meagher, J.W. and Chambers, S.C. (1970). Pathogenic effects of *Heterodera avenae* and *Rhizoctonia solani* on wheat. *Australian Journal of Agricultural Research* 22: 189-194.

Meagher, J.W., Brown, R.H. and Rovira, A.D. (1978). The effects of cereal cyst nematode (*Heterodera avenae*) and *Rhizoctonia solani* on the growth and yield of wheat. *Australian Journal of Agricultural Research* 29: 1127-1137.

Meier, U., Bachmann, L., Buhtz, H., Hack, H., Klose, R., Märländer, B. and Weber, E. (1993). Phänologische Entwicklungsstadien der Beta-Rüben (*Beta vulgaris* L. ssp.). Codierung

und Beschreibung nach der erweiterten BBCH-Skala (mit Abbildungen). *Nachrichtenblatt Deutscher Pflanzenschutzdienst* 45: 37-41.

Melakeberhan, H. (2002). Embracing the emerging precision agriculture technologies for site-specific management of yield-limiting factors. *Journal of Nematology* 34: 185-188.

Müller, J. (1980a). Ein verbessertes Extraktionsverfahren für *Heterodera schachtii*. *Nachrichtenblatt Deutscher Pflanzenschutzdienst* 32: 21-24.

Müller, J. (1980b). Wechselwirkungen zwischen *Heterodera schachtii* und Bodenpilzen an Zuckerrüben. *Phytopathologische Zeitschrift* 97: 357-363.

Müller, J. (1990). Anforderungen an die Bodenuntersuchung auf den Rübenzysten-nematoden (*Heterodera schachtii*) im Hinblick auf die Schadensschwelle bei Zuckerrüben. *Journal of Plant disease and Protection* 97: 563-569.

Mundt, J.T., Glenn, N.F., Weber, K.T., Prather, T.S., Lass, L.W. and Pettingill, J. (2005). Discrimination of hoary cress and determination of its detection limits via hyperspectral image processing and accuracy assessment techniques. *Remote Sensing of the Environment* 96: 509-517.

Moriarty, F. (1964). The monoxenic culture of beet eelworm (*Heterodera schachtii* Schm.) on excised roots of sugar beet (*Beta vulgaris* L.). *Parasitology* 54: 289-293.

Moshou, D., Bravo, C., Wahlen, S., West, J., McCartney, A., de Baerdemaeker, J. and Ramon, H. (2006). Simultaneous identification of plant stresses and diseases in arable crops using proximal optical sensing and self-organizing maps. *Precision Agriculture* 7: 149-164.

Nagel, K.A., Kastenholz, B., Jahnke, S., van Dusschoten, D., Aach, T., Mühlich, M., Truhn, D., Scharr, H., Terjung, S., Walter, A. and Schurr, U. (2009). Temperature response of roots: impact on growth, root system architecture and implications for phenotyping. *Functional Plant Biology* 36: 947-959.

Naito, S., Yamaguchi, T., Sugimoto, T. and Fujisawa, I. (1976). Studies on root rot of sugar beets, Anastomosis groups of *Rhizoctonia solani* Kühn isolated from diseased petioles, crowns and roots. *Proceeding of the Sugar Beet Research Association, Japan* 17: 37-44.

Nejad, S. and Dern, R. (1979). Über die Populationsentwicklung von Rübennematoden (*Heterodera schachtii*) nach Anbau von Zuckerrüben in Hessen-Nassau. *Gesunde Pflanzen* 31: 73-75.

Norman, G.G. and Fritz, N.L. (1965). Infrared photography as an indicator of disease and decline in citrus trees. *Proceedings Florida State Horticulture Society* 78: 59-63.

Nowatzki, J., Andres, R. and Kyllo, K. (2009). Agricultural remote sensing basics. Bulletin AE-1262. NDSU Extension Service. Internet source accessed on 11.10.2010. [http://hdl.handle.net/10365/5408].

Nürnberg, U. (Ed). (1965). Biologie und Geschichte unserer Kulturpflanzen. Akademische Verlagsgesellschaft Geest & Portig, Leipzig, Germany, pp. 94-106.

Nutter, F.W., Tylka, G.L., Guan, J., Moreira, A.J.D., Marett, C.C., Rosburg, T.R., Basart, J.P. and Chong, C.S. (2002). Use of remote sensing to detect soybean cyst nematode-induced plant stress. *Journal of Nematology* 34: 222-231.

Ogoshi, A. (1996). Introduction - the genus *Rhizoctonia*. In: Sneh, B., Jabaji-Hare, S., Neate, S. & Dijst, G. (Eds). Rhizoctonia *species: Taxonomy, molecular biology, ecology, pathology and disease control*. Kluwer Academic Publishers, Dordrecht, Netherlands, pp. 1-11.

Olthof, T.H.A. (1983). Effect of plant age and transplanting damage on sugar beets infected by *Heterodera schachtii*. *Journal of Nematology* 15: 555-559.

Oostenbrink, M. (1960). Estimating nematode populations by some elected methods. In: Sasser, J.N. & Jenkins, W.R. (Eds). *Nematology*. University of North Carolina Press, Chapel Hill, USA, pp. 85-102.

Ophel-Keller, K., McKay, A., Hartley, D., Herdina and Curran, J. (2008). Development of a routine DNA-based testing service for soilborne diseases in Australia. *Australasian Plant Pathology* 37: 243-253.

Pearce, R.B., Sümer, S., Doran, S.J., Carpender, T.A. and Hall, L.D. (1994). Non-invasive imaging of fungal colonization and host response in the living sapwood of sycamore *(Acer pseudoplatanus* L.) using nuclear magnetic resonance. *Physiological and Molecular Plant Pathology* 45: 359-384.

Penuelas, J., Baret, F. and Filella, I. (1995). Semi-empirical indices to assess carotenoids/chlorophyll a ratio from leaf spectral reflectance. *Photosynthetica* 31: 221-230.

Penuelas, J., Pinol, J., Ogaya, R. and Filella, I. (1997). Estimation of plant water concentration by the reflectance water index WI (R900/R970*). International Journal of Remote Sensing* 18: 2869-2875.

Pitcher, R.S. (1978). Interactions of nematodes with other pathogens. In: Southey, J.F. (Ed). *Plant nematology*. Her Majesty´s Stationery Office, Ministry of Agriculture, Fisheries and Food, London, UK, pp. 63-77.

Petherbridge, F.R. and Jones, F.G.W. (1944). Beet eelworm (*Heterodera schachtii* Schm.) in East Anglia, 1934-1943. *The Annals of Applied Biology* 31: 320-332.

Polychronopoulos, A.G. (1970). Effect *of Heterodera schachtii*, alone, or in combination with *Rhizoctonia solani*, on sugar beet seedlings. *Annals of the Institute of Phytopathological Benaki* 9: 118-133.

Polychronopoulos, A.G., Houston, B.R. and Lownsberry, B.F. (1969). Penetration and development of *Rhizoctonia solani* in sugar beet seedlings infected with *Heterodera schachtii*. *Phytopathology* 59: 482-485.

Powell, N.T. (1971). Interactions between nematodes and fungi in disease complexes. *Annual Review of Phytopathology* 9: 253-274.

Qin, J., Burks, T.F., Ritenour, M.A. and Bonn, W.G. (2009). Detection of citrus cancer using hyperspectral reflectance imaging with spectral information divergence. *Journal of Food Engineering* 93: 183-191.

Rascher, U., Nichol, C.J., Small, C. and Hendricks, L. (2007). Monitoring spatio-temporal dynamics of photosynthesis with a portable hyperspectral imaging system. *Photogrammetric Engineering and Remote Sensing* 73: 45-56.

Raski, D. J. (1950). The life history and morphology of the sugar beet nematode *Heterodera schachtii* Schmidt. *Phytopathology* 40: 135-152.

Reynolds, H.W. and Hanson, R.G. (1957). *Rhizoctonia* disease of cotton in presence or absence of the cotton root-knot nematode in Arizona. *Phytopathology* 47: 257-261.

Rheinischer Rübenbauer-Verband E.V. (2008). Versuche 2008, im Rahmen der Arbeitsgemeinschaft Zuckerrübenanbau und in Zusammenarbeit mit den Dienststellen der Landwirtschaftskammer NRW, den Zuckerfabriken der Bezirksgruppe NRW, den Zuckerrübenzüchtern und dem Institut für Zuckerrübenforschung. Internet source accessed on 11.10.2010. [http://h1437631.stratoserver.net].

Richards, B.L. (1921). A dry rot cancer of sugar beets. *Journal of Agricultural Research* 22: 47-67.

Roberts, D.L. and Herr, L.J. (1979). Soil population of *Rhizoctonia solani* from areas of healthy and diseased beets within four sugar beet fields differing in soil texture. *Canadian Journal of Microbiology* 25: 902-910.

Röntgen, W.C. (1895). Über eine neue Art von Strahlen. I Mitteilung. *Satzungsberichte der Würzburger Physik-medic Gesellschaft* 137: 41.

Rondeaux, G., Steven, M. and Baret, F. (1996). Optimization of soil-adjusted vegetation indices. *International Journal of Remote Sensing* 55: 95-107.

Rouse, J.W., Haas, R.H., Schell, J.A. and Deering, D.W. (1974). Monitoring vegetation systems in the Great Plains with ERTS. *Proceedings of the Third Earth Resources Technology Satellite-1 Symposium*. December 1973, Greenbelt, Maryland, USA.

Rupe, J., Kirkpatrick, T., Bajwa, S. and Cartwright, R. (2005). Application of precision agriculture technology to define and manage nematodes and diseases of soybean. International Plant Nutrition Institute. Internet source accessed on 11.10.2010. [http://www.inpofos.org].

Ruppel, E.G. (1991). Survival of *Rhizoctonia solani* in fallow field soil and buried sugarbeet roots at three depths. *Journal of Sugar Beet Research* 28: 141-153.

Sanwald, E. (1979). Die spektralen Reflexionseigenschaften gesunder und durch Zystennematoden geschädigter Zuckerrübenpflanzen und ihre Abbildung auf Infrarotluftaufnahmen. PhD Thesis University Freiburg, Germany, p. 165.

Savitzky, A. and Golay, M.J.E. (1964). Smoothing and differentiation of data by simplified least squares procedures. *Analytical Chemistry* 36: 1627-1639.

Schacht, H. (1859). Über einige Feinde und Krankheiten der Zuckerrübe. *Zeitschrift des Vereins für die Rübenzuckerindustrie im Zollverein* 9: 239-250.

Schlang, J. (1991). Anbau resistenter Zwischenfrüchte zur biologischen Bekämpfung des Rübenzystennematoden. *Zuckerrübe* 40: 476-488.

Schlang, J. (1996). Resistenter Ölrettich ist die beste Waffe gegen Rübennematoden. *LZ Rheinland* 18: 18-19.

Schmitz, A., Tartachnyk, I.I., Kiewnick, S., Sikora, R.A. and Kühbauch, W. (2006). Detection of *Heterodera schachtii* infestation in sugar beet by means of laser-induced and pulse amplitude modulated chlorophyll fluorescence. *Nematology* 8: 273-286.

Schowengerdt, R.A. (Ed). (1997). Remote Sensing, Models and Methods for Image Processing. Elsevier, San Diego, USA, p. 522.

Shackel, K., Labavitch, J., Matthews, M., Greve, L.C., Walton, J. and Perez, A. (2002). Magnetic resonance imaging: a nondestructive approach for detection of xylem blockages in *Xylella fastidiosa*-infected grapevines. *Pierce´s Disease Research Proceedings from 2002*. Internet source accessed on 11.10.2010. [http://files.piercesdisease.org].

Shepard, D. (1968). A two-dimension interpolation function for irregularly-spaced data. *Proceedings of the 23rd Association for Computing Machinery national conference*. 1968, New York, USA, pp. 517-524.

Shurtleff, M.C. and Averre, C.W. (Eds). (1997). Glossary of plant-pathological terms. American Phytopathological Society Press, St. Paul, USA, p. 323.

Shwetank, J.K. and Bhatia, K.J. (2010). Review of rice crop identification and classification using hyperspectral image processing system. *International Journal of Computer Sciences and Communication* 1: 253-258.

Sikora, R.A. and Carter, W.W. (1987). Nematode interactions with fungal and bacterial plant pathogens - fact or fantasy. In: Veech, J.A. & Dickson, D.W. (Eds). *Vistas on Nematology*. Society of Nematology, Hyattsville, USA, pp. 307-312.

Steddom, K., Jones, D., and Rush, C. (2005). A picture is worth than thousand words. Internet source accessed on 8.09.2009. [http://www.apsnet.org/online/feature/remote].

Stelter, H. and Meinl, G. (1967). Die Auswirkungen des Befalls mit *Heterodera rostochiensis* und *Rhizoctonia solani* auf Entwicklung und Knollenertrag von Kartoffelpflanzen in Gefäßen. *Journal of Plant Diseases and Protection* 74: 671-675.

Taubenhaus, J.J., Ezekiel, W.N. and Neblette, C.B. (1929). Airplane photography in the study of cotton root rot. *Phytopathology* 19: 1025-1029.

Taylor, C.E. (1990). Nematode interactions with other pathogens. *The Annals of Applied Biology* 116: 405-416.

Thornton, C.R. and Gilligan, A. (1999). Quantification of the effect of the hyperparasite *Trichoderma harzianum* on the saprophytic growth dynamics of *Rhizoctonia solani* in compost using a monoclonal antibody-based ELISA. *Mycological Research* 103: 443-448.

Tucker, C.J., Townshend, J.R.G. and Goff, T.E. (1985). African land-cover classification using satellite data. *Science* 25: 369-375.

Utsuzawa, S., Fukuda, K. and Sakaue, D. (2005). Use of magnetic resonance microscopy for the nondestructive observation of xylem cavitation caused by pine wilt disease. *Phytopathology* 95: 737-743.

von Blottnitz, H. and Curran, M.A. (2005). A review of assessments conducted on bio-ethanol as a transportation fuel from a net energy, greenhouse gas, and environmental life cycle perspective. *Journal of Cleaner Production* 15: 607-619.

Wallace, H.R. (1955). Factors influencing the emergence of larvae from cysts of the beet eelworm *Heterodera schachtii*. *Journal of Helminthology* 29: 3-16.

Wallace, H.R. (1983). Interactions between nematodes and other factors in plants. *Journal of Nematology* 15: 221-227.

Weinhold, A.R. and Sinclair, J.B. (1996). *Rhizoctonia solani*: Penetration, colonization and host response. In: Sneh, B., Jabaji-Hare, S., Neate, S. & Dijst, G. (Eds). Rhizoctonia *species: Taxonomy, molecular biology, ecology, pathology and disease control*. Dordrecht, Kluwer Academic Publishers, Netherlands, pp. 163-174.

Whitney, E.D. and Duffus, J.E. (Eds). (1986). Compendium of beet diseases and insects. American Phytopathological Society Press, St Paul, USA, p. 76.

Wiegand, C.L., Richardson, A.J., Escobar, D.E. and Gerbermann, A.H. (1991). Vegetation indexes in crop assessments. *Remote Sensing of the Environment* 35: 105-119.

Wyse-Pester, D.Y., Wiles, L.J. and Westra, P. (2002). The potential for mapping nematode distributions for site-specific management. *Journal of Nematology* 34: 80-87.

Wyss, U. (1992). Observations on the feeding behaviour of *Heterodera schachtii* throughout development, including events during moulting. *Fundamental and Applied Nematology* 15: 75-89.

Wyss, U. (1997). Root parasitic nematodes - An overview. In: Fenoll, C., Grundler, F.M. W. & Ohl, S. A. (Eds). *Cellular and Molecular Aspects of Plant-Nematode interactions*. Kluwer Academic Publishers, Wageningen, Netherlands, pp. 5-22.

Yang, C. and Everitt, J.H. (2002). Relationships between yield monitor data and airborne multidate digital imagery for grain sorghum. *Precision Agriculture* 3: 373-388.

Yang, C., Everitt, J.H. and Bradford, J.M. (2008). Yield estimation from hyperspectral imagery using spectral angle mapper (SAM). *Transactions of the ASABE* 51: 729-737.

Zens, I., Steiner, U. and Dehne, H.-W. (2002). Auftreten, Charakterisierung und Kontrolledes Erregers der Rübenfäule, *Rhizoctonia solani*, in Nordrhein-Westfalen.

Landwirtschaftliche Fakultät der Universität Bonn, Schriftenreihe des Lehr- und Forschungsschwerpunktes USL 91, p. 99.

ACKNOWLEDGEMENTS: